CS/NIH-RCB/2018-2019

GROUNDWATER MODELLING OF A HARD ROCK CATCHMENT- A CASE STUDY

B. K PURANDARA
B VENKATESH

NATIONAL INSTITUTE OF HYDROLOGY
HARD ROCK REGIONAL CENTRE
BELAGAVI

Abstract

Karnataka is one of the most frequent drought prone states of India due to the wider distribution of hard rock aquifers. The water availability situation in various parts of the state is alarming, particularly in Kolar, Bengaluru, Chickaballapur, Tumakuru, Chithradurga, Bidar, Kalburgi, Raichur, Vijayapura and Belagavi districts. The depth of occurrence of groundwater in these districts has gone up to 350-400 meters (1600 to 1800 feet) from the previous range of 150 m to 200 m. It is expected that, this scenario may spread rapidly to other parts of the state, if adequate water conservative measures are not taken. The main reason for this situation is unscientific way of exploitation of the precious groundwater to grow commercial crops like sugarcane, arecanut, paddy and other heavy water duty crops. In this context, one of the major river basin of Karnataka is selected for detailed investigation and modelling of groundwater system based on field conditions.

Malaprabha sub-basin of Krishna basin is heavily dependent on groundwater not only for irrigation, but also for other uses such as domestic, industrial and livestock population, because of the limited availability and supply of surface water. "Dynamic Groundwater Resources Estimation" report published by Central Ground Water Board and Groundwater Directorate Karnataka (2009), jointly identified thirty five talukas (blocks) as over exploited, whereas in 2013, it has increased to 44 talukas. In Belagavi district four taluka viz. Bailahongal, Savadatti, Ramadurga (watershed 4D7C8) which forms the part of Malaprabha sub basin and Athani taluk (watershed 4D7F1 & 4D7F2) are classified as over exploited blocks. In the over exploited blocks, drilling activities for groundwater tapping is restricted by the government authorities which resulted in public aggression. Farmers in this part of the region face conditions of hydrologic extremes very frequently due to the uncertainty in the rainfall pattern and climate change. In this context, it is highly essential to develop a reliable and well-conceived models for estimating the groundwater availability and to guide the society for adopting to the worst scenario of water scarcity from time to time. Therefore in the present study Malaprabha sub-basin in northern part of Karnataka has been studied and groundwater modelling study has been carried out.

Table of Contents

Chapter 1 1
1.1 General 1
Chapter 2 5
2.1 Elsewhere 6
2.2 National Scenario 16
Chapter 3 24
3.1 General 24
3.2 Demographics: 25
3.3 Climate 25
3.3.1 Summer season 26
3.3.2 Rainfall Pattern 27
3.3.3 Winter Season 28
3.3.4 Evaporation 28
3.4 Geomorphology of the area 28
3.5 Drainage Characteristics of the Basin 30
3.6 Land use Land cover of the area 31
3.7 Soils 33
3.7.1 Alfisols: 34
3.7.2 Entisols 34
3.7.3 Inceptisols: 34
3.7.4 Ultisols 34
3.7.5 Vertisols 34
3.8 Geology and Hydrogeology of the area: 34
3.8.1 Granites 37
3.8.2 The Meta Greywackes: 37
3.8.3 The sedimentary provinces (Quartzites/Dolomites/Conglomerates) 37
3.8.4 Deccan traps 37
3.8.5 Laterites 38
Chapter 4 41
4.1 Hydrological and Hydrogeological Investigation 41
4.2 Rainfall Analysis 41
4.2.1 Trend Analysis 41
4.3 Mann-Kendall test and Sen's slope estimate 42
4.4 Geomorphology: 42

4.5 Morphometric Analysis 43
4.6 Infiltration and Saturated Hydraulic Conductivity of Soil 45
4.6.1 Infiltration 45
4.6.2 Determination of Infiltration and Hydraulic conductivity using Disc Permeameter 45
4.6.3 Hydraulic conductivity and Sorptivity 47
4.6.4 Guelph Permeameter 48
4.7 Estimation of Groundwater recharge by Empirical Mehods: 50
4.8 Estimation of Ground water Availability using Groundwater Estimation Committee Norms. 51
4.8.1 Estimation of Ground Water Draft 52
4.8.2 Estimation of Ground Water Recharge 52
4.8.3 Estimation of normal rainfall recharge during monsoon season 54
4.8.4 Rainfall Infiltration Factor Method 55
4.9 Geophysical Survey: 56
4.9.1 ELECTRICAL RESISTIVITY METHODS 56
4.10 Surface and Groundwater Modelling 58
4.10.1 Surface and Groundwater Interactions: 58
4.10.2 Description of SWAT model 58
4.10.3 Principle 59
4.11 Groundwater Modelling 59
4.11.1 Principle: 60
Chapter 5 60
5.1 Rainfall Analysis 60
5.2 Geomorphological Characteristics of the Malaprabha sub basin 63
5.2.1 Morphometry of the Malaprabha Sub-basin: 63
5.3 Terrain characteristics of the Basin 66
5.3.1 Slope 67
5.4 L S Factor 67
5.4.1 Aspect: 68
5.4.2 Topographic Wetness Index: 69
5.4.3 Convergence Index: 70
5.5 Hydraulic Properties of Soils 71
5.5.1 Infiltration 71
5.5.2 Saturated Hydraulic Conductivity of the Soils 73

5.6 Static Groundwater Levels 75
5.6.1 Lithologic Unit wise analysis of Observation wells 76
5.6.2 Metagreywackes 78
5.6.3 Conglomerate, arenite and shale 81
5.6.4 Argillite, quarzite and conglomerate 81
5.6.5 Basalts 82
5.7 Groundwater Recharge Estimation using Empirical Methods 83
5.8 Comparision of Empirical Formulas 87
5.9 Correlation Analysis of Empirical Methods for Groundwater Recharge Estimation 88
5.10 Groundwater Resources Estimation 88
5.10.1 Dynamic Groundwater Resource Estimation by Groundwater Estimation committee norms (GEC-2015) 88
5.11 Groundwater Resource Estimation of 4D7C9(Non-Command): 88
5.12 Geophysical Studies 89
5.12.1 Data acquisition and interpretation: 90
5.12.2 VES Curves of Grainitic Terrain 91
5.12.3 Basaltic formation 92
5.12.4 Metagreywackes 94
5.12.5 Quarztie Formation 96
5.13 Groundwater Hydraulics 99
Chapter 6 102
6.1 Introduction 102
6.2 APPLICATION OF SWAT MODEL 103
6.2.1 Input data for SWAT 103
6.2.2 Calibration and Validation of the SWAT model 105
6.2.3 Validation of the Model 107
6.2.4 Surface and Groundwater Interactions: 107
6.3 Conceptual Frame work of the Study Area 109
6.3.1 Model Design 112
6.3.2 Horizontal extent 112
6.3.3 Vertical extent 112
6.3.4 Discretization 113
6.3.5 Boundary Conditions 113
6.3.6 Initial conditions 114

6.3.7 Estimation of Groundwater Recharge using Infiltration Parameter: 114
6.3.8 Horizontal and Vertical Conductivity: 115
6.4 Estimation of Groundwater Draft: 117
6.4.1 Steady state calibration 117
6.4.2 Model calibration 118
6.4.3 Calibration target and uncertainty 118
6.4.4 Trial and error calibration 119
6.4.5 Sensitivity analysis 120
6.4.6 Recharge 120
6.4.7 Evaluation of calibration 123
6.4.8 Model Validation 125
6.4.9 The Flow budget 128
6.5 Transient Model 128
6.5.1.1 Kharif Season(June-Sep): 128
Chapter 7 132
7.1 Conclusions and Scope for future work 132

List of Figures

Figure 3-1 Location Map of the Study Area 24
Figure 3-2 Map showing the Villages covered under study area. 25
Figure 3-3 Monthly Average temperature 27
Figure 3-4 Map showing the spatial distribution of Normal Rainfall 27
Figure 3-5 Plot of rainfall, Average Tempeature, Evaporation 28
Figure 3-6 Digital Elevation model of the basin 28
Figure 3-7 Map showing spatial distribution of Geomorphic units 29
Figure 3-8 Map showing the Drainage network and Tanks of Malaprabha Catchment 30
Figure 3-9 Land use Land Cover pattern of Malaprabha Catchment 32
Figure 3-10 Spatial distribution of soil types in the Malaprabha Catchment 33
Figure 3-11 Lithological units of Malaprabha Catchment 36
Figure 3-12 Hydrogeological Map. 38
Figure 3-13 Quartzite exposure are dam site dipping towards down stream 39
Figure 3-14 Quartzites trending NW-SE dipping horizontally 39

Figure 3-15 Lithology distribution in Malaprabha sub basin 40
Figure 4-1Double ring infiltrometer 46
Figure 4-2 Disc Permeameter 46
Figure 4-3 Guelph Permeameter 49
Figure 4-4 Electrical Resistivity Method 56
Figure 4-5 Wenner Array 57
Figure 4-6 Schlumberger Array 57
Figure 4-7 SWAT Flow chart 59
Figure 4-8 Groundwater Modelling flow chart 60
Figure 5-1 Average, Maximum and Minimum Rainfall (mm) 63
Figure 5-2 **S**lope map (in radians) 67
Figure 5-3Map showing **L S Factor** 68
Figure 5-4 Aspect map of Malaprabha sub basin 69
Figure 5-5 showing Topographic Wetness Index. 70
Figure 5-6 Map showing Convergence Index. 71
Figure 5-7 Landuse wise rate of infiltration 73
Figure 5-8 showing the Land use wise Hydraulic conductivity of the soils below 60 cm 75
Figure 5-9 Location of Observation Wells 75
Figure 5-10 Groundwater Hydrograph of Desur 77
Figure 5-11 Groundwater Hydrograph of Gunji 77
Figure 5-12 Groundwater Hydrograph of Khanapur 78
Figure 5-13 Groundwater Hydrograph of Bailahongal 78
Figure 5-14 Groundwater Hydrograph of Murkumbi 79
Figure 5-15 Groundwater Hydrograph of Ambadagatti 79
Figure 5-16 Groundwater Hydrograph of Beedi 79
Figure 5-17 Groundwater Hydrograph of Chikkabagewadi 80
Figure 5-18 Groundwater Hydrograph of M.K.Hubli 80
Figure 5-19 Groundwater Hydrograph of Parishwad 80
Figure 5-20 Groundwater Hydrograph of Katkol 81
Figure 5-21 Groundwater Hydrograph of Korkoppa 81
Figure 5-22 Groundwater Hydrograph of Gondi 82
Figure 5-23 Groundwater Hydrograph of K.Chandargi 82
Figure 5-24 Comparitive Graph of Groundwater recharge Estimation by various empirical methods 88

Figure 5-25 Vertical Electrical Soundings carried out in the Granitic terrain 91
Figure 5-26 Vertical Electrical Soundings carried out in Basaltic formation.....93
Figure 5-27 Vertical Electrical Soundings carried out in Meta Greywacke formation. 95
Figure 5-28 Vertical Electrical Soundings carried out in Quarzitic formation.....97
Figure 6-1 Malaprabha catchment demarcated into sub-units by using SWAT model 105
Figure 6-2 Observed and simulated discharge values for the calibration period.....106
Figure 6-3 Observed and simulated discharge values for the validation period 107
Figure 6-4 Water balance components obtained through SWAT model 108
Figure 6-5 Water balance obtained from the Soil Water Assessment tool 109
Figure 6-6 Fence diagram of the Borewells in the Malaprabha sub basin.....110
Figure 6-7 The Conceptualized Model of the Malaprabha sub-basin.....112
Figure 6-8 Boundary conditions 113
Figure 6-9 Starting heads (Groundwater levels) 114
Figure 6-10 Recharge rates for Groundwater Modeling 115
Figure 6-11 Distribution of hydraulic conductivity 116
Figure 6-12 Hydraulic conductivity sensitivity 120
Figure 6-13 The sensitivities of the Recharge rates 121
Figure 6-14 Contour map of simulated heads before the Calibration.....122
Figure 6-15 Contour map of simulated heads after the Calibration.....123
Figure 6-16 The Scatter plot before Calibraiton 124
Figure 6-17 The Scatter plot after Calibraiton 124
Figure 6-18 Computed V/S Observed Groundwater heads for Beedi observation well 126
Figure 6-19 Computed V/S Observed Groundwater heads for Desur observation well 126
Figure 6-20 Computed V/S Observed Groundwater heads for Parishwad observation well.....127
Figure 6-21 Computed V/S Observed Groundwater heads for Bailahongal observation well.....127
Figure 6-22 Computed V/S Observed Groundwater heads for Sampgaon observation well.....127
Figure 6-23 Simulated Groundwater heads for the Kharif Seaon(June to Sep) 129
Figure 6-24 Simulated Groundwater Heads for Rabi season.....130

Figure 6-25 Simulated Groundwater Heads for Summer season.....131

List of Tables

Table 3-1 Weather data of Khanapur station (WRDO, Bengaluru) 26
Table 3-2 Monthly average Temperatures 26
Table 3-3 Percentage spread of the individual geomorphic units 30
Table 3-4 Morphometry of the Malaprabha catchment 31
Table 3-5 Geographical extent of Land use/ Cover in the Malaprabha catchment 32
Table 3-6 The geographical Extent of Soil Types 33
Table 3-7 Stratigraphic sequence observed in the area 35
Table 3-8 Geographic extent of Geomorphological units of the catchment 36
Table 4-1 Methods involved in Morphometric Analysis 43
Table 5-1 Rainfall Statiscal Analysis of Sub basin 62
Table 5-2 Morphometry of Malaprabha sub basin 63
Table 5-3 Stream Length,ratio, Bifurcation ratio 64
Table 5-4 Drainage density, texture, stream frequency, Elongation ration 64
Table 5-5 Relative relief Longest axis, Relief ratio 66
Table 5-6 Infiltration Rate in Different stretches of Malaprabha catchment 72
Table 5-7 Saturated Hydraulic Conductivity in different stretches of Malaprabha catchment 74
Table 5-8 Observation well details 76
Table 5-9 Comparison of Groundwater recharge by Empirical Methods 84
Table 5-10 The Apparent resistivity values obtained from various locations of the granitic terrain 92
Table 5-11 The Apparent resistivity values obtained from various locations of basin in basalt formation 93
Table 5-12 The Apparent resistivity values obtained from various locations of basin in Meta Greywackes 96
Table 5-13 The Apparent resistivity values obtained from various locations of basin in Quartzites 98
Table 5-14 Formation wise Pumping details of Malaprabha sub basin 99
. Table 6-1 Fitted values of the parameters as obtained after the calibration 106
Table 6-2 Water balance components estimated using the SWAT Model 109
Table 6-3 Hydraulic conductivity, Vertical Hydraulic conductivity, Specific yield taken into the model 116
Table 6-4 Groundwater draft 117

Table 6-5 119
Table 6-6 Observed and calculated heads Before Calibration 121
Table 6-7 Observed and calculated heads After Calibration 123
Table 6-8 Groundwater flow budget for the steady state flow. 128
Table 6-9 Flow Budget for Kharif Season(June-Sep).....129
Table 6-10 Flow budget for Rabi season (Oct - Jan) 130

Chapter 1

Introduction

1.1 General

The history of groundwater hydrology dates back to the time of Darcy's hypothesis which enabled us to understand both quantitative and qualitative issues related to occurrence, distribution, flow and transport characteristics (downward movement of chemicals) in the subsurface horizon of the earth. However, due to the limited availability of data pertaining to groundwater movement, delineation and quantification of groundwater resources were mostly based on hydrogeological and hydrological investigations. In the latter years, those data were used to develop a set of type curves which helped all through in the groundwater assessment and management. Over the years, various results of regional hydrogeological studies have proved that the groundwater systems are highly dynamic and complex, particularly in hard rock areas of India which covers more than 65% of the country. Therefore, methodologies involving hydrogeological data regionalization are important in contrast to hydrogeological basins occupied by strata bound sedimentary aquifers. Hard rocks are characterized by a set of discontinuities such as joints, fractures and shear zones (Singhal, et al., 1999). The groundwater occurs under both unconfined and semi-confined conditions. Unconfined conditions found in the mantle of weathered rock, alluvium, and laterite overlying the hard rock, while within the fissures, fractures, cracks, joints, and lava flows water occurs in the semi-confined state.

Hydrological responses in hard rock region vary significantly, with time and space due to various climatic factors and also due to changes in land use/land cover. The groundwater storage and its flow in a hard rock terrain are controlled primarily with the secondary effective porosity that is formed through a network of fractures, weathering and/or mineral alteration and also due to impervious barrier through lithological contacts or dykes (Singhal, 2008). In addition, paleo-channels and/or paleo-valleys hidden in the subsurface also support an inherited preferential groundwater flow and recharge (De Vries et al., 2000; Maus et al., 1999; Owen and Dahlin, 2010; Revil et al., 2005). As a result of such vibrant characteristics, extreme hydrological condition may appear, i.e. in some cases increased recharge with a continuous rising of water table leading to water-logging problems. Meanwhile, due to deforestation and land preparation, there are instances of substantial decrease in infiltration capacity, resulting

in increased peak surface runoff and lowered groundwater levels in shallow aquifers. Further, such activities also give rise to reductions in well yields, spring discharges and dry weather stream flows. The occurrence of groundwater in volcanic rocks normally is under perched, unconfined and confined conditions. In the case of perched aquifers, the regional water table depends primarily on the presence of impervious formations, such as sills, ash beds and dense basalt flows. Confined aquifers are reported from where the pervious lava beds are sandwiched between impervious sedimentary beds (Stearns, 1942; Fetter, 1988). Confined conditions are also possible, if the vesicular or fractured basalt is lying between massive units (Singhal, 1973). The availability of groundwater under artesian condition is quite common in the Deccan traps (Kittu, 1990; Rana and Vishwakarma, 1990). From the discussion it is evident that, the groundwater flow and its response to changes in the hydrological system are mostly dependent on the geometry (horizontal extent and thickness) and anatomy (internal character, distribution and type of porosity) of hydrogeological bodies (aquifers and aquitards). Therefore, hydrogeological characteristics in directly refers to the age and tectonic activities of the region which in turn control the degree of diagenesis and the relationship between the inter-granular and fissure porosity of rocks. Consequently, these features determine the magnitude and distribution of their hydraulic parameters (transmissivity and permeability, storativity). Comparatively crystalline (igneous and metamorphic) or sedimentary (highly cemented and/or folded rocks) rocks generally lose their primary inter-granular porosity and instead develop fracture porosity. The common feature of a hard rock environment, designated as a 'hydrogeological massif', is a vertical sequence of three zones, termed upper weathered, central fractured and lower massive (Krasny 1996a). As in the case of the inter-granular environment, the permeability of fractures and of fault zones typically decreases through geological time due to different geological processes such as hydrothermal alteration, mineral precipitation and mechanical clogging (Mazurek 2000).Therefore, in any hard rock environment geologically young fractures are the most important for groundwater flow, but as noted by Banks et al.(1993), such fractures might not be recorded by standard field geological and geophysical methods. Relatively soluble rocks such as carbonates, gypsum and salt deposits are the only exceptions to this general rule as their permeability increase with time. This is especially the case with bedrock, which is usually represented by crystalline formation. The groundwater residence time in the crystalline rocks may vary from only a few years in shallow weathered horizons to as much as several thousand years in deep fractures. Therefore, in recent days, scientists

and groundwater professionals looked for an alternative method to that of regular conventional approach.

In recent years, in spite of having significant variability in the occurrence and distribution, groundwater use showed a phenomenal increase in all parts of the World including India, for both irrigation and drinking purposes. This essentially stressed the need to understand the existing aquifer system and its characteristics for the sustainable development of groundwater resources and to improve the management strategies. In order to achieve the management goal, mathematical models have been developed to predict the fate and movement of groundwater flow and physiochemical aspects in natural as well as hypothetical scenarios. Such models are widely used in water resources planning and management. Surface water and groundwater models have been used to estimate water balance managing and allocating. According to the convenience of the model development, classical surface and groundwater models were mostly simulated separately and supposed to use simple interaction of surface-subsurface water in their model boundary. Groundwater models are broadly used to understand the groundwater flow and transport processes using mathematical equations based on physical assumptions. These assumptions typically involve the flow paths, aquifer parameters, the heterogeneity or anisotropy of aquifer systems and the solute transport processes. Because of the simplifying assumptions embedded in the mathematical equations, there are number uncertainties in the prediction of groundwater movement, particularly in hard rock areas. This is mainly due to the more dynamic and complex nature observed in the occurrence and distribution of groundwater in weathered and fractured aquifers. Hard rock aquifers are discontinuous, anisotropic in nature and devoid of primary porosity. Therefore, the groundwater recharge process in such aquifers are very low and showed decline in groundwater table particularly in Peninsular India covering large areas of Deccan trap.

One of the basic parameter required to predict the groundwater level is the recharge characteristics of the aquifer which varies significantly with time and space. However, the estimation of groundwater recharge in crystalline and other hard rocks is faced with greater problems as compared with sedimentary rock aquifers, on account of their heterogeneity. With reference to groundwater distribution, it is a fact that hard rock aquifers are prevalent in semi-arid and arid areas (Maréchal et al. 2004; MacDonald et al. 2009) and are often the primary water source for large populations (Titus et

al. 2009). This indicates that these aquifer types are vulnerable to drought and overexploitation (Villholth et al. 2013) and hence critical to understand and to model in order to support water security, resilience and sustainable groundwater management (Ahmed et al. 2008). However, integrated catchment-scale assessments in these settings, where the temporal-spatial variation of recharge is determined as an integral aspect of the modelling, are presently relatively rare (Ahmed et al. 2008). In India groundwater models have been used by various researchers, however, it is mostly restricted to hypothetical conditions rather than real time analysis. Though in the recent years many of the professional engineers and Scientists have employed lumped models for planning and management of groundwater resources. However, such models completely ignore the distributed character of the groundwater regime. Thus, they are based upon rather conservative concepts like safe yields and are incapable of accounting for the stream-aquifer interaction and the dependence of lateral recharge on the water table pattern. According to the convenience of the model development, classical surface and groundwater models were mostly simulated separately and supposed to use simple interaction of surface-subsurface water in their model boundary. When groundwater use was hugely rising and hydrological elements of whole water system are needed to fully manage, the coupling simulation of both surface and subsurface system.

Karnataka is one of the most frequent drought prone states of India due to the wider distribution of hard rock aquifers. The water availability situation in various parts of the state is alarming, particularly in Kolar, Bengaluru, Chickaballapur, Tumakuru, Chithradurga, Bidar, Kalburgi, Raichur, Vijayapura and Belagavi districts. The depth of occurrence of groundwater in these districts has gone up to 350-400 meters (1600 to 1800 feet) from the previous range of 150 m to 200 m. It is expected that, this scenario may spread rapidly to other parts of the state, if adequate water conservative measures are not taken. The main reason for this situation is unscientific way of exploitation of the precious groundwater to grow commercial crops like sugarcane, arecanut, paddy and other heavy water duty crops. In this context, one of the major river basin of Karnataka is selected for detailed investigation and modelling of groundwater system based on field conditions.

Malaprabha sub-basin of Krishna basin is heavily dependent on groundwater not only for irrigation, but also for other uses such as domestic, industrial and livestock

population, because of the limited availability and supply of surface water. According to the local community, there is a significant increase in groundwater abstraction for irrigation from 90's and according to the present study, it showed 2-3 fold increase in the recent years. "Dynamic Groundwater Resources Estimation" report published by Central Ground Water Board and Groundwater Directorate Karnataka (2009), jointly identified thirty five talukas (blocks) as over exploited, whereas in 2013, it has increased to 44 talukas. In Belagavi district four taluka viz. Bailahongal, Savadatti, Ramadurga (watershed 4D7C8) which forms the part of Malaprabha sub basin and Athani taluk (watershed 4D7F1 & 4D7F2) are classified as over exploited blocks. In the over exploited blocks, drilling activities for groundwater tapping is restricted by the government authorities which resulted in public aggression. Farmers in this part of the region face conditions of hydrologic extremes very frequently due to the uncertainty in the rainfall pattern and climate change. In this context, it is highly essential to develop a reliable and well-conceived models for estimating the groundwater availability and to guide the society for adopting to the worst scenario of water scarcity from time to time. Therefore in the present study Malaprabha sub-basin in northern part of Karnataka has been studied and groundwater modelling study has been carried out with the following objectives by using Groundwater Modeling System (GMS- MODFLOW-).

1. Analysis of rainfall variability, trend and groundwater recharge estimation by conventional methods (using rainfall data)

2. Hydrological and hydrogeological investigations (field and laboratory methods) to determine model (Groundwater Modeling System- GMS) parameters for calibration and validation.

3. Estimation of hydrological components such as runoff and recharge factors using ArcSWAT model

4. Groundwater modelling of Malaprabha sub basin under different stress conditions (Khariff, rabi and summer) using GMS system.

Chapter 2

Literature Review

2.1 Elsewhere

Toth (1963) used for the first time analytical solutions to investigate groundwater flow in hypothetical small drainage basins. He found theoretically the existence of hierarchically nested groundwater flow systems: local, intermediate (sub-regional) and regional. Latter, **Freeze and Witherspoon, 1968** attempted numerical models to simulate steady state regional flow patterns in hypothetical layered aquifer systems. Such numerical models have the advantage in simulating three-dimensional groundwater flow in heterogeneous and anisotropic groundwater basins. Such models were used to analyze the effects of water table configuration and hydraulic conductivity on regional flow patterns and to quantify basin yields. A transient saturated-unsaturated numerical model was later developed by **Freeze (1971)** to investigate the relation between infiltration rates, water table rise and base flow hydrograph. The model was further used to predict maximum basin yield as a function of pumping pattern and recharge and discharge characteristics of a hypothetical basin. Groundwater modeling is increasingly recognized as a powerful quantitative tool available to hydrogeologists for evaluating groundwater systems. A groundwater model is a simplified version of the real system that approximately simulates the input/ output stress and response relations of the system

Application of groundwater flow models to large scale aquifer system simulation started in 1978, with the **Regional Aquifer System Analysis (RASA)** program of U.S. Geological Survey (Sun and Johnson, 1994). During the 18 years of the program (1978–1995), 25 regional aquifer systems were intensively studied. These include the famous High Plains aquifer system, the California Central Valley aquifer system and, among others, the Florida and Great Basin aquifer systems. The major contributions of the program were: (1) creation of regional hydrogeological databases; (2) construction of hydrogeological frameworks (conceptual models); (3) understanding of responses of regional aquifer systems to natural stresses (predevelopment) and human interferences (abstraction and land use changes); and (4) the compilation of a national groundwater atlas.

In recent years, computer-based numerical groundwater flow models were constructed and used to characterize flow systems and to simulate the effects of groundwater development and land use changes. Mathematical models used in most cases were the USGS 3D finite difference model (Trescott, 1975) and the MODLFOW (McDonald and Harbaugh, 1988). Significant advances in regional flow system analysis were

driven by the application of 3D groundwater flow models. Since its release in 1988, MODFLOW has become the industrial standard worldwide for groundwater modeling because of its flexible modular structure, complete coverage of hydrogeological processes and public domain free availability.

Modeling of large groundwater basins became much easier with the rapid development in software engineering, computer capacity and wide use of Geographic Information Systems (GIS). Several Windows-based graphic user interfaces for MODFLOW have been developed in 1990s. The most widely used are Processing Modflow (Chiang and Kinzelbach, 2001), Visual Modflow (Waterloo Hydrogeological, 2001), Groundwater Modeling Systems (GMS) (Brigham Young University, Environmental Modeling Research Brigham Young University Environmental Modeling Research Laboratory, 2000), and Groundwater Vista (Rumbaugh and Rumbaugh, 2005).

Wang (1997) envisaged that Steady-state groundwater and contaminant transport models were applied to simulate conservative or non-conservative contaminant transports in simple isotropic or complex geohydrological conditions. Calvete & Vera (1998) formulated a hydrogeological model having two aquifer system connected through an leaky aquitard using numerical approach. The model estimated the potential environmental effects of the large irrigation project of Los Monegros II and helped to quantify the hydrogeology of the area. The above study concluded that anisotropy plays a major role in some parts of the lower aquifer. The geometric average of model conductivity is almost two orders of magnitude larger than the average conductivity derived from small-scale field tests.

Gburek (1999) modelled the pollutant transport within a layered and fractured aquifer of an upland agricultural watershed in Pennsylvania, USA. The simulation results from a previous study by the same author (Gburek, 1998) on a groundwater flow simulation using Visual MODLFOW under springtime steady-state recharge was used as the basis for the study of areal-format water-shed flow paths.

Kuchling (2000) modelled the groundwater flow and TDS plume transport arising from miningoperations at Daivik diamonds project in Canada. **Abdulla et al (2000)** forged a three-dimensional groundwater flow model using MODFLOW to simulate water level change in the complex multi-aquifer systems of the Azraq basin, Jordan. The conceptual model used for the study consists of three hydrogeological layers and were

successful to predict the safe yield for the Upper aquifer system (25 MCM per annum). Further,

Jia (2003) simulated the groundwater flow in the Luancheng county of Hebei Province, China to understand the groundwater level fluctuations. **Kim (2003)** developed a GIS based Pre- and Post-processing tool for Visual MODFLOW to manage input data for flow analysis.

Meriano (2003) developed a groundwater flow model for a drainage basin in Canada. With their forecast they demonstrated the susceptibility of deeper aquifers to urban contaminants and suggested the importance of long term planning for water quality. Yunjie (2003) used Visual MODFLOW to simulate groundwater flow with the prevailing hydrogeological conditions at a sandstone-type uranium deposits.

Kilb (2005) used GIS tools and Visual MODFLOW to model the effects of groundwater mounding on the water table elevation of two flooded recharge basins situated on the northwest side of Stony Brook University's West Campus in New York, USA. The results showed that the groundwater flow on the northwest part of Stony Brook campus is strongly influenced by recharge mounding under the basins. Also, there was a possibility that the basins were flooded due to a combination of mounding, clogging, and large, continuous inputs of water to the basins.

Idrysy & Smedt (2006) developed a hydrological and a hydrogeological model for the Trifa aquifer which is most productive agricultural plain of north-eastern Morocco. Two layers groundwater flow model was created using MODFLOW in the PMWIN environment. The groundwater recharge and the pumping quantity of the groundwater for irrigation are calculated using the distributed hydrological model WetSpass. It conceded that the reduction in groundwater abstraction by at least 25% may be necessary to achieve sustainability conditions. **Abdulla & Al-Assad (2006)** used MODFLOW to build a groundwater flow model of Mujib aquifer to simulate the behavior of the flow system under different stresses. The model was calibrated for both steady state and transient condition. It revealed from the sensitivity analysis that the model was sensitive to specific yield. The water balance for the steady state condition of the aquifer indicated that the total annual outflow is greater than the inflow. **Hu (2006)** explores the application constraints with Visual MODFLOW in groundwater simulations. **Yuan-fang (2006)** studied the groundwater flow and levels around a river in China to ensure its quantity to meet the water demand of a city**. Roadcap (2001)** simulated the effects of pumpage from a series of ten groundwater wells on a particular aquifer and its surrounding wells.

Palma & Bentley (2007) developed the groundwater flow system in a sub-basin of the Leon-Chinandega aquifer using numerical models to investigate the effects of further groundwater development. Two flow systems are identified in the aquifer and clearly stated that the steady state simulations cannot capture the critical aspects of the groundwater system and transient simulations are required to estimate the important hydrological factors such as minimum base flow. **Johnson (2007**) used a MODFLOW package to construct a groundwater flow model in a mountainous hard rock area to prioritize the collection of data by doing a sensitivity analysis. **Yizhong (2007**) simulated a two-dimensional unconfined groundwater flow and the migration of nitrate contaminant for a period of 42 years in Shijia Zhuang, China.

Fei (2008) simulated the groundwater flow for a plain reservoir in Sheyang, China. They predicted the exploitable groundwater capacity with different water levels in the reservoir.

Zume (2008) modelled the groundwater flow in the semiarid north-western Oklahoma, USA to assess the impact of exploiting groundwater on the streamflow depletion in the Alluvium and Terrace aquifer of the Beaver-North Canadian River in the north-western Oklahoma, USA. With the help of streamflow routing package of the software, changes induced by pumping on base flow and stream leakage were studied. **Ayenew et al (2008)** developed a three dimensional steady-state finite difference groundwater flow model which was used to quantify the groundwater fluxes and analyzed the subsurface hydrodynamics in the Akaki catchment by giving particular emphasis to the well field that supplies water to the city of Addis Ababa. The model was used to forecast groundwater flow pattern, the interaction of groundwater and surface water, and the effect of pumping on the well field under different scenarios. Zume & Tarhule (2008) made an attempt to evaluate the impacts of groundwater exploitation on stream flow depletion in the Alluvium and Terrace aquifer of the Beaver-North Canadian River (BNCR) in north- western Oklahoma, USA. Ground water pumping was specified in the model and Stream–aquifer interaction was simulated with the stream flow routing package which has the additional capability to track the amount of water in each simulated stream segment. Stream stage was computed iteratively using Manning's roughness coefficient. Simulations were performed for both steady and non-steady state conditions. The study concluded that non-flood flow in Beaver North Canadian River network depends heavily on base flow contributions from the alluvial aquifer. **Dams et al (2008)** studied the impact of land-use changes, from 2000 until 2020, on the

hydrological balance and in particular on groundwater quantity, as results from a case study in the Kleine Nete basin, Belgium. An attempt was made to couple land use change model with a water balance and a steady state ground water model. Water balance components, groundwater level and baseflow are simulated using the WetSpass model in conjunction with a steady-state MODFLOW groundwater flow model. Results show that the average recharge decreases with 2.9, 1.6, 1.8 and 0.8% for scenario A1, A2, B1 and B2, respectively, over the 20 years period. Although these averages appear to indicate small changes in the groundwater system, spatial analysis shows that much larger changes are located near the major cities in the study area. Hence, spatial planning should take better account of effects of land-use change on the groundwater system and define mitigating actions for reducing the negative impacts of land use changes. **Wake (2008)** created a MODFLOW model in order to study the surface water-groundwater interaction in a rectangular study area in the Kleine Nete catchment of the Aa river basin. The results showed good correlation between the simulated and observed water levels and it was noticed that the groundwater flow was not significantly influenced by the pumping wells but mostly by the boundary conditions. Won Kim et al (2008) suggested a new approach for integrating the quasi-distributed watershed model 'SWAT' with fully distributed groundwater model 'MODFLOW'. The method proposed for the integration included the exchange of characteristics of the hydrological response units (HRU) in SWAT model with the cells in the MODFLOW model. The application demonstrates that an integrated SWAT–MODFLOW is capable of simulating the spatio-temporal distribution of groundwater recharge rates, aquifer evapotranspiration and groundwater levels and that it enables an interaction between the saturated aquifer and channel reaches.

Jovanovic (2009) used Visual MODFLOW to calculate the spatial distribution of NOx concentrations in groundwater. The research work was to study the impact of nitrogen dynamics on land and ground at Riverlands Nature Reserve, South Africa. **Fouépé Takounjou et al (2009)** carried out a study aimed to ascertain groundwater flow and mass transport Modeling in the Anga'a river watershed in Yaounde, Cameroon. Surface-groundwater interaction in the region was also studied using MODFLOW and MT3DMS. A two layered model was developed, where the upper layer comprised of unconfined clay/sandy weathered zone and the lower one was considered semi-confined fracture zone. Results showed that the surface topography controls the groundwater flow conditions in the Anga'a river watershed and also

concluded that some contamination occurred within the basin but it would take 50 years to reach the fish ponds located in the region.

Shi (2010) applied Visual MODFLOW to evaluate the impact caused by the leakage of a sewage plant accident pool on groundwater. Ammoniacal Nitrogen (NH3-N) migration from the accident spillage was simulated. **Faghihi (2010** predicted the reaction of an aquifer to different environmental stress scenarios in the Qazvin plain of Iran. **Feng (2010)** predicted the groundwater depression funnel and variations in groundwater levels due to different exploitation extents. A transient groundwater flow model was developed for the North China Plain in order to assess its groundwater development potential (Shao et al., 2009). A regional groundwater flow model was also constructed for the Cretaceous aquifer system in Ordos Basin (Hou and Zhang, 2008). The model consisted of 3 layers, 330 rows and 160 columns with a uniform grid size of 2 km by 2 km. The model was calibrated under the steady state and used for analyzing groundwater flow patterns and assessing groundwater resources. And, in addition, a 3D transient groundwater flow mode1 was established for the Beijing P1ain in order to analyze groundwater flow systems and water balance (Wang et al., 2009). The transient model simulation time was from l995 to 2005. The model was used to explore options for sustainable groundwater resources development. A limited review of groundwater modeling in China was provided by Wang et al. (2010).

Al-Dousari et al (2010) applied SWAT model to provide continuous simulation of overland flow, channel flow and transmission losses of Raudatain watershed in northern Kuwait and Umm Al Aish watershed in Central Kuwait. The results showed high groundwater recharge potential (about 50 MCM) which showed a good correlation with the one estimated using remote sensing approach. **Bejranonda et al (2010)** attempted to semi-couple SWAT and MODFLOW to determine the flow behaviour and hydrological components in the Upper Great Chao Phraya Basin of Thailand. It was found that the coupling methodology is a key to obtain satisfactory results in the case of natural hydrological processes.

Ahmad et al (2010) developed a 3 D flow model to optimize the supply demand in the urban settlement near Kahota Industrial Triangle area, located adjacent to the Soan River, Islamabad, Pakistan. Transient simulation was carried out with the constant discharge rates of groundwater by means of pumping wells, storage factor, porosity, and observed drawdown matched with the simulated drawdown. The results obtained indicated that, the direction of flow move initially from groundwater regimes to the

Soan River and reversed from the Soan River to the groundwater regimes as the drawdown deepens. **Mamunul et al (2012)** evolved a groundwater flow model using Visual Modflow to assess hydrogelogical conditions and for reliable assessment of the groundwater resources for future development in Rajshahi City Corporation, Bangladesh. The model scenarios showed that the declining trend of groundwater level in dry season in the vicinity of Padma happen due to lowering of peak river water level and substantial use of groundwater.

Vandecasteele (2010) studied a catchment in Northern Ethiopia during the rainy season in 2006. They developed a groundwater flow model for the catchment with a perched water table. The soil water budget was calculated for the period 1995-2006. The lumped groundwater model used in the study was developed by **Tomer et al. (2010)** and was based on a combination of groundwater budget and water table fluctuation technique. The simulated results obtained from both the models were quite encouraging and helped to take adequate water management measures in the study area.

Lei (2011) studied the seepage field along the centre line of an airport runway. Four different engineering conditions by excavating ditches were presented and simulated for the effect of floodwater on the groundwater seepage field on the runway. **Yugen (2011)** forecasted the water inflow impact in a bauxite mine in China. The forecast was used as a precautionary study to prevent water-in rush accident in the mine. **Saghravani (2011)** predicted the transport of phosphorus around a landfill in Malaysia for 10 years. **Da (2011)** built a model to simulate the pit dewatering process for a river delta region. The model result was suggested as a credible design reference for the construction of the dewatering scheme. **Byragi Reddy and Mekonen Aregai (2011)** summarized the significant environmental and socioeconomic changes took place in middle highlands of Tigray, Ethiopia. The study focused on evaluating the relationship of land cover dynamics and changes in water resource potentials in areas around Laelay-Koraro. Results indicate that the conversion of land cover types contributed to a number of observable challenges expressed in terms of high rates of land degradation influenced by factors such as an expansion of cultivated land, built up area and poor land management practices. The land cover dynamics assessed using remote sensing and the farmers view on trends of change support the overall changes overtime.

Xi-lian (2012) used the software to study the changes in groundwater flow field after the construction of a factory in Qufucity, China. Lead contamination was simulated for two different conditions created by the construction work. **Haque (2012)** modelled the recharge fluctuation rates of a groundwater source in Bangladesh. Also, they showed

the reasons for groundwater shortage during dry seasons using modelling. **Ismail (2012)** simulated the performance of a horizontal well to understand the optimum pumping rate that would safely achieve the desired drawdown in an area surrounding the horizontal collector well. Horizontal well hydraulic properties were assumed and a transient groundwater flow model was developed. Also, a steady-state model was built to predict the capture zone characterization. **Wang (2013)** used Visual MODFLOW as an Environmental Impact Assessment (EIA) tool. They ascertained the impact of soil and water conservation in weakening the surface run-off and strengthening the underground run-off using modelling.

Beltran (2013) used Visual MODFLOW with ArcGIS and Surfer to simulate the sub-surface water flow in and around a solid waste dumpsite in Mexico and modelled the migration path lines of contaminants.

De Condappa et al (2012) applied SWAT and a groundwater model to assess the impact of Agriculture Water Management (AWM) in the Jaldhaka watershed, a tributary of Brahmaputra River, located in India, Bhutan and Bangladesh.

Haque et al (2012) applied MODFLOW for the reliable assessment of the groundwater resource for future development in Rajshahi City Corporation area in Bangladesh. The results revealed that the recharge in the aquifer system occurs through rainfall and return flow. The area faces shortage of water in the dry seasons especially in the vicinity of river Padma due to substantial use of groundwater and lowering of river water level resulting in declination of groundwater level. Based on the study, it was suggested that conjunctive use of Padma River water should be promoted.

Youssef et al (2012) applied MODFLOW for planning and managing the groundwater problems and for predicting the change in the groundwater system of the El-Moghra Aquifer in Wadi El-Farigh (Egypt). The study area is considered as a water scarce region with low rainfall, high evaporation, long dry summers and short warm winters. The aim of this study was to forecast the impact of the groundwater irrigation expansion projects on the sustainability of the aquifers. The results of the simulation process reveal that the implementation of the current development policy have serious impacts on the aquifer storage.

Baier et al (2013) attempted to use mathematical Modeling for simulating groundwater and heat flow in complex hydrogeological structures (presence of fault zones) of the Benesov-Usti aquifer system in the Czech Republic. MODFLOW **HUF** package along

with MT3DMS was used for this study. The study revealed that the conventional approach of using MODFLOW with **BCF** and **LPF** packages to simulate heat flow failed due to simplified discretization of the model domain. Hence, the model was discretized into 21 vertical layers in order to represent the complex and detailed hydrogeology of the region using HUF package of MODFLOW. According to model results, the areas with higher temperatures were more influenced by upward flow of heated groundwater than by higher natural heat flow from bedrock. **Ehsan Shirkhani et al (2013)** performed quantitative simulation of Mahidasht plain water table in Kermanshah province of Iran using Visual MODFLOW. Simulated and observed levels showed a reasonably good match. However, the water budget indicated that there is a loss of aquifer water, which may lead to lowered groundwater table, increased water scarcity in the region as well as cause additional problems of water salinity. The study concluded with the suggestions to improve surface water availability in the region through construction of new canal network, thus reducing the dependability of the farmers on groundwater for agriculture and other needs.

Zhai (2014) assessed the drainage of a limestone aquifer. The study was carried out in a mining area. The model result precisely identified the poor drainage condition in the eighth mining area and suggested remedial measures. **Aigler & Ge (2013)** developed a model to evaluate the groundwater- withdrawal potential of the Fraser River watershed, a mountainous drainage system in north-central Colorado, USA. Modeling results suggested that the surface recharge is the major source of groundwater in the watershed which could sustain current and future withdrawals, given that the current recharge condition is maintained. **Li et al (2013)** formulated a model for the convenience of groundwater management in Tianjin city. Groundwater levels were simulated by using the groundwater numerical model, which are taken as the blue line and red line to control the groundwater level exploitation by comparing the real-time monitoring groundwater levels with the control water levels. **Albhaisi (2013)** made an attempt to understand the impact of land use/land cover in the upper Berg catchment, Western Cape, South Africa. The catchment has undergone many changes in recent years, not least of all the construction of a dam on the upper reach. To reduce water loss due to evapotranspiration, non-native hill slope vegetation upstream of the Berg River Dam was cut down. It was hypothesised that recharge has been increased due to this change in vegetation. Multi-temporal Landsat images from 1984, 1992, 2002, and 2008 were used to predict the impact land use changes on groundwater recharge. For the simulation of groundwater recharge the distributed hydrological model WetSpa was

used. Forest plantations lost 72% (18.8 km2) of their areal extent between 1984 and 2008, due to deforestation as part of a plan to implement the ecological Reserve as required by national water policy; the area of barren land increased by 15.7 km2 in the same period. The high increase in precipitation, especially in the period of 2005–2009, combined with the change in land use in the study area resulted in a highly increased (278%) groundwater recharge. Simulated groundwater recharge shows strong spatial differences for each evaluated year. The effect of the rapid clearing of non-native hill slope vegetation upstream of the Berg River Dam for the land use scenario of 2008 was tested to check if clearing is an important factor in the increase of groundwater recharge. A systematic increase of about 8% per year for the 21-year period, due to the change in land use from the different years to that of 2008, is predicted, which confirms that the clearing of the non-native hill slope vegetation is of considerable importance for the increase in groundwater recharge.

Zare et al (2014) using MODFLOW predicted the extent of waterlogging in Miandaraband plain of Iran over a period of 10 years (from the start of the network operation). Due to the construction of the network of irrigation/drainage canals of the Gavoshan dam, the region experienced raised groundwater table and suffered from the problem of waterlogging, as the groundwater extraction in the region was low. The effect of the operation of the irrigation network on the groundwater table in the region was simulated after 1, 5 and 10 years. The results indicated that the water table in the area experienced a rise of 5.2 meters in 10 years. The study reported that, the waterlogging will be extended up to 56.28% in ten years, (according to the model prediction after 1 year 6.59% and after 5 years 37.5%). Rostamian et al (2014) used SWAT to model runoff and sediments in Beheshtabad and Vanak watersheds in the northern Karun catchment in central Iran. Also, Sequential Uncertainty Fitting (SUFI2) interface within SWAT-CUP (Calibration and uncertainty Programs) package was used for calibration and uncertainty analysis of the model. Both basins were mostly agricultural, where majority of the area was rainfed. The study concluded that the model is successful in assessing different land management options and also helpful for the selection of a suitable management policy.

Qadir (2016) studied the groundwater sustainability for agricultural activities near the Indus Riverin Pakistan. Water table depth maps and groundwater budget calculations were interpreted. The condition for the simulation was taken by considering the before and after scenarios of a river canal construction. The model results forecasted the continued drawdowns for the entire period of simulation (35 years).

Persson (2016) modelled the transport of perfluorooctanesulfonic acid (PFOS) in groundwater at the old fire drill site of Bromma Stockholm airport in Sweden. They found that it would take approximately 570 years for the PFOS to be carried by groundwater from the site to the airport area.

Baharuddin (2016) simulated the sub-drains' performance to investigate a water seepage problem at a Botanic park in Kuala Lumpur, Malaysia. The simulation was carried out for transient conditions and successfully determined the cause of water seepage issue in the area.

Nabil (2016) modelled the effluents from a steel industry that pollute the Meboudja River in

Algeria. Groundwater flow and mass transport model were simulated using Visual MODFLOW. **Lee (2016)** simulated the impacts of seasonal pumping on stream depletion. Visual MODFLOW was used to quantify stream aquifer interactions caused by the seasonal pumping of groundwater. Stream Depletion Factor (SDF) was found to be the reason for the seasonal variation of the stream depletion rate.

Park (2016) undertook a feasibility study to determine the minimum embedded depth of vertical barrier to prevent possible contaminant leakage from an off-shore landfill. The study was successful.

Vijay (2016) used modelling to assess the safe yield of groundwater withdrawal and quantified the future demand of water supply for the city of Puri, India, which is being subjected to constant sea water intrusion and continuous freshwater withdrawal due to pumping. **Steiakakis (2016)** studied the drought-induced impacts using Visual MODLFLOW. They investigated the combined effects of groundwater exploitation and climate variability on karst aquifers. Saline water intrusion was simulated using the SEAWAT package of the software. Suggestion to adjust the scheme of groundwater exploitation was recommended to prevent seawater intrusion.

2.2 National Scenario

Narasimha Reddy et al. (1994) estimated the regional groundwater budget in the Dullapally watershed, a hard rock area, using water-balance models and validated with numerical flow models in a transient state.

National Institute of Hydrology, Roorkee, India (1997) carried out groundwater modeling in Ghataprabha sub-basin of Krishna River basin using MODFLOW. They calibrated and validated the model for both study state and transient state. Results

indicated, that the wells are getting dried up in some parts of the command area whereas in some parts there are problems of water logging.

Thangarajan et al (1999) developed a multi-layer groundwater model for the Thamalakane River valley which is located in Okavango Delta, Botswana where three major aquifers are separated by two aquitards in the valley portion. The top two aquifers are freshwater bearing zones and the bottom one is saline. The hydrological set-up of the basin is complex, as the groundwater flow directions are opposite in the upper- unconfined and in the lower-confined aquifers. The hydrodynamic behaviour was then studied under two prediction scenarios to evolve appropriate management decisions for locating the well field (large diameter wells) in the upper aquifer by making use of induced river infiltration during the flood season. It revealed from the aquifer response that upper-unconfined aquifer system could sustain the pumping rate of 6000 m^3/day from the shallow production large diameter wells.

Mahesh Kumar (2004) developed a steady-state groundwater flow for Northeast Musi Basin using the finite difference method and MODFLOW package by assuming 8–10% of annual recharge.

Tiwary (2005) modelled the migration of hexavalent chromium from chromite deposits of the Sukinda valley in Odisha, India. The path lines of migration of Cr6+ were simulated for 20 years. **Bin (2005)** applied well boundaries package of the software to simulate 23 faults (rocks) of compressoshear and water-resisting types on the path of groundwater flow to study the effect of faults on the flow.

Sarada (2006) developed a steady-state groundwater flow model of the upper Musi basin using a MODFLOW package. The groundwater draft (output) was estimated to be approximately 177.5 mcm; the river leakage was estimated to be 120 mcm; and the outflow to be 0.4 mcm.

The entire Musi basin is simulated by **Massuel et al. (2007)**. In this study, the authors found the mean annual simulated recharge to be 1,176 mcm (17% of total rainfall), whereas the annual pumping was estimated to be 1,235 mcm. In the present study, a transient-state groundwater flow model has been developed for the catchments of the Osmansagar and Himayatsagar reservoirs by using 21% recharge from the total rainfall. Purandara et al (2004) studied the Mass balance calculations for Na, K, Ca, Mg, Cl, SO 4 and HCO 3 for the study area showed that the major source of contamination is through non-point sources. It is also observed that the river water quality during the non-monsoon season (February, 2000) almost resembles with the groundwater quality

of the adjoining aquifer. However, during post-monsoon period (October, 1999) a wide variation was found between groundwater and surface water quality which can be attributed to the movement of fertilizers and agricultural ashes with monsoon flows reaching the stream along with overland flow. The major source of contamination in the Malaprabha river was found to be due to the non-point sources (more than 90%). An immediate attention from the concerned authorities is required in order to protect the land from further salinization.

Rejhani (2008) simulated a 2-D groundwater flow to study the overexploitation of groundwater and to analyse the aquifer response to various pumping strategies in the Balasore coastal basin, India.

Five pumping scenarios were used for the simulation. **Mondal (2009)** developed a mass transport model for the migration of tannery effluent contaminants around a tannery industrial belt. It was reported that the migration phenomenon was affected mainly by advection rather than dispersion. The contaminant transport emanated from the tannery belt and moved towards eastern side of a river downstream.

Mondal et al. (2011) estimated the average groundwater at various sections of the paper. For example, the recharge in a hard rock area in southern India is approximately 80–250 mm=year, which is equivalent to 12–37% of the annual rainfall. The total groundwater abstraction is approximately 80.43% of the annual groundwater recharge. In the study area, the Environmental Protection Training and Research Institute (EPTRI) and the National Geophysical Research Institute (NGRI) has found that the total input and output for the catchments of the Osmansagar and Himayatsagar reservoirs are 33.69, 36.99 mcm and 83.62, 82.68 mm, respectively, under 8–10% of recharge conditions. Gurunadharao et al. (2008) found the groundwater draft in the catchments of the Osmansagar and Himayatsagar reservoirs to be 35 and 77 mcm, respectively.

A groundwater flow model developed by **Ahmed & Umar (2009),** simulated the behavior of the flow system and evaluated the water balance of Yamuna-Krishni interfluves, India for effective groundwater management. Sarvarian (2010) used Visual MODFLOW to identify capture zones for wells in Urmia plain, Iran. MODPATH package of the software was used for this work. Also, they determined the influence of injection wells of wastewater on capture zones of pumping wells.

Rajamanickam et al (2010) applied Visual MODFLOW to simulate groundwater and solute transport in the Amravathi river basin in Karur district, Tamil Nadu (India). The

objective of the study was to understand the impact of industrial effluents (textile bleaching and dyeing units) on groundwater quality. The study revealed that 14600 kilo liters of partially treated effluent was discharged daily into the river. This has adverse effects on the water quality, aquatic life and agricultural output in the region. Further, the flow and transport model was run from 1994 to 2009 under 5 different scenarios. These scenarios represented the different stress conditions that can be subjected to the system, like increased or reduced effluent discharge, introduction of zero liquid discharge (ZLD) scheme and construction of artificial recharge structures. The model results showed reduced TDS values in the case of ZLD and artificial recharge structures. The study suggested to introduce new strategies for reduction of chemical wastes (such as ZLD) in the region and also supported the construction of percolation tanks, check dams etc. to increase groundwater recharge. **Saravanan (2011)** modelled groundwater flow for textile effluent affected areas in Tirupur basin, India and demarcated the groundwater protection zones. These modelled zones were ranked and their need for keeping them pollution-free was stressed. **Purandara et al (2010)** The application of SWIM has been demonstrated for different land use in parts of WG of North Kanara district of Karnataka, India. The advantage of the model is that it can be used both for laboratory and field studies to simulate the soil water and solute transport and can also be used for understanding the impact of different land use management hydrologic regime of the area. In this study, simulations using the SWIM has been substantiated by the field experiments to understand the runoff generation dynamics under different land– use conditions. Following are some of the important conclusions drawn from the study 1. The impact of afforestation showed a considerable increase in infiltration and hydraulic conductivity and also generates infiltration excess overland flow at higher rainfall intensities. The results obtained through SWIM model indicated that there is marked differences in recharge percentages as the land cover changes (i.e., converting the land from degraded has been brought under Acacia plantation in the present case). This higher groundwater recharge may contribute to the dry season flows in the streams. 3. The current study clearly indicated that selective reforestation/afforestation with specific species may lead to improve the surface hydraulic properties and encourage greater percolation and conversely, inhibits the occurrence infiltration excess overland flow.

Kumar et al (2011) attempted to develop a model, to evaluate the existing trend and availability of groundwater in time and space and its movement for proper planning of groundwater utilization in Nadia district, West Bengal. The groundwater flow pattern

indicated that the occurrence of base flow which feed both the Rivers Bhagirathi and Jalangi throughout the year. It can be inferred from the optimization that the all existing deep Borewells should be run with reduced unit draft of 556.5 m3/day while all existing shallow Borewells should be pumped unit draft of 41 m3/day.

Mondal et al (2011) applied Visual MODFLOW to develop steady state and transient simulation model for a tannery belt near Dindigul town, Tamil Nadu (India). The aim of the study was to determine the groundwater velocity and to assess aquifer response under different input stresses. The model was conceptualized as single layered having varying thickness. A total of 96 wells were assigned as pumping wells throughout the area. Other boundary conditions included river, groundwater recharge and evapotranspiration. The model was run and calibrated in three stages viz. steady state, transient and prognostic model under transient state. The steady state calibration was done for April 2001 whereas the transient model was calibrated from April 2001 to February 2009. Further, the model was used for prediction of water levels for the next 6 years i.e. from March 2009 to December 2015. The predictive simulation was carried out in three schemes by first keeping the initial abstraction rate of 2009, then increasing the rate by 10 % in the second scheme and finally increasing the rate by 20% of the initial value. A scenario of artificial recharge was also assumed, where the recharge was increased. The corresponding results showed that the water level in the region kept declining in the first three schemes. However, the water level showed a rise in the case of artificial recharge. Through this study, the authors found that the groundwater velocity is more sensitive to recharge from rainfall, hydraulic conductivity and specific yield. The study concluded with the suggestion of augmenting the groundwater resources with artificial recharge methods, with the construction of tanks and check dams in the uplands to increase the groundwater recharge. **Varalakshmi (2011)** modelled the groundwater flow for a hard rock aquifer to determine the average input, output and the withdrawal levels of water in the aquifer system. **Rao (2011)** assessed the groundwater contamination around a dumpsite near TCCL at Ranipet, India. Migration of TDS and chromium plumes in the groundwater were simulated for 30 years.

Paramesswari (2012) used Visual MODFLOW to prepare a pictorial representation of the geohydrological profile of their study area to represent the layers of soil in the study area.

Rajamanickam (2013) modelled the groundwater around the Amaravathi river basin of Karur District, Tamil Nadu to study the effect of discharging partially treated

effluents from textile bleaching and dyeing units. Total Dissolved Solids (TDS) migration was simulated for 15 years under five different scenarios. Kant (2013) modelled the groundwater levels in the Sonar sub-basin in Madhya Pradesh. The aquifers situated in the alluvial plains of Madhya Pradesh were modelled to find the fluctuations in water levels.

Needhidasan (2013) highlights the usage of Visual MODFLOW and GIS techniques for groundwater assessment studies as a part of conservation of groundwater resources. The research was carried out in Thirukkazhukundram Taluk of Kanchipuram District in Tamilnadu, India. Visual MODFLOW was used for simulation of water levels in the observation wells. The model was calibrated using data from 2010 and 2011. The model results showed satisfactory correlation with the observed data after calibration. He concluded that GIS could be used very effectively for studies along with Visual MODFLOW which may give satisfactory simulation results. He also emphasized that the success of the model depends largely on the availability of more distributed data.

Krishnaswamy et al (2013) carried out investigations on the hydrologic effects of forest use and reforestation of degraded lands in the humid tropics and reported its implications for local and regional hydrologic services. However, such issues have been relatively less studied when compared to the impacts of forest conversion. In particular, the ‘‘infiltration-evapotranspiration trade-off’’ hypothesis which predicts a net gain or loss to baseflow and dry-season flow under both, forest degradation or reforestation. In this context, few observations were made in parts of Western Ghats region of Karnataka to understand the hydrologic responses and groundwater recharge and hydrologic services linked with three ecosystems, i.e. (i) remnant tropical evergreen forest (NF), (ii) heavily-used former evergreen forest which now has been converted to tree savanna, known as degraded forest (DF), and (3) exotic Acacia plantations (AC, Acacia auriculiformis) on degraded former forest land. Instrumented catchments ranging from 7 to 23 ha representing these three land-covers (3 NF, 4 AC and 4 DF, in total 11 basins), were established and maintained between 2003 and 2005 at three sites in two geomorphological zones, Coastal and Up-Ghat (Malnaad). Four larger (1–2 km2) catchments downstream of the head-water catchments in the Malnaad with varying proportions of different land-cover and providing irrigation water for areca-nut and paddy rice were also measured for post-monsoon baseflow. The study concluded that the groundwater recharge is the most temporally stable under natural forest, although substantial recharge occurs under all three ecosystems, which helps to sustain dry-season flow downstream in higher order streams that sustain local communities and

agro-ecosystems. In addition to spatial scale effects, greater attention also needs to be given to the role of hydrogeology within the context of the above hypothesis and its implications for hydrologic services.

Vikrant Vishal et al (2014) applied MODFLOW to simulate groundwater recharge in the semi-arid region of Delhi territory in India. The NCT of Delhi is an area with political state boundaries, and no real aquifer boundaries. The boundary conditions in the model were assigned as river boundaries along the Yamuna River, Western Yamuna canal and Najafgadh drain. The study area was divided into nine zones for the estimation of groundwater recharge. The results exhibited high variation in the recharge, which the researchers concluded, would seem to reflect the diversity in the geology of the study area as well as the ongoing urbanization which influenced the overall recharge in the region. Kumar (2014) developed a groundwater flow model to quantify groundwater in Choutuppal Mandal, Andhra Pradesh. The water budget estimate was also made.

Mirudhula (2014) applied Visual MODFLOW to develop a groundwater flow model for the Lower Bhavani basin of Tamil nadu. Ground water recharge was estimated using the VISUAL MODFLOW and the amount of recharge from the lined and unlined canals was estimated by using ZONEBUDGET package. The results of the model indicated that the seepage from the lined canals was 20% lesser than that from unlined canals. Based on the results, it was concluded that the main length of the canal should be lined while the minor distributaries may be left unlined. This will help to reduce the seepage and conveyance losses from the main canal and ensure adequate water supply for agricultural purposes.

Pradeep Kumar (2014) developed a MODFLOW model to quantify groundwater in Choutuppal Mandal, Nalgonda district in Andhra Pradesh (India). The study area consists of mostly agricultural lands, where, cotton, paddy, red gram and castor are the important crops grown. The MODFLOW model was developed as a two layered weathered and fractured model having total thickness of 40 meters. Constant head, groundwater recharge and pumping wells were the boundary conditions assigned to the model. A total of 19 wells were taken into consideration. A steady state simulation was performed in MODFLOW and was calibrated using observed water levels of September 2013. The simulated water levels were found to closely match the observed water levels with correlation co-efficient of 0.993.

Varalakshmi et al. (2014) used MODFLOW to model groundwater in the catchments of Osmansagar and Himayatsagar. Conceptualization of model was carried out using Visual MODFLOW as an interface. They reported groundwater decline by 45 m by the end of 2020 if current rate of withdrawal is continued. Surinaidu et al. (2012) studied the impact of climate change on the agriculture water requirement of the upper Bhima basin in southern India. Groundwater is the major source of irrigation in the region. Visual MODFLOW was used to simulate the groundwater by different climate change scenarios. They reported groundwater decline by 6m over 30 yrs of simulation. To maintain groundwater level with in safe limit, they suggested to reduce current pumping rate by 5-10 %.

Parameswari (2015) analysed the leachate migration from a dump yard at Perungudi, Chennai, India. The groundwater flow model was calibrated for transient conditions and chloride migration was simulated for 12 years. The model results were helpful to assess the contaminant's influence on the water supply wells located downstream of the landfill. **Surinaidu (2015)** applied Visual MODFLOW to study groundwater seepage issues in subsurface tunnels. They created a three dimensional finite difference model with the help of inferences made from hydro-geo-morphological features and geological lineaments to investigate the groundwater seepages and then suggested solutions

Nagraj et al. (2017) carried out groundwater modeling studies Hiranyakeshi watershed of Ghataprabha sub-basin of hard rock region. A 3-D groundwater flow model, viz. Visual MODFLOW was used for the study with two conceptual layers. The first layer is a weathered zone which is about 20-30m from the top, followed by a second laye rof fractured zone which is about 30-40m from the first. The model was simulated for a period of seven years (2008-2014), under transient case. The results from the modeling shows that for the next 10 years the water table is believed to decrease more than 50m in the study area. To overcome this critical stage, the present draft should be reduced by nearly 50%.

Chapter 3

Study Area

3.1 General

Malaprabha River originates in the Western Ghats at an altitude of 792 meters at Kanakumbi village, Khanapur taluka, Belagavi District, Karnataka state. Malaprabha sub-basin lies between latitude 15° 28' 27.75" N to 16° 5' 43.62" N and longitude 74° 12' 34.5" E to 75° 17' 8.59" E. The catchment area of the sub basin is 2902 km^2. The study area covers parts of Belagavi, Khanapur, Bailahongal, Savadatti and Ramadurga Taluks of Belagavi district. It flows North-East and North-West and joins the river Krishna at Kudalasangam in the Bagalkot district of Karnataka. The Bennihalla and the Hirehalla are the principal tributaries of the river Malaprabha. To harness the water of the Malaprabha river, a dam is constructed at Naviluteerth village, Savadatti taluk of Belagavi District to impound 1377 MCM (37.7 TMC) of water. The location of the Malaprabha sub basin is shown in Figure 3.1

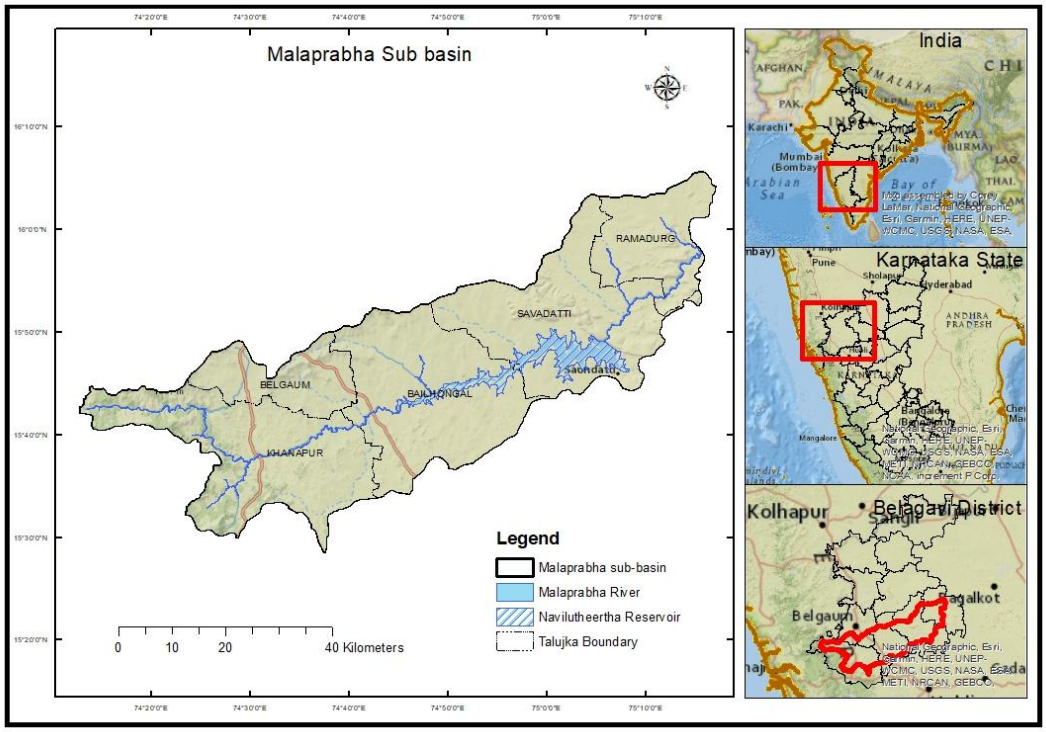

Figure 3-1 Location Map of the Study Area

3.2 Demographics:

The study area covers 398 villages in Belagavi, Bailahongal, Savadatti and Ramadurga taluks of Belagavi District of Karnataka state with a total population of 9, 62,351. The main occupation for lively hood is agriculture about 70% of the region is under agriculture practice. The income of the farmers is mainly depending on the Commercial Crops like Sugar Cane, Tobacco, Cabbage and Cauliflower. The villages covered in the Malaprabha sub basin are shown in Figure 3.2

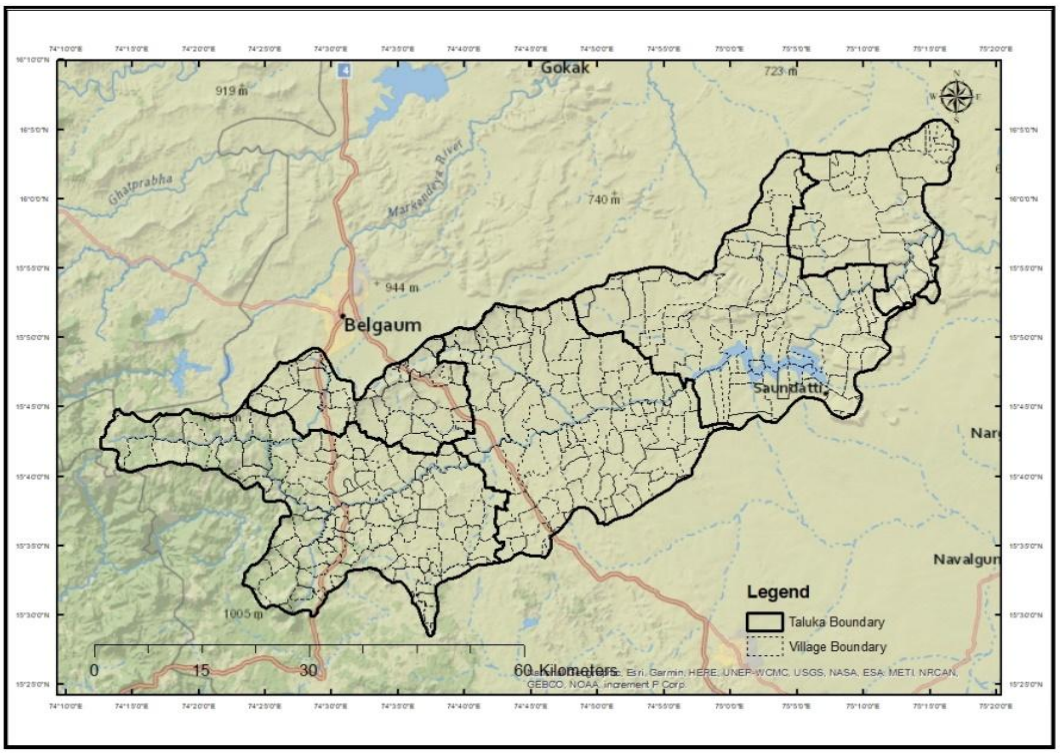

Figure 3-2 Map showing the Villages covered under study area.

3.3 Climate

The majority of the catchment area falls under Semi-arid climatic conditions. There is a distinct climatic pattern defining three different climatic seasons. They are summer season, Rainy season and winter season.

Table 3-1 Weather data of Khanapur station (WRDO, Bengaluru)

Year	Average of Temp (min)	Average of Temp (max)	Average of Humidity (%)	Average of Wind Speed (m/sec)	Average of Vapour Pressure (mb)	Average of Evaporation (mm)/day
1980	21.32	30.87	86.20	1.95	21.69	3.87
1981	19.10	31.59	83.97	1.86	20.59	7.24
1982	18.53	32.80	85.82	1.68	22.23	3.69
1983	17.89	31.99	84.24	1.73	20.82	3.89
1984	18.75	32.29	84.59	1.80	21.13	3.79
1985	18.46	31.82	84.05	1.55	20.98	4.09
1986	18.83	32.05	84.35	1.62	21.24	4.15
1987	18.89	32.40	84.46	1.32	21.07	3.57
1988	18.51	32.18	86.81	1.29	22.37	3.81
1989	18.31	31.89	109.33	1.45	21.32	3.46
1990	18.46	31.80	88.06	1.56	21.56	3.76
1991	18.49	32.13	85.86	1.46	22.84	3.58
1992	17.93	31.71	87.27	1.32	22.26	4.08
1993	18.37	31.48	88.39	1.19	22.40	4.10

3.3.1 Summer season

The summer season prevails between March to June months. The average temperature varies between 36^0 and 39^0C during the season. The Northern part of the area experience hot climatic conditions, whereas the temperature are milder on the upper part of the catchment (i.e.,Western part)(28^0-29^0C). The monthly average temperature from the year 1901 to 2001 is calculated shown in the Table 3.2 and plotted in Figure-3.3

Table 3-2 Monthly average Temperatures

Month	Jan	Feb	Mar	Apr	May	Jun	Jul	Aug	Sep	Oct	Nov	Dec
Temparature in ^{o} C	16.65	17.62	20.45	22.78	23.56	22.50	21.85	21.88	21.44	21.18	19.12	17.26

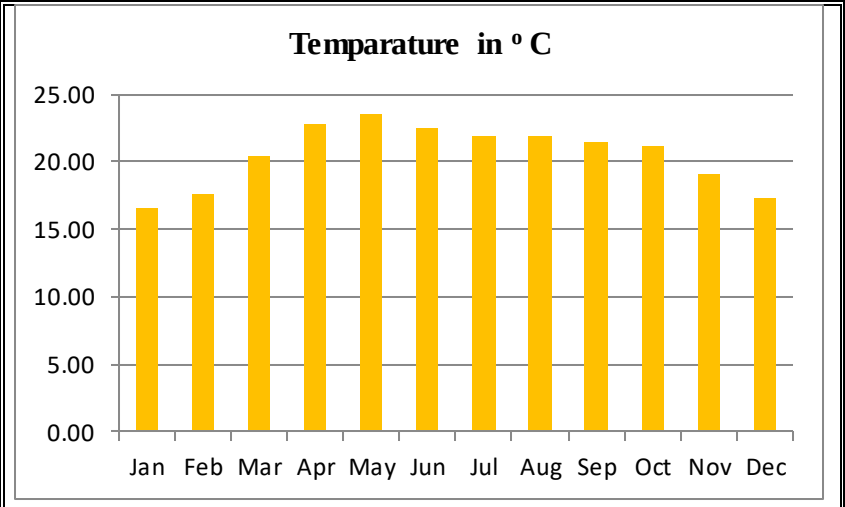

Figure 3-3 Monthly Average temperature

3.3.2 Rainfall Pattern

More than 90% of rainfall is received during southwest monsoon (June to September) and the rest from October to December. Spatial distribution of rainfall shows large variations all over the basin. The rainfall received in the upper catchment (4D7C9-Watershed) is significantly higher compared to the lower catchment (4D7C8 Watershed). In the upper catchment the annual average rainfall is 1776 mm (highest average rainfall of 5216 mm is recorded from Kankumbi station) and lowest is observed at Kadasagatti (478.28 mm). The average rainfall of Malaprabha sub basin is 1219 mm. The rainfall showed declining trend towards eastern and north eastern side. Numerous seasonal springs are observed during Monsoon season in Upper catchment. The spatial distribution of rainfall is shown in Figure 3.4

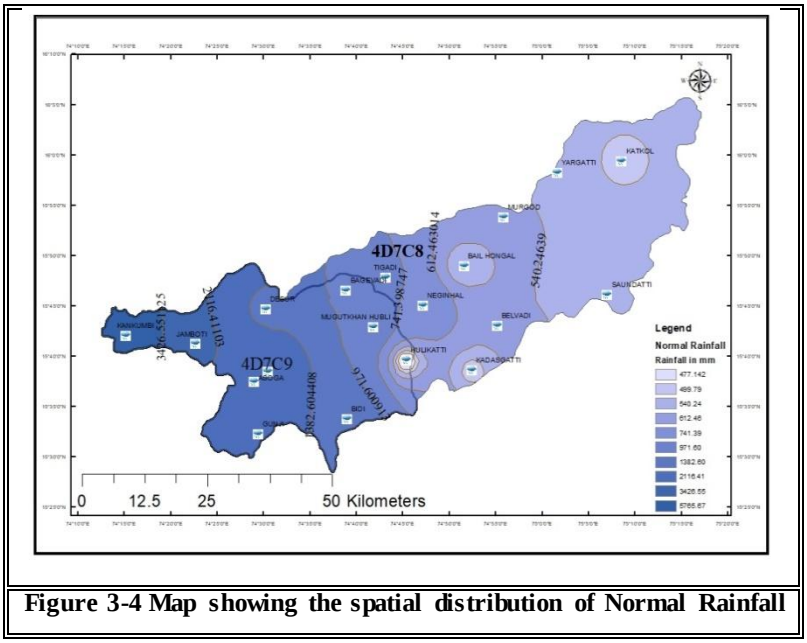

Figure 3-4 Map showing the spatial distribution of Normal Rainfall

3.3.3 Winter Season

The winter cold starts after the recession of rainfall i.e. from October to February. Temperature recorded in the western region is relatively low and varies from 8^0 to 14^0C. However, it shows increasing trend towards eastern side which ranges between 25^0 C and 32^0C. (As per the data available with the Water Resources Department, Karnataka).

3.3.4 Evaporation

Daily, Monthly and Annual temperature, relative humidity, atmospheric pressure and wind velocity are shown in the Table 3.1 . It influences transpiration from plants and loss of water from reservoirs, water conveyance systems and loss of moisture in the upper layer of soil.

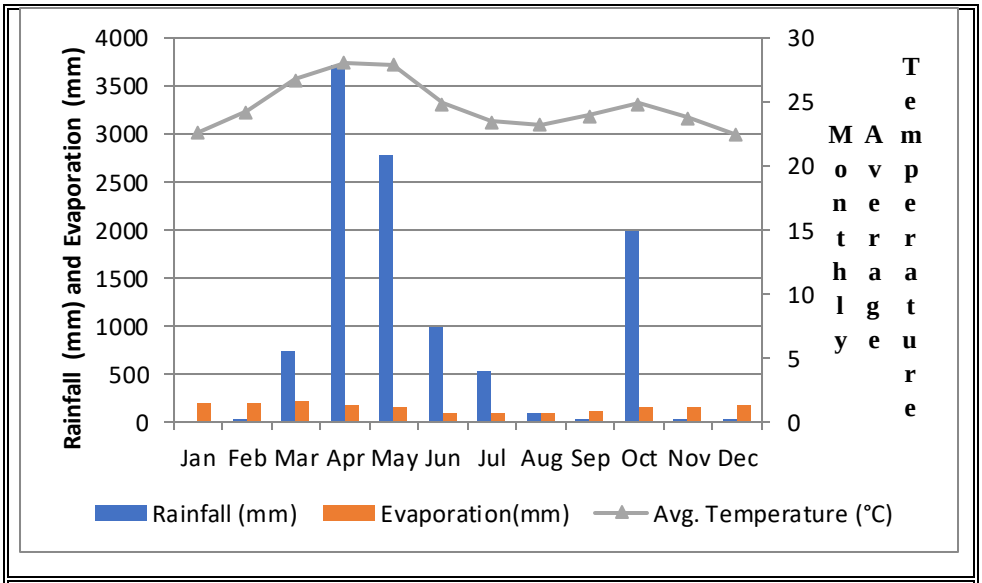

Figure 3-5 Plot of rainfall, Average Tempeature, Evaporation

3.4 Geomorphology of the area

Figure 3.6 shows the digital Elevation map of the study area. The relief of the basin varies between 953m and 475m from the mean sea level.

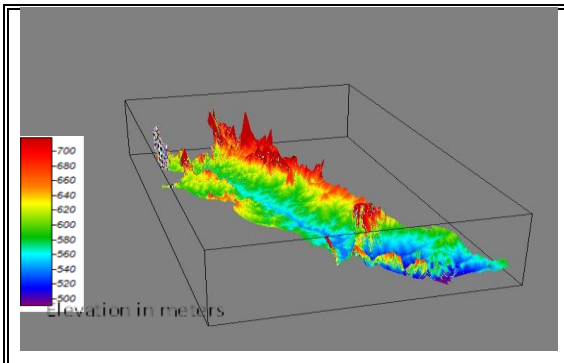

Figure 3-6 Digital Elevation model of the basin

The study area follows closely spaced contours on the water divides with convex-concave slope, and the broadly spaced contours in the valley bottom specify gentle and flat valley bottoms. Thus, the basin is divisible into three distinct morphological zones. These are,

i. Convex hill summit (more than 900m)
ii. Concave and gentle mid-crest (800 - 900 m) and
iii. Flat valley bottom (less than 800 m)

This change in morphological character from hill crest to valley bottom of the basin is largely responsible in the change in behavior of water flow between the hill-slope and foot slope. In the entire catchment, the area lying above 800 m contours exhibit convexo-concave hill-slope which has fully erosional environment. This is the zone of maximum overland flow and minimum infiltration. However, 86.5% of the total basin which includes gentle and flat slope zones lie below 800 which has a depositional environment with maximum recharge capacity and comprises of colluvium materials. The extent of the individual geomorphic units are shown in Figure 3.7.

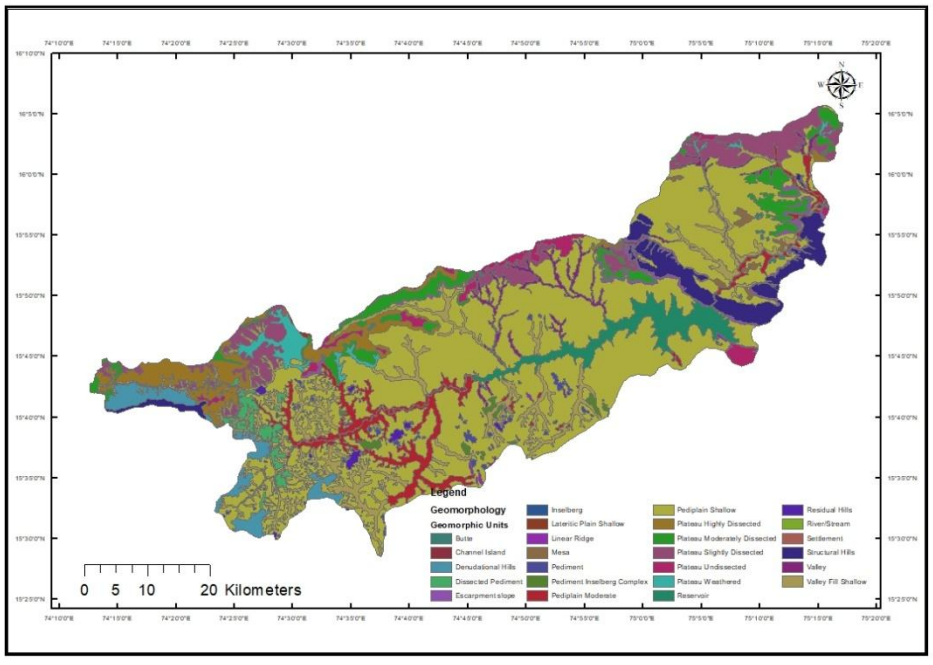

Figure 3-7 Map showing spatial distribution of Geomorphic units

The Geomorphic units play an important role in controlling the infiltration rate. Hilly portions show very low to zero Infiltration rates whereas pediplains will have considerable infiltration rates. The percentage distribution is shown in Table-3.3 (Source:KSRSAC).

Table 3-3 Percentage spread of the individual geomorphic units

Geomorphic unit	**Area (Ha)**	**% of the area**
Hills	21704	7.5
Lateritic Plain	119	0.06
Pediment	5330	1.84
Pediment Inselberg Complex	1479	0.51
Pediplain	188358	64.9
Plateau	61372	21.15
Reservoir	10250	3.53
River/Stream	1479	0.51
Grand	290223	100

3.5 Drainage Characteristics of the Basin

The drainage pattern observed in the study area (Figure 3.8) is of dendritic with typical representation of hard rocks (basalts, granites, gneisses etc.). The total numbers of water bodies (Tanks, Lakes, Reservoir) present in the area are 538 which are spread over an extent of 13,576 hectares.

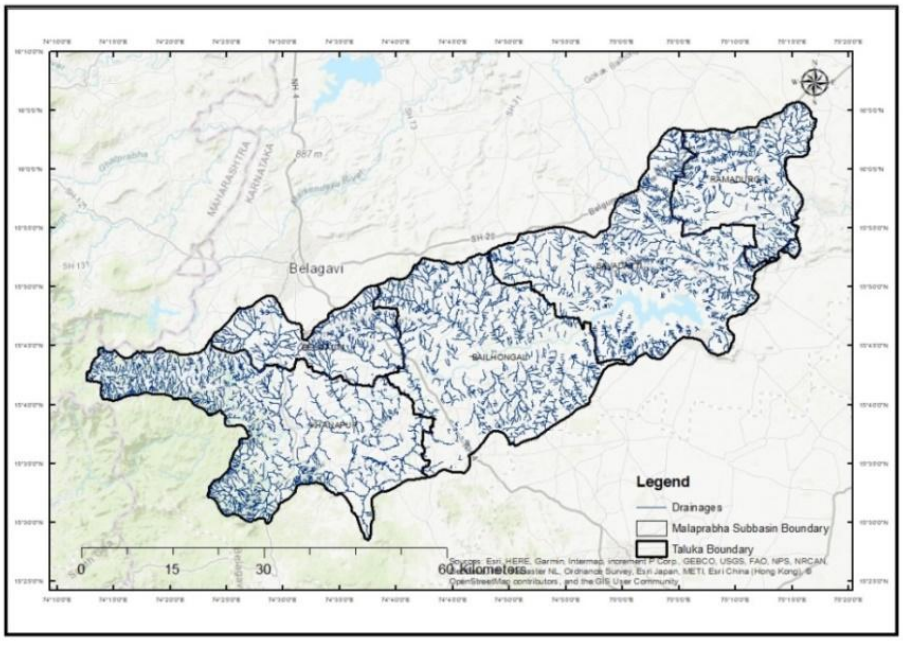

Figure 3-8 Map showing the Drainage network and Tanks of Malaprabha Catchment

Morphometric characteristics of the sub-basin is shown in Table 3.4. The highest order of stream observed in the Malaprabha river is of 5th order having a length of 75 km.

Table 3-4 Morphometry of the Malaprabha catchment

S.No	Morphometry	Length in Kilometers
1	Total No of First Order streams	2392.00
2	Total length of First Order streams	1808.58
3	Total No of Second Order streams	701.00
4	Total length of Second Order streams	551.63
5	Total No of Third Order streams	113.00
6	Total length of Third Order streams	98.96
7	Total No of Fourth Order streams	27.00
8	Total length of Fourth Order streams	21.29
9	Total No of Fifth Order streams	1.00
10	Total length of Fifth Order streams	75.00

3.6 Land use Land cover of the area

Land use pattern of the basin is very complex which comprises of forest, agriculture, shrubs and barren land. The major portion of the area is covered under agriculture (70%) and forest (10%). The spatial distribution of the Land use is as shown in Figure-3.9 and the Geographical extents of the Land use are shown in Table-3.5

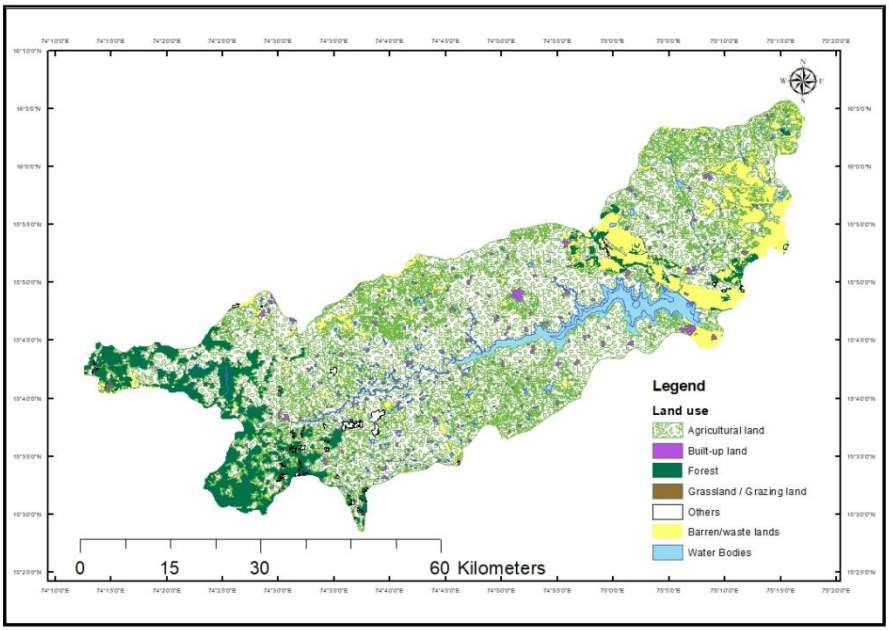

Figure 3-9 Land use Land Cover pattern of Malaprabha Catchment

Percentage distribution of land use land cover shows that the forest cover is only 9.58% which is fully restricted to headwater catchment. Agriculture in the Malaprabha catchment is very significant (more than 70%) which clearly indicates the quantity of water use required for the agriculture growth. This may be one of the major causes of groundwater depletion and reduction in surface water flow during non-monsoon months.

Table 3-5 Geographical extent of Land use/ Cover in the Malaprabha catchment

Land Use/ Land cover group	**Area Covered in (Ha)**	**% Of the area**
Agricultural land	216496.03	74.60
Built-up land	4640.09	1.60
Forest	27802.15	9.58
Grassland / Grazing land	99.12	0.03
Others	1773.20	0.61
Wastelands	26094.53	8.99
Water Bodies	13320.78	4.59
Total Area in Hectares	290225.90	100

3.7 Soils

The spatial distribution of soils is shown in the Figure-3.10. The classification of soils is based on the United States Department of Agriculture (USDA) soil taxonomy.

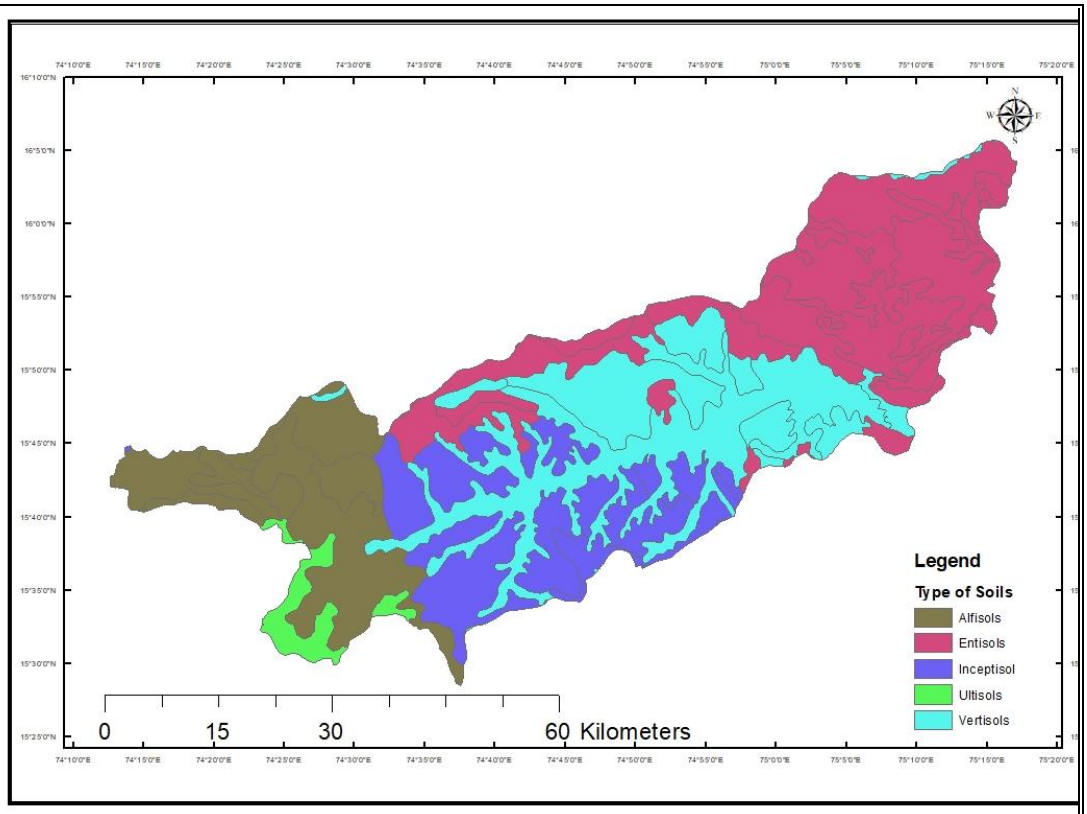

Figure 3-10 Spatial distribution of soil types in the Malaprabha Catchment

There are four major soil types in the study area. Entisols are the most dominating ones spread over the hilly portions of the catchment and in the downstream part of the catchment. This is followed by vertisols, inceptisols and alfisols. The percentage distribution of individual soil types is shown in Table 3.6

Table 3-6 The geographical Extent of Soil Types

S.No	Order of the soil	Area (Ha)	% Of the area
1	Alfisols	52065	17.94
2	Entisols	94658	32.62
3	Inceptisol	53502	18.43
4	Ultisols	7975	2.75
5	Vertisols	82025	28.26
Total area			290225

3.7.1 Alfisols:

Seventeen percentage of the study area is covered by alfisols these are enriched with aluminum and iron. Clay is the most dominating constituent of the soil horizon with relatively higher fertility status. This part of the catchment showed higher recharge capacity due to both soil characteristics and presence of thick layer of leaf litter in thick forest area. It is also observed during the investigation that the zone below 'A' horizon of soil is less permeable and leads to inter flow conditions in the region.

3.7.2 Entisols

Entisols are generally restricted to 'A' horizon of the soil profile and is highly weathered and unconsolidated in nature (quartzite and Dolomites). About 32% of the region is covered by entisols, particularly in the downstream of the study area. This type of soil exhibit higher recharge due to coarse grained soils and high porosity of the rock material.

3.7.3 Inceptisols:

Fine grained in nature and devoid of iron Oxide, aluminum oxide and organic matter. It is observed that the porosity of the soils is higher due to finer grain size however the permeability is found to be quite minimum. Further it is also noticed that the organic matter content is lower, there by hindering the recharge potential of the area. In the study area, spread over the meta greywackes which covers about 18 % of the study area in Bailahongal taluk.

3.7.4 Ultisols

Ultisols occupy about 2.75% of the study area. Which are derived basically from the Laterites and mainly found in the western part of the Khanapur Taluka. The texture of the soil showed fine grains in 'B' horizon of the soil profile. Therefore, the percolated water appears as base flow during the dry season.

3.7.5 Vertisols

A type of clayey soil with little organic matter which occurs in regions having distinct wet and dry seasons. This type of soil covers about 28.26% and are spread all along the Malaprabha River banks.

3.8 Geology and Hydrogeology of the area:

The catchment of Malaprabha consists of igneous rocks of plutonic origin and basaltic rocks of volcanic origin, Dolomite and Sandstone of sedimentary origin and greywacke and meta greywackes of metamorphic origin. Lateritic capping of Recent origin are

found in the higher elevations. The stratigraphic sequence observed in the area is shown in the Table-3.7

Table 3-7 Stratigraphic sequence observed in the area

Stratigraphy	Rock_group	LithologicUnit	Rock_type
Palaeocene to recent	Residual capping	Laterite	Residual cappings
Upper proterozoic	Consolidated sediments	Conglomerate, arenite and shale	Badami
		Argillite, quarzite and conglomerate	Bagalkot
		Dolomite bhq and chert-breccia	
		Dolomite,limestone,argillite	
		Sand stone conglomerate	Bhima
Archaean to lower proterozoic	Metamorphic rocks	Greywacke / argillite	Chitradurga
		Lower -meta greywacke	
		Lower -meta greywacke	
		Quartzite / quartz-sericite schist	
Archaean	Plutonic rocks	Pink & grey granite	Closepet granite

Geologically, about 32.87% (95401 Ha) of the study area is occupied by greywackes mainly in parts of Khanapur and Bailahongal taluka. Rock formation are of metamorphic origin trending NNW to NW with dipping angle 55^0 to 70^0 having low intensity of weathering and devoid of secondary structures at the deeper levels (*Source: Geological Survey of India published quadrangle maps*). Figure 3.11 shows the geographical distribution of rock formation in the study area. From the Figure it is evident that the occurrence of groundwater is quite limited in the central part of sub basin which is presumed to be due to the presence of argillites and black soils. It is also noticed that, more than thirty percent of the area consists of sandstones, conglomerates

and dolomitic limestones of sedimentary origin. These are horizontally bedded, trending NE to SW and are observed in the Eastern portion of the sub basin mainly found in parts of Savadatti and Ramadurga talukas.

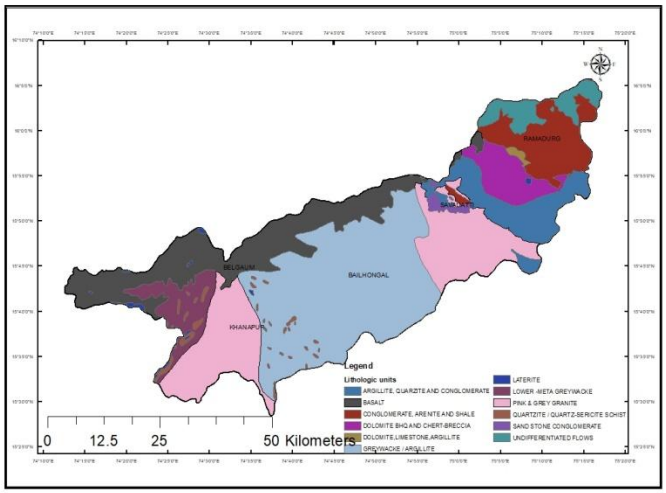

Figure 3-11 Lithological units of Malaprabha Catchment

Pink and grey granites covers 19.84% of the area in Khanapur and Savadatti taluks which are of plutonic origin and the weathering is observed up to 30-40 m below which they are massive. Basalts are the volcanic flows present in the Northern portion of the sub basin overlain by granites, meta greywackes and quartzite. These are layered flows and they consist of red bole beds as inter trappeans. Table 3.8 indicates the distribution of rock types in percentage,

Table 3-8 Geographic extent of Geomorphological units of the catchment

Lithologic units	Area of lithologic units (Ha)	% of area
Greywacke / argillite	95401	32.87
Pink & grey granite	57589	19.84
Basalt	49149	16.93
Conglomerate, arenite and shale	23215	8
Argillite, quarzite and conglomerate	21931	7.56
Lower -meta greywacke	13415	4.62
Dolomite bhq and chert-breccia	13276	4.57
Undifferentiated flows	9743	3.36
Quartzite / quartz-sericite schist	2815	0.97
Sand stone conglomerate	1850	0.64
Laterite	1041	0.36
Dolomite,limestone,argillite	804	0.28

Grand	290229	100

3.8.1 Granites

The pink granites and gneisses of Archaean age are distributed in parts of Khanapur and Savadatti talukas. The ground water occurrence in this area is restricted to phreatic zone. which extend up to 30m and in most of the region water is abstracted through dug wells. In the case of bore wells, there is a large variation in the yield of the wells which is attributed to change in weathering status, fracture density and joint structures. The previous studies indicate that the NE-SW lineaments are the most potential zones for ground water occurrence followed by E-W, NNE-SSE lineaments.

3.8.2 The Meta Greywackes:

Meta greywackes are found in parts of Khanapur, Bailahongal and Belagavi taluks. These rocks cover major portion of the sub basin. The weathered zone in these rocks are extended up to 45-50 m beyond this depth the meta greywackes are massive. Hence shallow borewells drilled upto 45 to 50 meters were observed.

3.8.3 The sedimentary provinces (Quartzites/Dolomites/Conglomerates)

Consolidated sedimentary rocks occur in Kaladgi formation mainly represented by quartzite, sandstone, shale and limestone which are seen in the North Eastern part of the study area (Ramdurga and Savadatti taluka). The primary porosity of these formations has been lost due to the process of consolidation and compaction. Limestone formation are the low yielding aquifers as they are horizontally bedded and devoid of solution activity except along the contact zones, however areas covered with cavernous limestones are found to be good aquifers. Sandstones of Ramdurga and Savadatti taluka are poor aquifers as they occur at higher altitudes forming ridges.

3.8.4 Deccan traps

North and north western part of the sub basin is covered by basalts. The vesicles and amygdaloidal structures present in the basalts act as porous media. Generally, these porous media are filled with the secondary materials like -quartz, zeolites and clays. Zeolitic traps with amygdaloidal and vesicular properties facilitate the occurrence and movement of ground water. Further, traps have shallow dip that facilitates the movement of the ground water through contact zone of the flows. The intratrapean red bole beds act as an aquiclude. The weathered zone occurs up to a depth of 20 m bgl and semi confined conditions occur below 20 to 40 m in the Deccan trap. The jointed and fractured Deccan traps carry the ground water to deeper depths. Depth of bore wells drilled in traps ranges from 40 to 175m. The Deccan trap shows a gradual thinning of

layers towards east and in such area it is noticed that the ground water yield is very low. The specific capacity of the wells in Deccan traps ranges from 0.05 to 341/min/m draw down. The yield of bore wells ranges from 40 to 1440 m^3/day. The transmissivity of the traps ranges from 1 to 369 m^2/day.

3.8.5 Laterites

Laterites derived from the traps are found in the western part of the sub-basin. These are highly porous and permeable in nature and acts as high recharge zones. The aquifer drains out naturally as subsurface out flow in the post monsoon period. The dug wells, tapping these aquifers located on sloping ground gets dried up during summer months even if the ground water extraction in the area is low. The distribution of hydrogeological units are shown in Figure 3.12

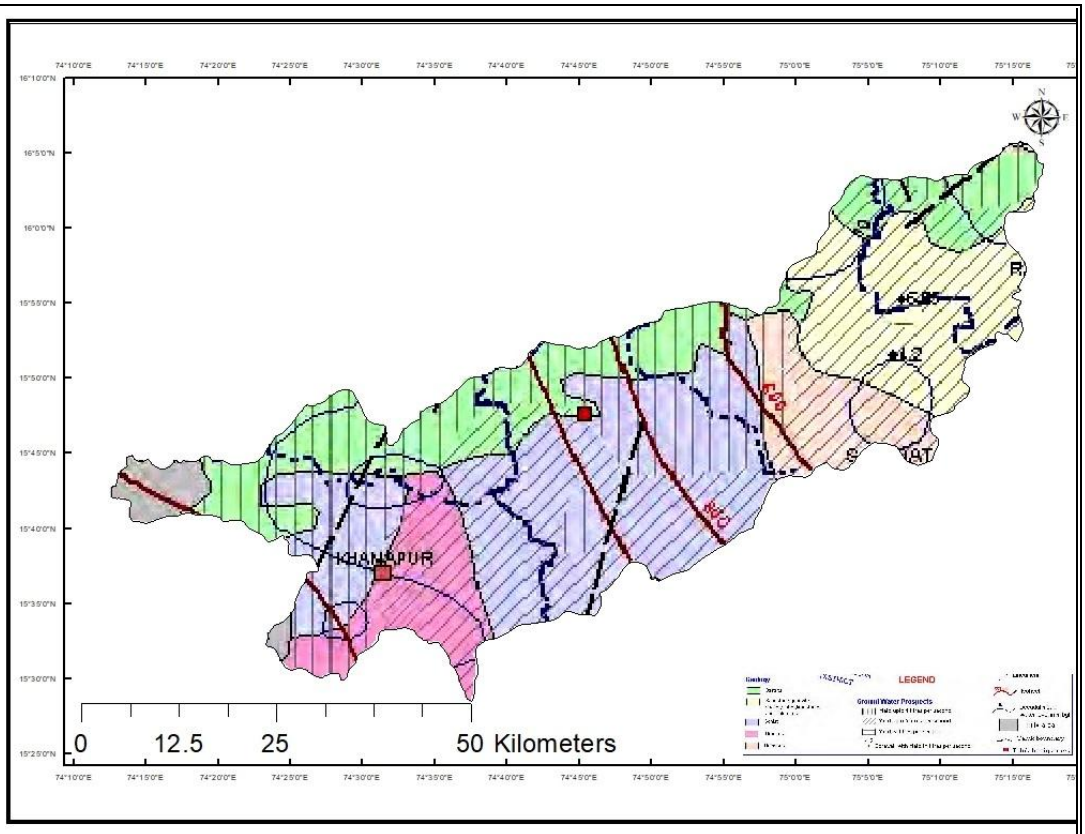

Figure 3-12 Hydrogeological Map.

The Malaprabha sub basin is having 11 types of lithological units and which are distributed widely from West of the basin to the East. The higher elevations of the basins are covered by Laterite capping over un differentiated basaltic flows in the Northern portion and Quartzite formations in North Eastern portion at Navilutheertha dam site. Though there is maximum rainfall received in the upper catchment because

of higher slopes much of the water goes as run off. The infiltered water in the upper catchment are utilised for the kaolinization process leading to the formation of clay. These clay patches act as aquicludes hence the occurrence of the groundwater in the upper catchment is restricted to unconfined zone.

The mid of the basin is covered by Meta-Greywackes and the terrain is almost flat, the vertical lineations and foliations are observed in this type of formation. The weathering thickness is extended up to 35 to 40 meters so shallow borewells are noticed in this area.

The northern portion of the sub basin is covered by Deccan trap basalts which are acting as surface water divide in the northern portion of the basin. The flows are terminated aburuptly and are over laid on Meta Greywackes, Quartzites, Dolomites, limestones. They are flat mounted hills and the groundwater development is meagre in this formation.

The quartzites occurring in the area are horizontally bedded trending NW-SE are mainly found nearer to the dam site. At the dam site the Quartzite beds are dipping towards the down stream (Figures 3.13 & 3.14) hence there is more chance of seepage from the horizontal bedding planes.

Few patches of Dolomitic Limestones and Limestones are found along the Eastern side of the basin are compact and massive. The occurrence of cavernous in limestone is rare phenomena hence low yielding wells are observed in the Ramdurga taluka .

Figure 3-13 Quartzite exposure are dam site dipping towards down stream

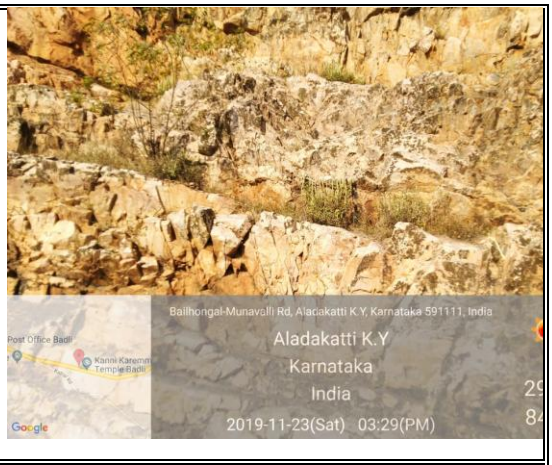

Figure 3-14 Quartzites trending NW-SE dipping horizontally

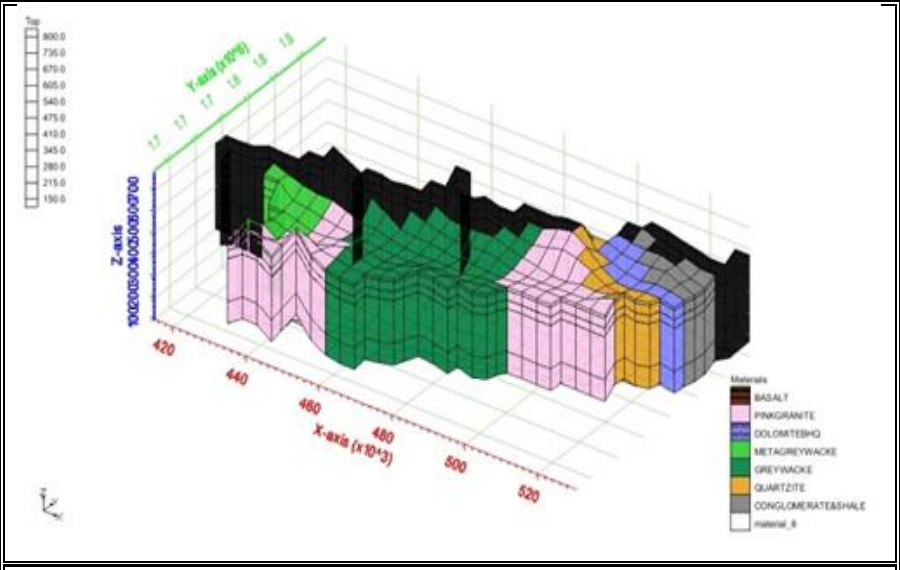

Figure 3-15 Lithology distribution in Malaprabha sub basin

Chapter 4

Methodology

4.1 Hydrological and Hydrogeological Investigation

Hydrological and hydrogeological analysis are the basic input for the modelling of groundwater systems in any given terrain conditions. Therefore, the present study combines both collection of secondary data and field observations and detailed experimental studies for the parameterization of various conditions involved in regional flow modelling. Some of the important analyses are the following:

1. Rainfall trend analysis by Mann Kendall test and Sen's slope method.
2. Morphometric analysis
3. Groundwater level monitoring and data analysis
4. Determination of hydraulic properties such as infiltration, saturated hydraulic conductivity and soil characteristics
5. Geophysical investigations and aquifer characterization
6. Estimation of Aquifer parameters using pumping test data analysis

4.2 Rainfall Analysis

4.2.1 Trend Analysis

The changes in rainfall trend can have a significant effect on the watershed conditions and groundwater availability. Hence, for the Watershed considered the Rainfall trend analysis is carried out to check the changes in the long-term rainfall. If there is significant change then it is quantified by the statistical tests performed.

There are several statistical methods available to evaluate trends in time series data. These include Wilcoxon rank sum test (also known as the Mann-Whitney U test), Sen 's test, and the Seasonal Kendall test. Mann-Kendall test for trend and Sen's slope estimates are statistical tests developed for detecting and estimating trends in the time series data.

Mann-Kendall test:

The Mann-Kendall Test, is a simple test for trend. Mann-Kendall is a non-parametric test and as such, it is not dependent upon the magnitude of data, assumptions of distribution, missing data or irregularly spaced monitoring periods. Mann-Kendall

assesses whether a time-ordered data set exhibits an increasing or decreasing trend, within a predetermined level of significance. The Mann Kendall test computes Kendall's tau nonparametric correlation coefficient and its test of significance for any pair of X, Y data.

Sen's nonparametric estimator of slope: To estimate the true slope of an existing trend (as change per year) the Sen's nonparametric method is used.

4.3 Mann-Kendall test and Sen's slope estimate

In this study two stages of statistical analysis are carried out jointly. First the presence of a monotonic increasing or decreasing trend is tested with the nonparametric Mann-Kendall test and secondly the slope of a linear trend is estimated with the nonparametric Sen's method (Gilbert).

Mann first suggested using the test for significance of Kendall's τ where the X variable is time as a test for trend. This was directly analogous to regression, where the test for significance of the correlation coefficient r is also the significance test for a simple linear regression. The Mann-Kendall test can be stated most generally as a test for whether Y values tend to increase or decrease with T (monotonic change).

H0: Prob [Yj > Yi] = 0.5, where time Tj > Ti. Null Hypothesis – No Trend

H1: Prob [Yj > Yi] ≠ 0.5 (2-sided test). Alternate Hypothesis – increasing or decreasing trend

The Mann-Kendall Test and Sen's slope estimate has been done for all the 19 rain gauges considered in and around the catchment and attributed into GIS platform for spatial analysis. The results of the Test for 5% significance level are as furnished in Table 5.3 and 5.4.

4.4 Geomorphology:

The variation in elevation profile has significant influence on the Hydrology of any catchment. With the advent of technology the elevation data is captured from the satellites like ASTER, CARTOSAT P5, and the Shuttle Radar Topography Mission (SRTM). The products of these satellites stored in the form of a raster grid known as a Digital Elevation Model (DEM). The DEM pixel values indicate the height of the pixel above the defined vertical datum. Although the DEM itself describes just the elevation of the land surface, it can be used to derive many interesting and useful data products. These derivatives are used in hydrological, visibility, ecology and morphological analyses. The present study includes the collection, analysis, evaluation, and interpretation of geographic information on the

natural and manmade features of the terrain, combined with other relevant factors, to predict the effect of the terrain on regional hydrology. The morphometric parameters were estimated based on the following methods (Table4.1).

4.5 Morphometric Analysis

Drainage morphology analysis is essential to any hydrological study. Hence, the determination of stream networks behaviour and their interrelation with each other is of great importance in many water resources studies.

Digital Elevation Map was extracted from CARTOSAT image by using SAGA(System for Automatic Geographic Analysis, a freely downloadable GIS software) system. GIS tools for drainage analysis has been employed to evaluate several drainage parameters. The morphometric analysis of the sub-watersheds in the upstream region revealed a predominantly dendritic drainage pattern which is formed by interlinking of the streams. The drainage density map obtained from the SAGA is compared with the Topo sheet map. The SAGA extracted map was devoid of majority of the first order streams particularly in downstream areas of the sub-basin. This could be attributed to change in land use/land cover changes where the area is encroached by agriculture crops. Table 4.1 shows the various methods involved in the estimation of morphometric parameters.

Table 4-1 Methods involved in Morphometric Analysis

Parameters	Formulae	References
Stream Order(U)	The smallest permanent streams are called “first order”. Two first order streams join to form a larger, second order stream; two second order streams join to form a third order, and so on. Smaller streams entering a higher-ordered stream do not change its order number.	Strahler (1964)
Stream Length (Lu)	The average length of streams of each of the different orders in a drainage basin tends closely to approximate a direct geometric ratio.	Horton (1945)
Stream Length Ratio (RL)	RL =(Lu/Lu)-1	Sreedevi et al
Bifurcation Ratio (Rb)	Rb =(Nu/Nu)+1	Horton (1932)

Areal Aspects		
Drainage density	Dd = Lu/A	Horton (1945) (Dd)
Drainage texture T	T = Dd x Fs	Smith (1950)
Stream Frequency (Fs)	Fs = ΣNu/A	Horton (1945)
Elongation ratio (Re)	$\mathrm{Re} = \frac{D}{L} = 1.12\sqrt{\frac{A}{L}}$	Schumm (1956)
Form factor (Ff)	$Ff=A/L^2$	Horton (1945)
Relief Aspects		
Relief R	R = H – h	Hadley and Schumm (1961)
Relief Ratio Rr	Rr = R/L	Schumm (1963)
Slope	Sb = H – h/L'	Mesa (2006)
Gradient Ratio	Gr =H – h/ L	Sreedevi et al (2005)

Accordingly, the above parameters were estimated in the GIS environment. GIS based maps were prepared to exhibit the morphological parameters of hydrological importance such as Slope, L S Factor, Aspect, Topographic Wetness Index, Convergence Index, Drainage Density etc.

4.6 Infiltration and Saturated Hydraulic Conductivity of Soil

4.6.1 Infiltration

Infiltration, the process of water entry through the soil surface, plays an important role in the soil water cycle as it controls how much, and at what rate water will enter into the soil. In turn, this can affect soil water storage, crop yield, irrigation efficiency and solute entry into the soil profile. The two main factors affecting infiltration are hydraulic conductivity and infiltration rate. Hydraulic conductivity refers to the ease of water movement through soil, both horizontally and vertically, and it decreases with a decrease in pore size and water content. Infiltration rate, the speed at which water enters the soil, is related to the soil's infiltration capacity; meaning its ability to absorb water. If water is applied at a rate less than the soil's infiltration capacity, all the water will move through the soil and the infiltration rate will be equal to the rate of delivery. Soil acts as a sponge to take up and retain water. Movement of water into soil is called *infiltration*, and the downward movement of water within the soil is called *percolation*, *permeability* or *hydraulic conductivity*. Pore space in soil is the conduit that allows water to infiltrate and percolate. It also serves as the storage compartment for water.

4.6.2 Determination of Infiltration and Hydraulic conductivity using Disc Permeameter

The disc permeameter is a field instrument used for measuring water infiltration into the soil, which is characterized by insitu saturated and unsaturated soil hydraulic properties. It is mainly used to provide estimates of the hydraulic conductivity of the soil near saturation.

Conventional techniques for measuring in-situ infiltration include the use of a single or double ring infiltrometer. Single and double ring infiltrometer only measures flow under ponded (saturated) conditions, and when used in soil with distinct macropores, preferential flow will dominate the flow. This does not reflect infiltration under rainfall or sprinkler irrigation. Therefore, many authors attempted to create a negative potential (tension) on the water flow. This is to exclude macropores in the flow process, hence only measuring the soil matrix flow. The disc permeameter was designed by Perroux and White (1988) from CSIRO. Figure 4.1 and 4.2 shows the experimental set up of doube ring infiltrometer and disc permeameter. The double ring infiltrometer was used for estimating field determined infiltration parameter under different land use land

covers, so that errors in the recharge estimate may be reduced. Further, disc permeameter was also used for the estimation of hydraulic conductivity and to understand the preferential flow paths occurring in the study area.

Figure 4-1Double ring infiltrometer

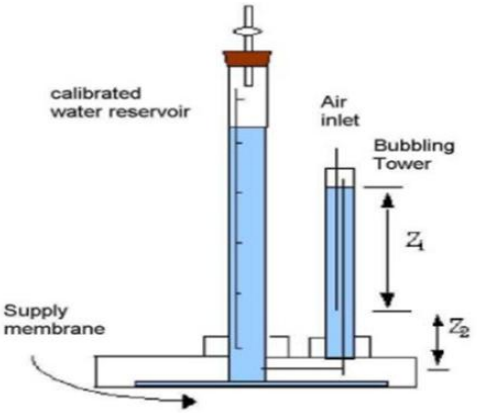

Figure 4-2 Disc Permeameter

4.6.2.1 Double Ring Infiltrometers :

Double ring infiltrometers are usually metal rings with 30 cm diameter with a height of 60 cm in length. The metal tube is so driven into the ground that it protrudes about 10 cm above the soil. Water is poured into this ring to a depth of 25-50 cm depending upon the presence of vegetation and humus on the soil surface. A constant water depth is maintained by adding measured volume of water. The volume of water added is noted at each interval of time and the average infiltration rate for the time interval can be computed. Usually, it takes about two to three hours for the infiltration rate to become constant.

4.6.2.2 Disc Permeameter

The disc Permeameter has become a popular apparatus for measuring in situ sorptivity (S), and hydraulic conductivity, (K), of the soil at some prescribed potential. Measurements of sorptivity (S), and hydraulic conductivity (K), are important for predicting how water will enter, redistribute within, and drain from soils. Methods that can rapidly and accurately measure S and K are valuable. The disc Permeameter (Per roux and White 1988) is a relatively new method that has gained popularity because of its simplicity, the speed at which measurements can be made, and because it does not greatly disturb the soil surface being measured (White and Sully 1987; White and Perroux 1987 and 1989; Smettem and Clothier 1989; Ankeny et al 1991). Different methods have been devised for calculating S and K are compared using same set of

data. These methods are all based on the approximate, but usefully accurate, solution of flow from a disc source found by Wooding (1968). This linearized solution uses a hydraulic conductivity (K) function of the exponential form (Gardner 1958):

$$K = Ks\, e^{\varphi/\lambda c} \qquad \textbf{(Eq 4.1)}$$

Where Ks is the saturated hydraulic conductivity (m s-1), λc is the macroscopic capillary length scale (m) and φ is the matric potential (m).

4.6.2.3 Principles of Operation

When a source of water, such as a wet circular disc or shallow pond, is placed on the soil

Surface, the initial stages of flow into the soil are dominated by the soil's capillary properties. As time progresses, both the size and geometry of the water source and the force of gravity influence the water flow rate. For uniform soils a time is eventually reached where the flow rate from the source becomes steady. This steady state flow rate is governed by capillarity, gravity, the size of the disc and the pressure at which water is supplied to the soil surface.

In this technique we make use of both the initial and steady-state flow rates to separate the capillarity and gravity contributions to soil water flow. In addition, by selecting the water supply pressure we can dictate the sizes of pore sequences or fissures which participate in the flow process.

4.6.3 Hydraulic conductivity and Sorptivity

The method for determining soil hydraulic properties from disc Permeameter measurements in the field is based on an analysis of the three-dimensional flow from a shallow circular pond or surface disc.

For a pond or disc of radius r_0, on a homogeneous soil , Wooding showed that when

water is supplied at a potential of ψ_0 the steady state volumetric flow rate q is

$$q = \pi r_0^2 (K_0 - K_n) + 4 r_0 \psi \qquad \textbf{(Eq. 4.2)}$$

The first term on the right essentially represents the contribution of gravity to the total flow from the surface disc and the second term contains the contribution due to capillarity. In the gravity term K_0 is the hydraulic conductivity at the supply potential

Ψ_0, and K_n is the hydraulic conductivity at the initial soil water potential Ψ_n. For relatively dry materials K_n is much smaller than K_0 and we can safely ignore its effect. The capillarity term contains the matric flux potential, which is related to the conductivity by

$$\psi = K_0\lambda_c$$

The macroscopic capillary length (λc), is related to the sorptivity, S_0, and the hydraulic conductivity (White and Sully, 1987),

$$\lambda c = bSo^2/(\Theta o - \Theta n) \qquad \textbf{(Eq. 4.3)}$$

is the initial moisture content at Θn is the moisture content at ψ_n, Θo is the moisture content at the supply potential, Θ_0, So is the sorptivity at Θ_n with supply potential ψ_0 and `b' is a dimensionless constant whose value lies between 1/2 and $\pi/4$. For field soils a good mean value for b is 0.55. With simplification and, dividing by the area of the disc, we find the steady-state flow rate per unit area

$$\boldsymbol{q = Ko + \frac{4bS2}{\theta s - \theta r}} \quad \textbf{(Eq. 4.4)}$$

Rearranging (Eq.4.4) to find the conductivity, we have

$$\boldsymbol{Ko = q - \frac{4bS2}{\theta s - \theta r}} \qquad \textbf{(Eq 4.5)}$$

During the early stages of flow from the disc, capillarity dominates flows irrespective of the disc. At short infiltration times the system behaves as if it were one-dimensional. In this case the cumulative infiltration is given by (Philip, 1969). Where Q is the total volume of water infiltrated and t is time from the commencement of infiltration. Sorptivity then is the Slope of the cumulative infiltration vs. $t^{1/2}$ plot to calculate the hydraulic conductivity from (4), the measurements required are the sorptivity, the steady state flow rate, the initial volumetric moisture content at the supply potential.

4.6.4 Guelph Permeameter

The instrument was used to characterize the saturated hydraulic conductivity of the soil at various depths in a borehole of depth up to 1.2 m. This data is helped to understand the hydrologic processes occurring along the soil profile and how much it contributes to shallow aquifer recharge. Though this is not a direct method for the estimation, the parameters are useful to characterize the soils regionally and in parameterization of SWAT model.

The Guelph Permeameter method (Reynolds et al. 1985) measure the steady state liquid recharge Q, necessary to maintain a constant depth of liquid (H), in an uncased cylindrical well of radius `a' finished above the water table. Constant head

level in the well hole is established and maintained by regulating the level of the bottom of the air tube which is located in the centre of the Permeameter. As the water level in the reservoir falls a vacuum is created in the air space above water. When the Permeameter is operating, equilibrium is established.

When a constant well height of water is established in a cored hole in a soil, a bulb of saturated soil with specific dimension is rather quickly established as shown in above figure. The bulb is very stable and its shape depends on the type of soil, the radius of the well and the head of water in the well. The shape of the bulb is numerically described by the C factor used in the calculations. Once the bulb shape is established, the outflow of water from the well reaches a steady state flow rate which can be measured. The rate of this constant outflow of water, together with the diameter of the well and height of water in the well can be used to determine the field saturated hydraulic conductivity of the soil.

The Richard analysis of steady state discharge from a cylindrical well in unsaturated soil, as measured by the Guelph Permeameter technique accounts for all the forces that contribute to three dimensional flow of water into soils, the hydraulic push of water into soil, the gravitational pull of liquid out through bottom of the well and the capillary pull o water out of the well into the surrounding soil. The Richard analysis is the basis for the calculation of field saturated hydraulic conductivity. The C factor is a numerically derived shape factor which is dependent on the well radius `a' and head `H' of water in the well.

Figure 4-3 Guelph Permeameter

4.7 Estimation of Groundwater recharge by Empirical Methods:

Rainfall is the most important source of ground water recharge in the country. The most commonly used methods for estimation of natural ground water recharge in India include empirical methods, ground water level fluctuation method and the ground water balance method. Based on the studies undertaken by different scientists and organizations regarding correlation of ground water level fluctuation and rainfall, some empirical relationships have been developed for computation of natural recharge to ground water from rainfall. Some of these empirical relationships for different hydrogeological situations in India are discussed as below and results are placed in table 5.9.

a) Chaturvedhi formula (1936):

Chaturvedhi derived a following empirical equation to calculate groundwater recharge.

$$Rg = 2(P - 15)^{0.4} \quad \textbf{(Eq 4.6)}$$

Where,

Rg- Groundwater recharge

P is the annual precipitation in Inches.

b) UP Irrigation Research Institute Formula(UPRI):

In 1954 UP Irrigation Research Institute modified equation as.

$$Rg = 1.35(P - 14)^{0.5} \quad \textbf{(Eq 4.7)}$$

Where, P is the annual precipitation in inches.

c) Bhattacharjee Formula (1954):

Bhattacharjee has proposed the following empirical formulae to calculate to groundwater recharge

$$Rg = 3.47(P - 38)^{0.4} \quad \textbf{(Eq 4.8)}$$

Where, P is the annual precipitation in centimeters.

d) Krishna Rao Formula (1970)

Krishna Rao developed the following empirical relation to calculate groundwater recharge based on climatic conditions.

$$R_g = K\,(P\text{-}X) \quad \textbf{(Eq 4.9)}$$

Where,

K is constant

P is the annual precipitation in milli meters. X is number of point rainfall.

The following formulae is applied to different climatic conditions of Karnataka

Rr = 0.20 (P-400) – for areas with annual rainfall between 400 and 600mm

Rr = 0.25 (P-400) – for areas with annual rainfall between 600 and 1000mm

Rr = 0.35 (P-600) – for areas with annual rainfall above 2000mm

e) Sehgal Formula (1973)

Sehgal has developed the following empirical relation to calculate groundwater recharge.

$$R_g = 2.5\ (P\text{-}16)^{0.5}$$ **(Eq 4.10)**

Where, P is the annual precipitation in inches.

f) Kumar and Seethapathi (2002)

The Kumar and Seethapathi developed empirical formula to determine the ground water recharge.

$$R_g = 0.63\ (P\text{-}15.28)^{0.76}$$ **(Eq 4.11)**

Where, P is the annual precipitation in inches.

Above discussed empirical methods to calculate Groundwater recharge are compared and placed in table 5.9 at section 5.7.

4.8 Estimation of Ground water Availability using Groundwater Estimation Committee Norms.

The basic objective of estimation of groundwater availability is to know the hydrogeological characteristics such as lithology, groundwater level fluctuations and distribution of groundwater, groundwater use etc. Detailed household survey to know the groundwater usage and also input from local farmers were collected and the specific data used to calculate the groundwater balance which is essential for the primary assessment of the groundwater occurrence in different parts of the catchment.

The dynamic groundwater resources of Malaprabha river basin was computed based on Groundwater Estimation Methodology 2015. The Malaprabha sub basin comprises of two watersheds 4D7C9 AND 4D7C8 .The dynamic Groundwater resources are estimated for these two watersheds.

As the study area comprises of hard rock areas, the specific yield was estimated by applying the water level fluctuation method for the dry season data, and then used the specific yield value in the water level fluctuation method for the monsoon season to get recharge.

4.8.1 Estimation of Ground Water Draft

Ground water draft is estimated for all the ground water uses viz. Domestic, Irrigation and Industrial. Domestic draft is estimated based on well census method or requirement method. Irrigation draft is estimated using well census method, cropping pattern.Industrial draft is estimated using well census method. Sum of all these drafts is the Gross ground water draft.

4.8.2 Estimation of Ground Water Recharge

Ground water recharge due to rainfall is to be estimated using ground water level fluctuation method and rainfall infiltration factor method.

4.8.2.1 Ground water level fluctuation method

The water level fluctuation method is applied for the monsoon season to estimate the recharge using groundwater balance equation. The groundwater balance equation for the monsoon season is expressed as,

$$RG - DG - B + IS + I = \Delta S \qquad \textbf{(Eq 4.12)}$$

Where,

RG = gross recharge due to rainfall and other sources including recycled water

DG = gross groundwater draft

B = base flow into streams from the area

IS = recharge from streams into groundwater body

I = net ground water inflow into the area across the boundary (inflow - outflow)

ΔS = increase in ground water storage.

In the present investigation, it is considered that inflow, base flow and stream aquifer interactions are negligible and therefore, the above equation is re written as

$R = \Delta S + DG = h \times Sy \times A + DG$ **(Eq 4.13)**

Where,

R= Possible recharge, which is gross recharge minus the natural discharges in the area during monsoon season (RG - B + I +IS)

h = rise in water level in the monsoon season

A = area for computation of recharge

Sy = specific yield, ΔS = change in ground water storage

DG = gross ground water draft

The recharge calculated from the above equation gives the available recharge from rainfall and other sources for the particular monsoon season. For non-command areas, the recharge from other sources such as recharge from water conservation structures including tanks and ponds and also from irrigation return flow were also considered, The recharge from rainfall is given by,

$$Rrf = R - Rgw - Rwc - Rt = hxSy \times A + DG - Rgw - Rt - Rwc$$ **(Eq 4.14)**

Where Rrf = recharge from rainfall

Rgw = recharge from groundwater irrigation in the area

Rwc = recharge from water conservation structures

Rt = Recharge from tanks and ponds

In command areas there are two more components in recharge due to other sources viz. recharge due to canals and return flow from surface water irrigation. Hence the rainfall recharge can be estimated using the following formula.

$Rrf = h \times Sy \times A + DG - Rc - Rsw - Rgw - Rt - Rwc$ (Eq 4.15)

Where,

Rrf= rainfall recharge

h = rise in water level in the monsoon season

Sy= specific yield

A = area for computation of recharge

DG= gross ground water draft in the monsoon season

Rc= recharge due to seepage from canals

Rsw= recharge from surface water irrigation

Rgw = recharge from ground water irrigation

Rt= recharge from tanks and ponds Rwc

4.8.3 Estimation of normal rainfall recharge during monsoon season

The rainfall recharge obtained by using above equations provides the recharge in any particular monsoon season for the associated monsoon season rainfall. This estimate is to be normalized for the normal monsoon season rainfall which in turn is obtained as the average of the monsoon season rainfall for the recent 30 to 50 years. The normalization procedure requires that, a set of pairs of data on recharge and associated rainfall are first obtained. To eliminate the effects of drought or surplus years, it is recommended that the rainfall recharge during monsoon season is estimated not only for the current year for which assessment is being made, but also for at least four more preceding years. Two possible methods are recommended for the normalization procedure. The first method is based on a linear relationship between recharge and rainfall of the form, R = a r

Where, R = rainfall recharge during monsoon season r = monsoon season rainfall a = a constant The computational procedure to be followed in the first method is as given below:

$$\text{Rrf Normal} = \sum_{i=1}^{N} R * \frac{\frac{r(Normal)}{r_1}}{N} \quad \text{---------- (Eq 4.16)}$$

The second method is also based on a linear relation between recharge and rainfall. However, this linear relationship is of the form,

R = ar + b ---------- (**Eq 4.17**)

Where, R = rainfall recharge r = rainfall a and b = constants. The two constants 'a' and 'b' in the above equation are obtained through a linear regression analysis. The computational procedure to be followed in the second method is as given below

$a = (NS_4-S_1S_2)/(NS_3-S_1^2)$----------(Eq 4.18)

$b=S_2-aS_1/N$----------(Eq 4.19)

where, N= No. of datasets and

The rainfall recharge during monsoon season for normal monsoon rainfall condition is computed as below:

$S1 = \sum_{i=1}^{N} r1 \;\; S2 = \sum_{i=1}^{N} R1 \;\; S3 = \sum_{i=1}^{N} r1 = \sum_{i=1}^{N} r12 \;\; S4 = \sum_{i=1}^{N} r1R$---------- (**Eq 4.19**)

The rainfall recharge during monsoon season for normal monsoon rainfall condition is computed as below:

Rrf (normal) = a * r (normal) + b ----------(**Eq 4.20**)

4.8.4 Rainfall Infiltration Factor Method

Recharge from rainfall in monsoon season can also be estimated based on the Rainfall Infiltration Factor method and is estimated using the following equation

Rrf = f x A x Normal rainfall in monsoon season

Where f = rainfall infiltration factor, A = area for computation of recharge

Percent Deviation (PD), is the difference between the two methods, i. e. water table fluctuation and rainfall infiltration factor method was estimated using the formula

PD = R_{if} (Normal, Wtfm) - R_{rf} (Normal,rifm)/R_{rf} (Normal,rifm)*100 ----------(**Eq 4.21**)

where,

Rrf (normal, wtfm) = Rainfall recharge for normal monsoon season rainfall estimated by the water table fluctuation method

Rrf (normal, rifm) = Rainfall recharge for normal monsoon season rainfall estimated by the rainfall infiltration factor method

The rainfall recharge for normal monsoon season rainfall is finally adopted as per criteria given below:

If PD is greater than or equal to -20%, and less than or equal to +20%, Rrf (normal) is taken as the value estimated by the water table fluctuation method.

If PD is less than -20%, Rrf (normal) is taken as equal to 0.8 times the value estimated by the rainfall infiltration factor method. If PD is greater than +20%, Rrf (normal) is taken as equal to 1.2 times the value estimated by the rainfall infiltration factor method.

4.9 Geophysical Survey:

4.9.1 ELECTRICAL RESISTIVITY METHODS

Electrical Resistivity Method is one of the Geophysical techniques used to investigate the nature of the subsurface formations.

In Electrical Resistivity methods current sent into the ground through a pair of electrodes, called current electrodes, and resulting potential difference across the ground is measured with the help of another pair of electrodes, called potential electrodes.

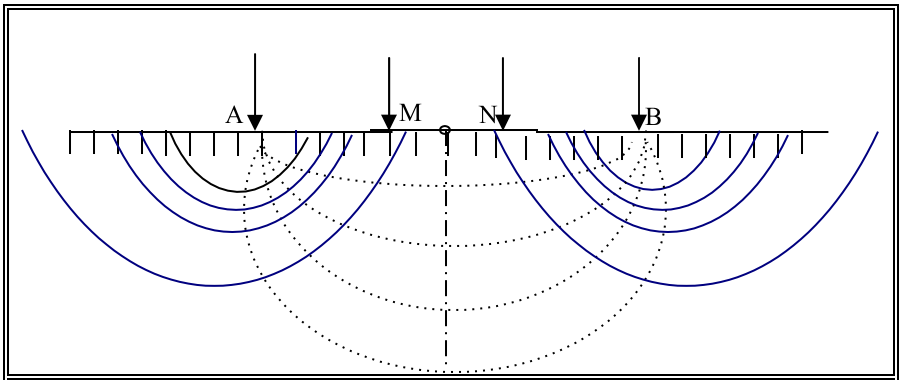

Figure 4-4 Electrical Resistivity Method

The ratio between the potential difference (ΔV) and the current (I) gives the apparent resistance, which depends on the electrode arrangement and on the resistivities of the subsurface formations. There are several types of electrode arrangements (configurations) of which Wenner and Schlumberger configurations are more popular.

In **Wenner** Configuration all the four electrodes are kept along a line at equal distances 'a'. For each measurement all the electrodes are moved simultaneously keeping the inner electrode spacing same. The current is sent normally through outer electrodes and potential difference is measured across the inner electrodes.

The resistance is multiplied by the configuration factor 2πa, to get the value of apparent resistivity (ρ_{aw})

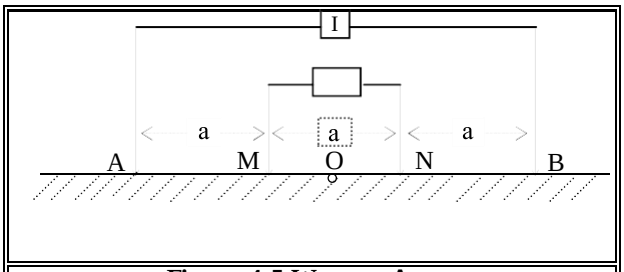

Figure 4-5 Wenner Array

$$\rho_{aw} = 2\pi a\, R \qquad \textbf{(Eq 4.22)}$$

Where $R=\Delta V/ I$

In Schlumberger Configuration all the four electrodes are kept in a line similar to that of Wenner but the outer electrode spacing is kept large compared to the inner electrode spacing, usually more than 5 times. For each measurement only current electrodes are moved keeping the potential electrodes at the same locations. The potential electrodes are moved only when the signal becomes too weak to be measured.

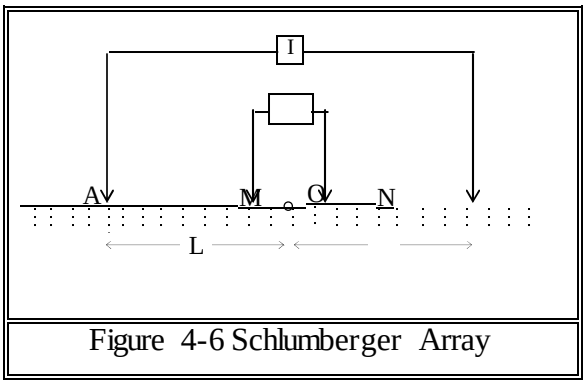

Figure 4-6 Schlumberger Array

The apparent resistivity for this configuration is computed with the formula;

$$\rho as = \Delta\,[(AB/2)2 - (MN/2)2]R/\ MN \qquad \textbf{(Eq 4.22)}$$

There are two types of procedures for making resistivity observation, namely Resistivity Sounding (also called Vertical Electrical Sounding, VES) and Resistivity Profiling (Horizontal Electrical Profiling). Resistivity profiling is employed to determine the lateral variations in the resistivity thereby establishing the existence of vertical bodies like dykes, fracture zones, geological contacts etc. The Vertical Electrical Sounding is used to estimate the resistivity and thickness of various

subsurface layers at a given location and is mainly employed in groundwater exploration to determine the disposition of the aquifers.

Vertical Electrical Sounding (VES):

In the present investigation, soundings were taken in selected sites based on geology. About 10-11 sections were taken in the Malaprabha sub-basin. Data obtained were analysed and interpretations were drawn based on resistivity curve characteristics.

4.10 **Surface and Groundwater Modelling**

In order to understand the amount of water available for Groundwter recharg the surface water distribution, quantification, land use wise rate of infiltration, Soil Water Assement tool is used.(SWAT)

4.10.1 Surface and Groundwater Interactions:

The surface and Groundwater Interactions are predicted using familiar software SWAT (Soil and Water Assessment Tool).

4.10.2 Description of SWAT model

Soil and Water Assessment Tool (SWAT) is a physically based distributed parameter model which has been developed to predict runoff, erosion, sediment and nutrient transport from agricultural watersheds under different management practices. The SWAT works in conjunction with ArcGIS with an extension ArcSWAT a graphical user interface for SWAT tool. The hydrologic cycle as simulated by SWAT is based on the water balance equation (1). Here the runoff volume is estimated by using the Soil Conservation Service (SCS) curve number technique (USDA, 1972).

$$SW_t = SW_o + \sum_{i=1} (R_{day} - Q_{surf} - E_a - W_{seep} - Q_{gw}) \ldots\ldots\ldots \quad \textbf{(Eq 4.22)}$$

Where, SWt is the final soil water content (mm H_2O), SWo is the initial soil water content (mm H_2O), t is time in days, R day is amount of precipitation on day i (mm H_2O), Q surf is the amount of surface runoff on day i (mm H_2O), Ea is the amount of evapotranspiration on day i (mm H_2O), wseep is the amount of percolation and bypass exiting the soil profile bottom on day i (mm H_2O), Qgw is the amount of return flow on day i (mm H_2O).

For simulation, a watershed is sub-divided into a number of sub-basins or sub watersheds. The use of sub basins in a simulation is particularly beneficial when

different areas of the watershed are dominated by land uses or soils dissimilar enough in properties to impact hydrology. The total runoff mainly depends on the actual hydrologic condition of each land cover soil type and slope present in the watershed. Therefore, the impact of each type of land use is considered to calculate runoff of the basin. After the overlay of the land-use, soil maps and slope, the distributions of the Hydrological Response Units (HRUs) were determined. HRUs divide the sub basin in to the area of similar land use, soil type and slope. Runoff is predicted separately for each HRU and routed to obtain the total runoff of the watershed. This increases accuracy and gives a much better physical description of the water balance.

4.10.3 Principle

SWAT requires many sets of spatial and temporal input data. As semi-distributed model, SWAT has to process, combine and analyze spatially these data using GIS tools. Therefore, to facilitate the use of the model, it was coupled with GIS software as free additional extension ArcSWAT for ArcGIS. The methodology for the runoff Modelling at the basin outlet using SWAT is depicted in flow chart Figure.

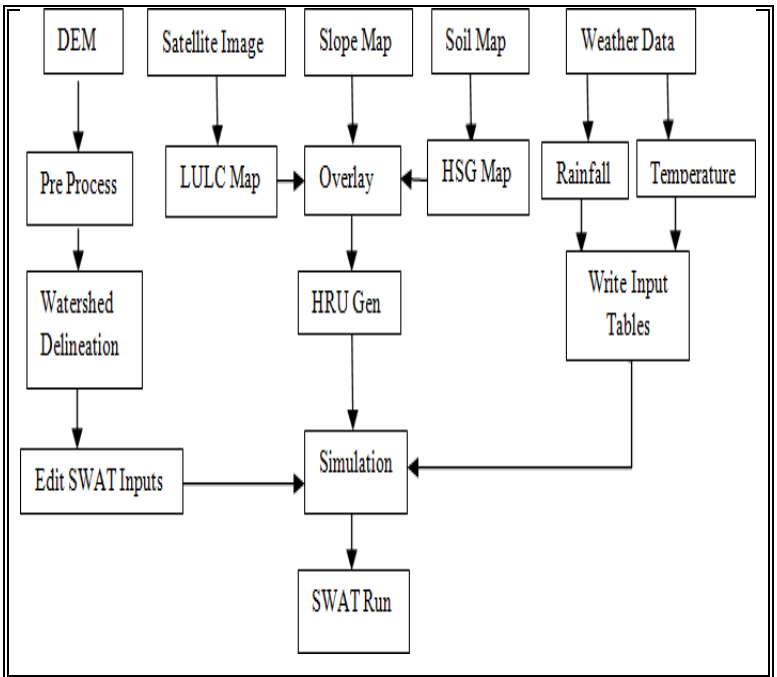

Figure 4-7 SWAT Flow chart

4.11 Groundwater Modelling

The output rainfall recharge obtained from the Soil water Assesment tool is used as recharge to Groundwater modelling in Groundwater Modelling System (GMS).

4.11.1 Principle:

Groundwater models include physical (laboratory) and mathematical models including process-based numerical models. Most groundwater models are developed for forecasting (prediction), and some of the models are used for the reconstruction of past conditions. There are also screening models and generic models for hypothesis testing. A model is the primary quantitative tool available in a groundwater investigation. A workflow for groundwater modelling begins with a question that addresses the modelling purpose.

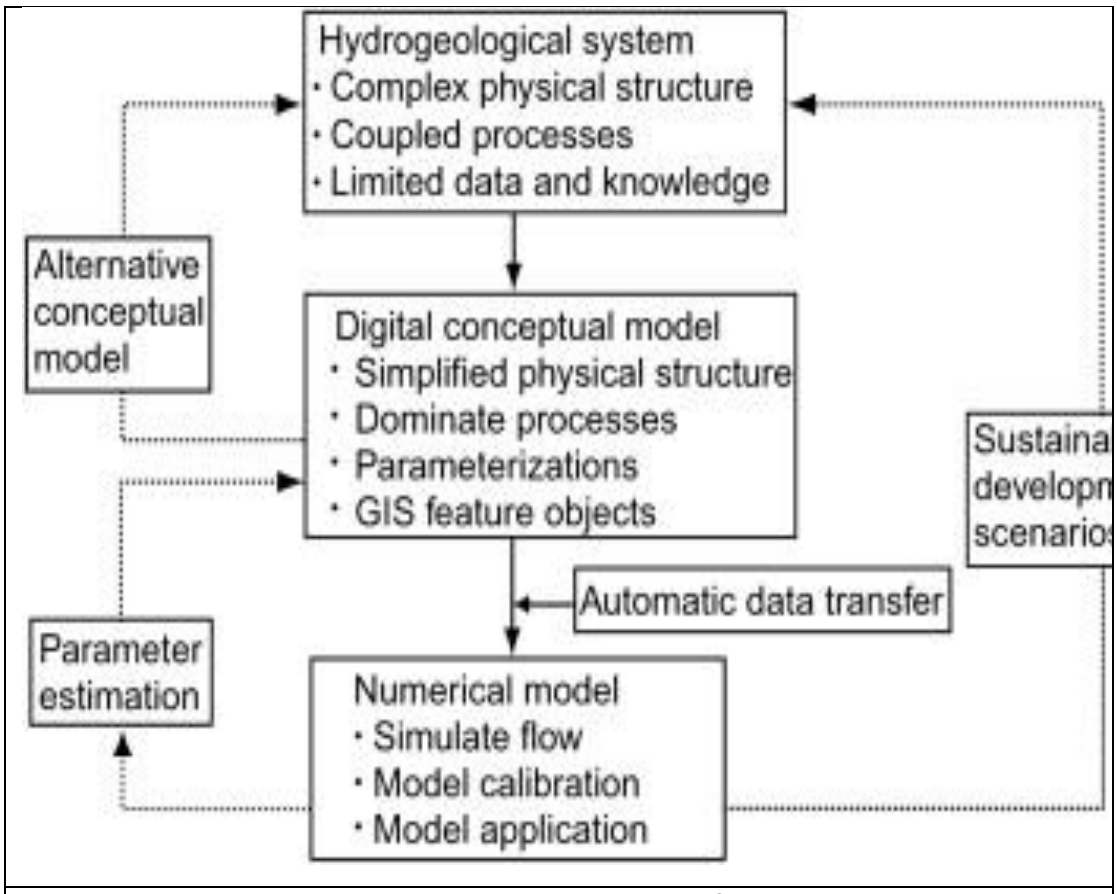

Figure 4-8 Groundwater Modelling flow chart

Chapter 5

5.1 Rainfall Analysis

A spatio-temporal analysis of rainfall over the study area was carried out using the data for 37 years for 18 raingague station observing the rainfall Figure (3.4). Long term averages were calculated for each individual station and are placed in the Annexure III and IV. The highest rainfall is recorded in the Kankumbi rain gauge

station (8150 mm during the Year 1994) which is located in the western part of the catchment. The lowest rainfall recorded in Hulikatti is 217 mm in the southern part of the Catchment with a mean annual rainfall of 1157.66 mm. The study area gets about 68% of the annual total rainfall during the monsoon season (June to Sept) and the remaining amount during the rest of the year.

A trend analysis was carried out using Sen's slope method as described in section 4.3. The results of trend analysis is presented in Table 5.1.

The monthly average rainfall and the coefficient of variation for all individual stations are shown in Table 5-1. Out of the total rainfall, 67.28 % occurs during the monsoon season i.e., from June to September. The Co efficient of Variation of the rainfall over the basin as a whole is 30 %, whereas the C.V. of the individual stations for their long-term data varies from 21.63 % to 43.38 %. The Co efficient of Skewness of the rainfall over the basin as a whole is -0.0774, whereas the Co efficient of Skewness of the individual stations for their long-term data varies from -0.8779 to 1.16%. The Standard deviation of the rainfall over the basin as a whole is 332.74, whereas the Standard deviation of the individual stations for their long-term data varies from 105.80 to 1462.86. The station wise average, Maximum and Minimum rainfall is plotted and is shown in the Figure 5.1

Table 5-1 Rainfall Statistical Analysis of Sub basin

Raingauge	Average	Maximum	Minimum	Standard Deviation	Co-efficient of variation	Co-efficient	Test Z	Significance	Sen's Slope
Kankumbi	5651.48	8150.80	1936.03	1462.86	25.88	-0.88	-1.91	+	-40.66
Jamboti	2344.40	3873.40	1673.60	463.60	19.77	-0.60	-1.73	+	-11.97
Asoga	1743.01	2978.30	877.50	564.97	32.41	0.13	0.64		5.87
Khanapur	1840.18	3149.80	510.79	573.34	31.16	-0.08	-0.33		-3.52
Gunji	1792.88	3138.10	449.91	653.25	36.44	0.00	1.73	+	23.66
Desur	1236.51	2534.70	542.40	457.82	37.02	0.50	-1.93	+	-15.91
Bidi	1127.97	1752.26	489.90	265.04	23.50	-0.55	0.31		2.53
Hirebagewadi	943.96	1514.50	587.72	237.16	25.12	-0.24	1.09		4.76
Mkhubli	843.24	1273.30	500.90	206.74	24.52	-0.52	0.35		0.86
Hulikatti	639.00	1229.80	217.00	233.03	36.47	0.40	-0.52		-1.86
Tigadi	770.31	1230.60	263.50	261.67	33.97	-0.22	1.96	*	9.14
Neginal	724.69	1418.90	321.00	229.52	31.67	0.41	-0.42		-1.75
Kadasagatti	499.54	1162.00	293.00	216.71	43.38	1.16	2.46	*	6.24
Bailahongal	484.62	739.61	271.81	105.80	21.83	-0.65	1.61		2.62
Belawadi	548.09	1121.80	249.80	231.91	42.31	0.76	3.78	***	10.99
Murgod	562.74	994.80	327.10	166.27	29.55	0.30	-1.22		-3.20
Yargatti	511.04	752.33	297.09	110.55	21.63	-0.74	1.82	+	3.32
Soundatti	549.66	931.60	307.80	134.13	24.40	-0.33	1.63		3.85
Katkol	491.97	739.61	271.81	110.81	22.52	-0.63	2.05	*	3.30

*** significance at 0.001 level; ** significance at 0.01 level; * significance at 0.05 level; + significance at 0.1 level

From the Table 5.1, it is evident that the highest declining trend is observed at Kanakumbi (-40.66) at 0.1 significant level. At the same time the Belawadi which is located in the eastern part of the study area records increasing trend at 0.001 significance level. However, it is important to note that, the stations which received higher rainfall and are located in the undulating hilly areas have registered a significant decreasing trend (Desur, Khanapur and Jamboti). The increasing trend in the rainfall has been recorded in the middle part of the catchment which has relatively flatter slopes. There have been reports indicating the impact of decreasing / increasing rainfall on river discharge as well as groundwater recharge. Singh and Kumar (1997) and Singh et al.,

(2006) observed that, a 10% decrease in rainfall has resulted in 3.5% of decrease in runoff. Further, Putty et al., (2000) have reported that, events with large (>80 mm a day) daily rainfall amount will significantly contribute to the annual rainfall, which in turn generate considerable quantity of river flow due to high rate of infiltration. Therefore, decreasing trend has a greater impact on runoff as well as on recharge pattern of the catchment.

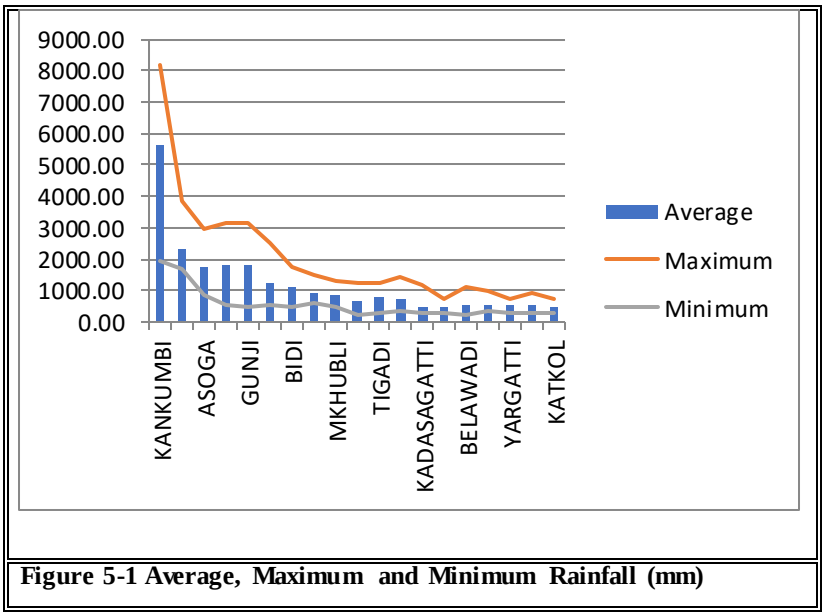

Figure 5-1 Average, Maximum and Minimum Rainfall (mm)

5.2 Geomorphological Characteristics of the Malaprabha sub basin

5.2.1 Morphometry of the Malaprabha Sub-basin:

Table 5.2 to 5.5 summarises the various geomorphological parameters determined using empirical and GIS approach.

Geomorphology plays a significant role in understanding the catchment characteristics, runoff process and groundwater dynamics. The estimated geomorphological parameters are discussed below.

Table 5-2 Morphometry of Malaprabha sub basin

Basin/sub-basin	Area in sq km2)	Length(km)	Stream nos in different orders					Order wise stream lengths				
			1	2	3	4	Total	1	2	3	4	Total
Malaprabha Sub-basin	2902.26	364.162	2392	701	113	27	3233	1808.59	551.64	98.96	21.29	2480.48

The Malaprabha sub basin covers an area of 2902.26 square kilometers, the highest order of the stream found in this basin is 5th Order. There are 2392 first order, 701 second order, 113 third order and 27 fourth ordered streams are found in the basin. This indicates the good surface hydrological system in the basin.

Table 5-3 Stream Length,ratio, Bifurcation ratio

Basin/sub-basin	Average Stream length (km)						Stream length ratio (Rl)				Bifurcation ratios			
	1	2	3	4	Avearge	2/1	3/2	4/3	Rl		Rb1	Rb2	Rb3	Mean Rb
Malaprabha Sub-basin	0.76	0.79	0.88	0.79	0.805	0.31	0.18	0.22	2.63		3.41	6.20	4.19	3.2

The average stream lengths of First, Second, Third and Fourth are 0.76,0.79,0.88,0.79 km in the basin are calculated in the GIS environment, the stream length ratio First to second, second to third, third to fourth are 0.31,0.18, 0.22,2.63 respectively and the Bifurcation ratio is a dimension less quantity. The bifurcation ratio of first, Second, Third is 3.41,6.2,4.19,3.2 respectively the Mean Bifurcation ratio (Rb) is 3.2 Bifurcation ratio is useful measure of flood proneness , the higher the bifurcation ratio, the shorter will be the time taken for discharge to reach the outlet, and higher will be the peak discharge – leading to a greater probability of flooding. Bifurcation ratio correlates positively with drainage density. Higher Bifurcation ratios also suggest that the area is tectonically active.

Table 5-4 Drainage density, texture, stream frequency, Elongation ration

Basin/sub-basin	Drainage density	Drainage Texture	Stream Frequency	Elongation ratio	Circularity ratio	Form factor
Malaprabha Sub-basin	(km-1)	(km-1)	(km-2)			
For the entire basin	0.85	8.8	1.11	1.8	0.27	0.2

5.2.1.1 Drainage density

It indicates the closeness of spacing between drainages and is a measure of the total length of the stream segment of all orders per unit area. Drainage density of this sub basin varies from 0.85 (Table 5.4). In general, it has been observed over a wide range

of geologic and climatic types, that low drainage density is more likely to occur in regions of highly permeable subsoil material under dense vegetative cover, and where relief is low. In contrast, high Drainage density is favored in regions of weak or impermeable subsurface materials, sparse vegetation and mountainous relief (Nag, 1998).

5.2.1.2 Drainage Texture

The drainage texture depends upon a number of natural factors such as climate, rainfall, vegetation, rock and soil type, infiltration capacity, relief and stage of development (Smith, 1950). The soft or weak rocks unprotected by vegetation produce a fine texture, whereas massive and resistant rocks cause coarse texture. Sparse vegetation of arid climate causes finer textures than those developed on similar rocks in a humid climate. Drainage texture is defined as the total number of stream segments of all orders per perimeter of the area (Horton). Smith (1950) classified drainage into five classes i.e., very coarse (<2), coarse (2-4), moderate (4-6), fine (6-8) and very fine (>8). Horton (1945) recognized infiltration capacity as the single important factor which influences drainage texture and considered drainage texture which includes drainage density and stream frequency. The drainage density values of watersheds range from 8.8 indicating very fine drainage texture for Malaprabha Sub catchment

5.2.1.3 Stream frequency

It is the total number of stream segments of all orders per unit area (Horton, 1932). Stream frequency values indicate positive correlation with the Drainage density of Malaprabha Sub Catchment. The stream frequencies of are mentioned in Table 5.4. The study revealed the stream frequency for all orders is 1.11 per square kilometer.

5.2.1.4 Elongation ratio

Schumn (1956) defined elongation ratio as the ratio between the diameter of the circle of the same area as the drainage basin and the maximum length of the basin. Analysis of elongation ratio indicates that the areas with higher elongation ratio values have high infiltration capacity and low runoff. A circular basin is more efficient in the discharge of runoff than an elongated basin (Singh and Singh, 1997). The values of elongation ratio generally vary from 0.6 to 1.0 over a wide variety of climate and geologic types. Values close to 1.0 are typical of regions of very low relief, whereas values in the range 0.6 to 0.8 are usually associated with high relief and steep ground slope (Strahler, 1964). These values can be grouped in to three categories namely (a) circular (>0.9), (b) oval (0.9 to 0.8), (c) less elongated (<0.7). The values of Elongation ratio is 1.8 in present

study area indicating that it falls in the Circular category.

5.2.1.5 Circularity ratio

Circularity ratio is the ratio of the area of the basin to the area of a circle having the same circumference as the perimeter of the basin (Miller, 1953). It is influenced by the length and frequency of streams, geological structures, land use/ land cover, climate, relief and slope of the watershed. In the present study (Table 5.4), the circularity ratio 0.27

5.2.1.6 Form factor

Form factor is defined as the ratio of basin area to the square of the basin length (Horton, 1932). The values of form factor would always be less than 0.7854 (perfectly for a circular basin). Smaller the value of (Form factor) more elongated will be the basin. The form factor for this sub basin is 0.20 indicates that the whole catchment is elongated. The elongated watershed with low value of Form factor indicates that the basin will have a flatter peak flow for longer duration. Flood flows of such elongated basins are easier to manage than from the circular basin.

Table 5-5 Relative relief Longest axis, Relief ratio

	Elevation	in 'm'	Relative relief	Longest axis	Relief ratio
Basin/sub-basin	Max 'H'	Min 'h'	(H-h) (km)	'L' (km)	(H-h/L)
Malaprabha Sub-basin	953	462	491	85	5.77

The highest relief lies in the western part of the catchment is about 953 meters above mean sea level and the lowest relief is observed in the Eastern part of the basin the difference of this gives the Relative relief and the longest length of the stream of the sub basin is 85 km. The ratio of longest axis to the Relief is 5.77 which indicate moderate erosion potential.

5.3 Terrain characteristics of the Basin

Slope, Aspect, LS factor, Topographic Wetness Index, Convergence Index and Drainage density were estimated by using SAGA software. The derived parameters are discussed below.

5.3.1 Slope

Figure 5.3 shows the slope map of the study area. The slope can be expressed either in percentage or radians. Slope plays a significant role in controlling infiltration and runoff processes. Infiltration is inversely related to slope, i.e. gentler the slope, infiltration is more and runoff is less. In the sub-basin, the slope ranges from 0 to 0.18 radians. The dark orange color shown in the figure 5.3 indicates the highest slope (range 0.1 to 0.18 radians) which is observed in the head water catchment and also near the Navilutheertha dam. 0.1 – 0.18 radians and 0 to 0.14 radians slope is observed at Malaprabha River and along its bank.

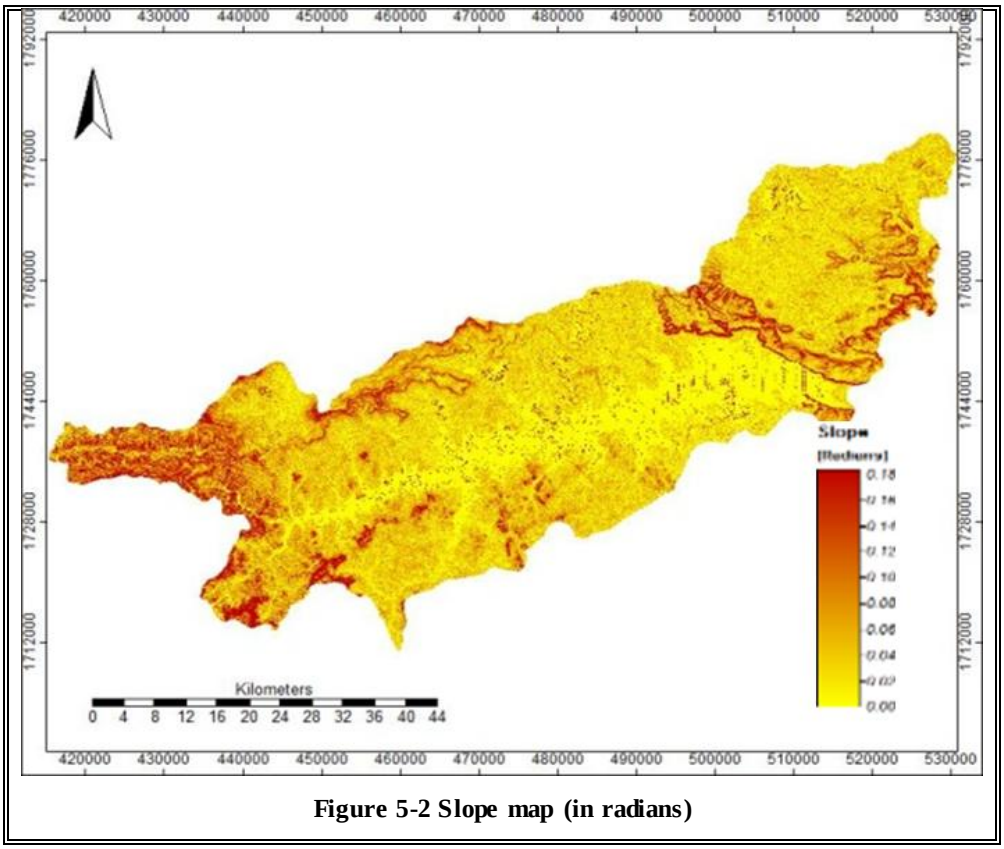

Figure 5-2 Slope map (in radians)

5.4 L S Factor

LS factor represents a combination of Slope and Slope length which is a very useful tool to understand the soil dynamics of the region. This is also significantly useful attribute for the estimation and prediction of erosion potential. The erosional areas

showed significantly lower infiltration rates and indicating lower recharge. Figure 5.7 is the LS map of the Malaprabha sub-basin.

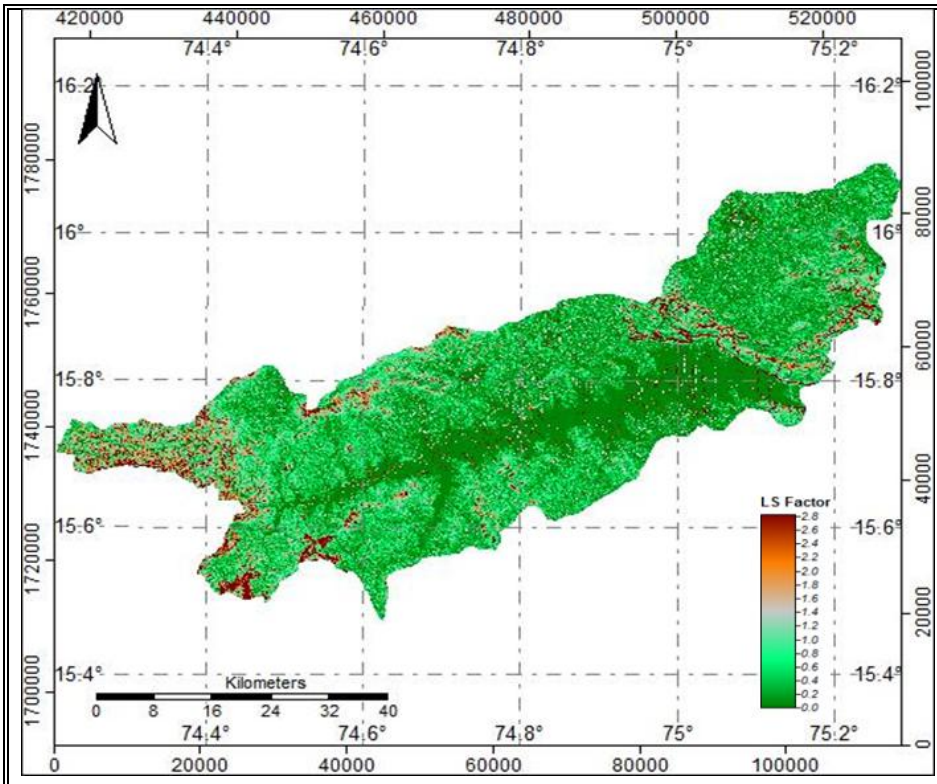

Figure 5-3Map showing L S Factor

5.4.1 Aspect:

Aspect is the compass direction of the slope (terrain faces) and broadly influences hydrological components such as vegetation, settlement, agriculture, precipitation, snow melting and wind direction. The direction of the aspect is 0° north and the 90° aspect marked to the east. The aspect map of the Malaprabha sub-basin is shown in Figure 5.5.

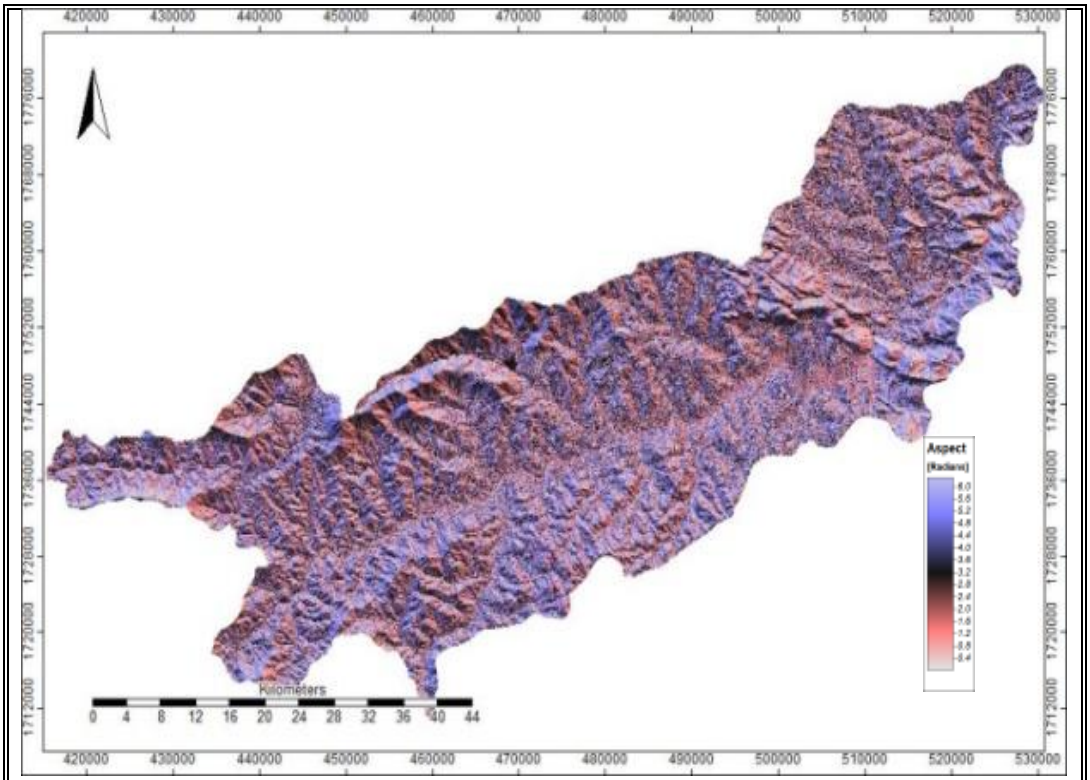

Figure 5-4 Aspect map of Malaprabha sub basin

5.4.2 Topographic Wetness Index:

Topographic Wetness Index (TWI) is termed as $\ln(\alpha)/ \tan \beta$, Where ' α ' denotes the local upslope area draining through a certain point per unit contour length and β Denotes slope angle. The estimated index is a function of both the slope and the upstream contributing area per unit width orthogonal to the flow direction (known as specific catchment area, SCA, $m^2 .m^{-1}$). TWI signifies the topographic control on hydrological processes and reflects the potential groundwater exfiltration caused by the effects of topography. Higher TWI value represented higher groundwater potential value. A higher TWI indicated a gentler slope and larger slope area

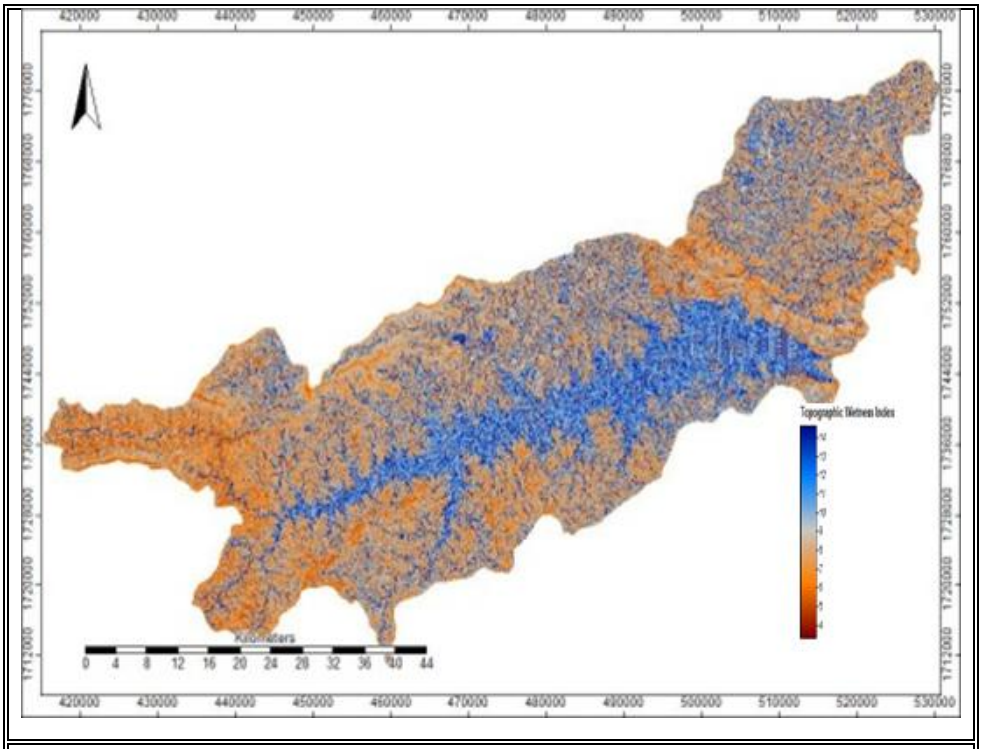

Figure 5-5 showing Topographic Wetness Index.

5.4.3 Convergence Index:

Convergence Index (CI) is used to distinguish flow convergent area from divergent region ([4] Kiss 2004, Thommeret 2009), which may be an essential parameter to understand the recharge characteristics and thus could be used for groundwater potential Modelling. CI could be calculated based on the aspect which can be extracted from DEM. The CI was obtained by calculating the average angle (i. e. θ in figure 5) between the aspect of adjacent cells and the direction to the central cell and then subtracting 90°. Positive CI values represented divergent area while negative CI values represented convergent area. Thus, a lower CI is associated with groundwater accumulation and the higher CI indicates higher groundwater potential in the region.

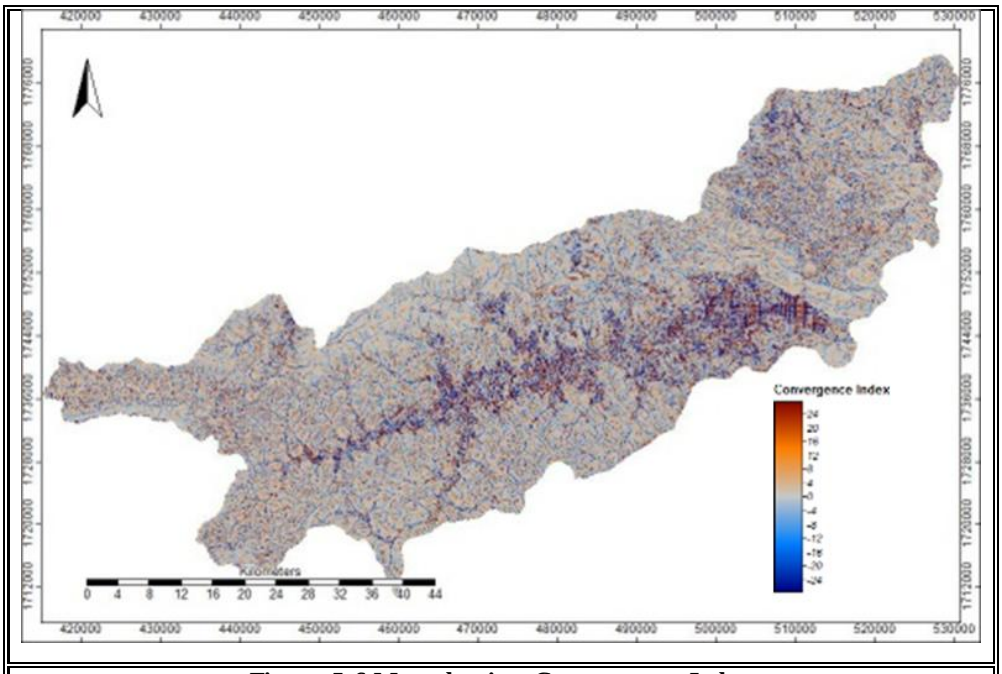

Figure 5-6 Map showing Convergence Index.

5.5 Hydraulic Properties of Soils

5.5.1 Infiltration

The mean infiltration characteristics of different kinds of soil (Table5.6), exhibit significant variation with respect to soil type and land use pattern. However, one of the interesting results obtained in the present study is that, the rate of infiltration is higher in the wet zone as compared to semi-arid and arid zone (soil type and texture were similar), irrespective of the land use pattern. The infiltration rate observed in the shrub of wet zone and wastelands of semi-arid and arid zone was considerably lower than other types of land covers. The major reason could be due to the thickness of soil type and thickness, runoff characteristics and the rainfall pattern occurring in three different zones. In an agriculture land, variation of hydraulic properties *shows* a different trend because of the impact of cropping pattern and irrigation processes adopted. In the case of barren land the infiltration is significantly lower than the agriculture land. The infiltration characteristics of soils in an agriculture land in arid and semi-arid indicate a wide variation between the two zones. Higher infiltration capacity of arid zone soils are associated with the abundance of large pores with aggregation of clayey particles present in the command areas (arid zone). Further, being parts of command area, application of irrigation and cropping pattern would also influence the rate of infiltration. On the other hand, in parts of the semi-arid zone of the present study area, the soils are affected by salinity problems as reported by earlier researchers. Another

striking feature observed is that the afforestation activities taken up in the semi-arid and arid region has improved the hydraulic properties of soil leading to higher rate of infiltration and hydraulic conductivity. It was quite higher than the rate of infiltration in shrubs and barren land. The high rate of infiltration in the forest covers of wet zone could be attributed to preferential flows taking place during the growth period. This flow occurs either when the macrospores and cracks open to the atmosphere or when the water pressure within macrospores and cracks is positive. One of the important reasons for having high rate of infiltration in tropical soil is due to the low viscosity of warm water.

Table 5-6 Infiltration Rate in Different stretches of Malaprabha catchment

Sl No.	Catchment zones	Land Use	Geology	Soil Texture	Infiltration Final Rate cm/hr
1	Head water catchment (Kankumbi to Khanapur)	Forest	Lateritic capping, Basalt, Lower Meta Greywacke,Basalt, pink Granite	Medium Loam	13.8
2		Shrub		Medium Loam	1.8
3		Agriculture		Medium Loam	6.6
4		Barren land		Heavy Loam	3.6
5	Khanapur to up to Renukasagar dam	Plantation	Basalt,Meta Greywacke,Basalt, pink Granite	Medium – Heavy Loam	5.4
6		Waste land with scrubs		Medium - Heavy Loam	1.2
7		Agriculture Land		Medium Loam	2.4
8		Barren Land/rocky exposures		Medium -Heavy Loam	0.8
9	Downstream of dam	Plantation		Medium – Heavy loam	4.8

10		Wasteland with scrubs	Basalts, Dolomitic Limestones,Argillites, Quartzites, Pink Granite.	Medium Heavy Loam	1.2
11		Agriculture land		Medium-Heavy Loam	5.4
12		Barren land/Rocky exposures		Medium - Heavy Loam	0.8

Figure 5.7 shows the infiltration map of the study area based on land use type.

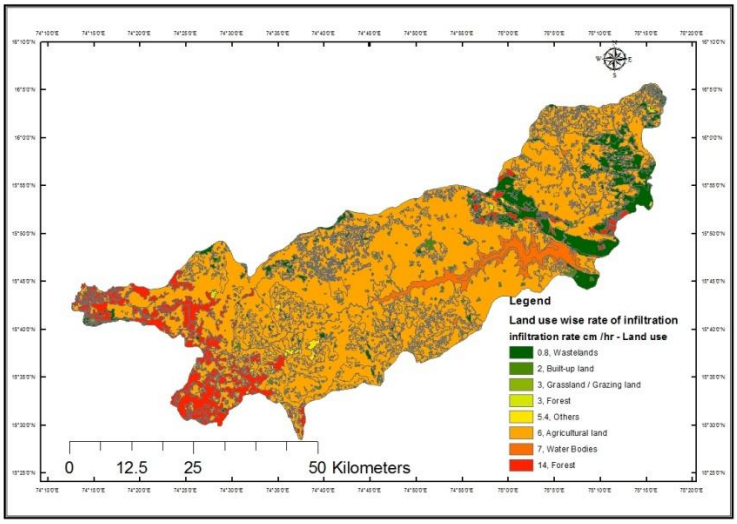

Figure 5-7 Land use wise rate of infiltration

5.5.2 Saturated Hydraulic Conductivity of the Soils

The saturated hydraulic conductivity observed for soils in the undisturbed forest is considerably high as compared to soils in the other land types such as shrubs/scrubs, wastelands, agriculture land and barren land. The present study shows that, in all the sites, the surface hydraulic conductivity is higher than the sub-surface conductivity. There is a marked variation between sub surface hydraulic conductivity of wet zone and semi-arid to arid zone. Therefore, it is surmised that the variation in saturated and unsaturated flow depends on the basic parameter viz. hydraulic conductivity. When the soil is saturated, the hydraulic conductivity tend to be higher and if the soil is unsaturated, some of the pores become air filled and the conductivity reduces depending on the grain-size distribution. Therefore, the transition from saturated to unsaturated

generally entails a steep drop in hydraulic conductivity, which may decrease by several orders of magnitude as suction increases from 0 to 1 bar. At still, higher suctions, or lower wetness values, the conductivity may be so low that very steep suction gradients, or very long times, are required for any appreciable flow to occur. Table 2 shows the Saturated soil moisture status under different hydrological regimes and saturated hydraulic conductivity at varying depths of soil (surface and below 60 cm)

Table 5-7 Saturated Hydraulic Conductivity in different stretches of Malaprabha catchment

Sl. No.	**Location/Agro-climatic zone**	**Saturated Moisture (in percent)**	**Residual Moisture (in percent)**	**Hydraulic Conductivity (Surface) cm/h**	**Hydraulic Conductivity (below 60 cm depth) cm/h**
Head water catchment (Kankumbi to Khanapur)					
1	Forest	42	19	5.8	4.2
2	Shrub	35	17	3.74	1.8
3	Agriculture land	38	15	3.00	1.4
4	Barren land	28	3.8	30	1.20
Semi-Arid (Khanapur to Renukasagar dam)					
5	Plantation	33	1.1	3.8	1.55
6	Wasteland/scrubs	21	5	3.4	0.21
7	Agriculture land	27	1.2	4.7	1.10
8	Barren land/rocky exposures	18	9.0	3.6	0.58
Arid zone (Downstream of Renukasagar dam)					
9	Plantation	35	2.0	3.4	0.85
10	Wasteland/scrubs	36	1.9	2.4	0.16
11	Agriculture	21	1.1	3.9	0.17
12	Barren/Rocky exposures	30	1.6	5.5	0.38

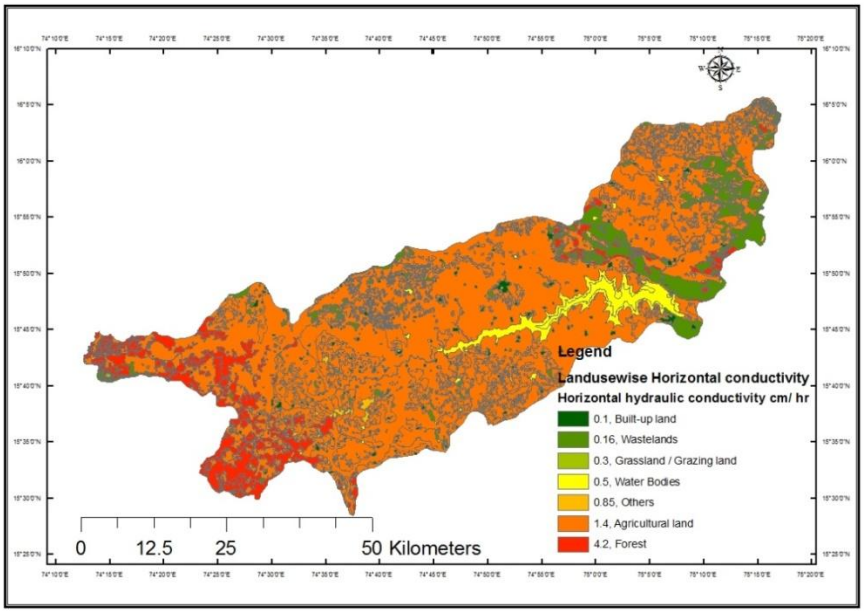

Figure 5-8 showing the Land use wise Hydraulic conductivity of the soils below 60 cm

5.6 Static Groundwater Levels

The details of the observation wells present in the catchment are shown in figure 5.10. There are 9 Observation wells in the upper catchment and 11 Observation wells in the Lower catchment which are distributed almost uniformly all over the study area.

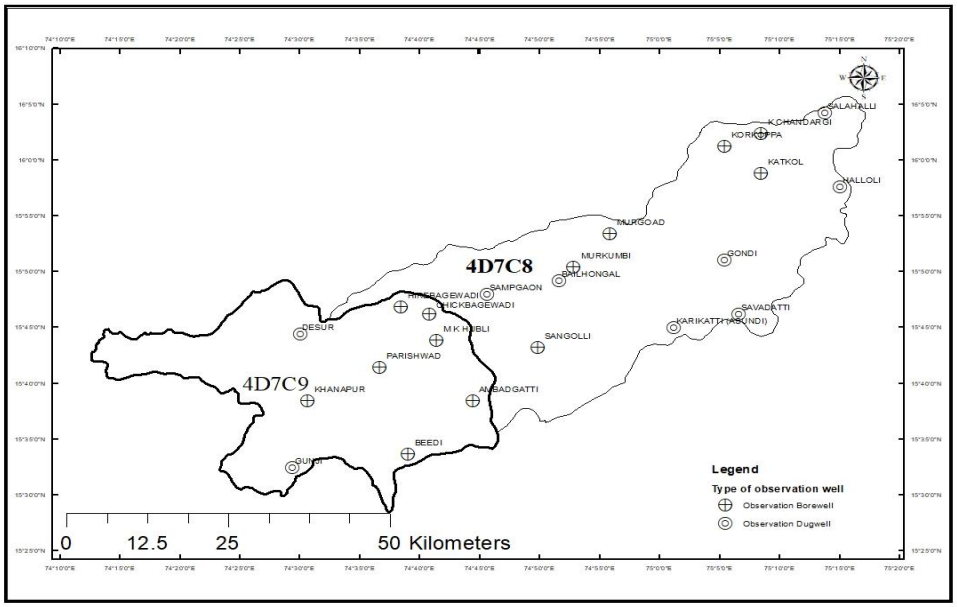

Figure 5-9 Location of Observation Wells

Table 5.8 summarizes the location of observation wells along with type of wells and altitude above mean sea level. Watershed code 4D7C9 represent the upper part of the catchment and 4D7C8 form the downstream part of the catchment.

Table 5-8 Observation well details

S.No	Watershed Code	Name of the Observation well	Taluka	Type	Latitude Deg/min	Longitude Deg/min	Altitude in meters above msl
1	4D7C9	Ambadagatti	Khanapur	Borewell	15.63	74.73	693
2	4D7C9	Beedi	Khanapur	Borewell	15.56	74.64	690
3	4D7C9	Chickbagewadi	Bailahongal	Dug Well	15.77	74.68	675
4	4D7C9	Desur	Belagavi	Dug Well	15.74	74.49	745
5	4D7C9	Gunji	Khanapur	Dug Well	15.53	74.49	678
6	4D7C9	Hirebagewadi	Belagavi	Borewell	15.77	74.63	694
7	4D7C9	Khanapur	Khanapur	Borewell	15.63	74.5	660
8	4D7C9	M k hubli	Bailahongal	Borewell	15.72	74.69	666
9	4D7C9	Parishwad	Khanapur	Borewell	15.69	74.61	683
10	4D7C8	Bailhongal	Bailahongal	Dug Well	15.82	74.85	697
11	4D7C8	Gondi	Savadatti	Dug Well	15.85	75.08	610
12	4D7C8	Halloli	Ramdurga	Dug Well	15.96	75.24	556
13	4D7C8	K.chandargi	Ramdurga	Borewell	16.04	75.14	645
14	4D7C8	Karikatti (asundi)	Savadatti	Dug Well	15.75	75.02	643
15	4D7C8	Katkol	Ramdurga	Borewell	15.98	75.13	652
16	4D7C8	Korkoppa	Savadatti	Borewell	16.02	75.08	660
17	4D7C8	Murgoad	Savadatti	Borewell	15.88	74.92	721
18	4D7C8	Murkumbi	Savadatti	Borewell	15.84	74.88	679
19	4D7C8	Sangolli	Bailahongal	Borewell	15.71	74.83	651
20	4D7C8	Savadatti	Savadatti	Dug Well	15.77	75.11	650

5.6.1 Lithologic Unit wise analysis of Observation wells

5.6.1.1 Granitic formation

Twenty percent of the total catchment is covered by granitic (Pink granite) formation and are located in the upper and Eastern part of the catchment. There are three observation wells (Desur, Gunji and Khanapur) which showed minimum average ground water level 1.42 meters below ground level and the maximum water level 7.22m. The fluctuation ranges from 2.09 to 6.31 meters. The observation wells Gunji and Desur are showing raise in water level trend because in this formation there is an impermeable clay layer below the unsaturated zone hence there is a less percolation to the groundwater. The Hydrographs are shown from figure 5.11 to figure 5.13

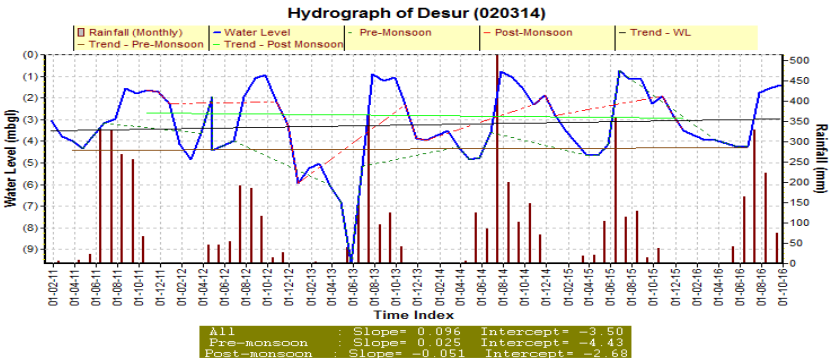

Figure 5-10 Groundwater Hydrograph of Desur

From the above hydrograph of Desur, it is noticed that, irrespective of lower rainfall received in the latter years, the groundwater level did not show any fluctuation due to the following reasons, (i) groundwater is used only for drinking water due to which abstraction of water was limited further, an additional water supply was given to villagers due to which abstraction became stand still.

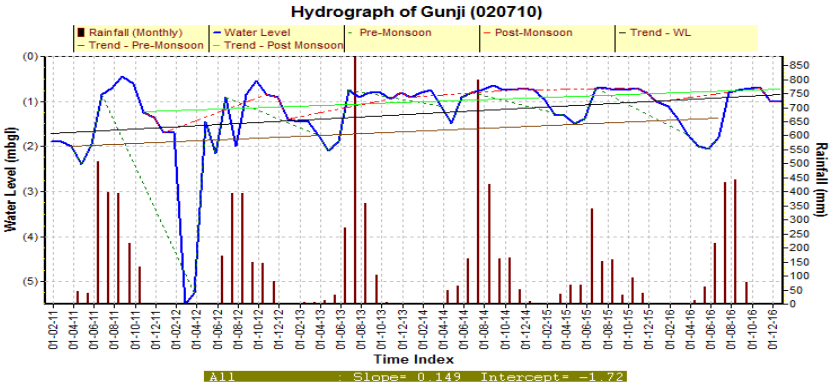

Figure 5-11 Groundwater Hydrograph of Gunji

Unlike the Desur open well, at Gunji, the recharge is influenced by the presence of agriculture growth surrounding the well and the catchment is covered by thick forests

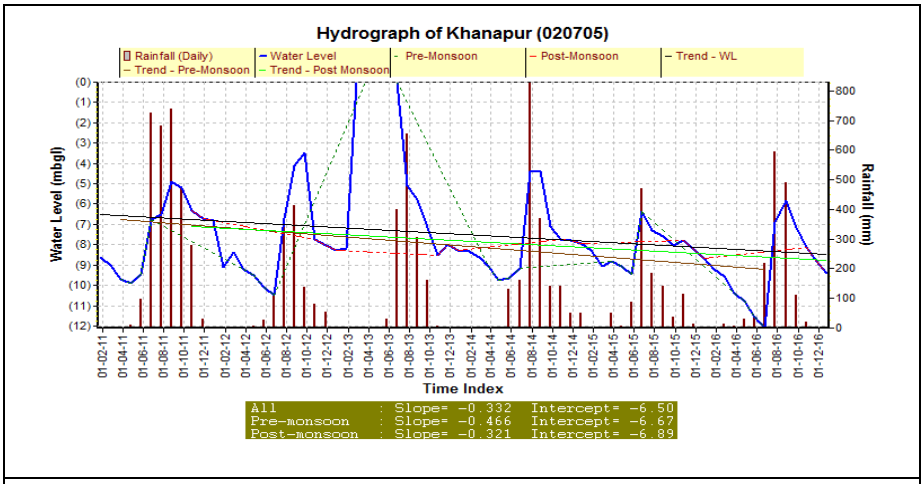

Figure 5-12 Groundwater Hydrograph of Khanapur

5.6.2 Metagreywackes

Nearly thirty eight percent of the total catchment is covered by Metagreywackes and Lower meta Greywackes which covers major portion of the basin are located in the middle part of the catchment. There are seven observation wells (Bailahongal, Murkumbi, Ambadagatti, Bidi, Chikkabagewadi, M.K.Hubli, Parishwad) which showed shows minimum average water level of 2.89 m and the maximum average water level 24.17 meters and the water level fluctuation ranges from 2.49 metrs to 24.17 meters. In these formations the fracture zone is restricted up to the 40 to 50 m. The borewells drilled beyond this depth shows the maximum water level. The Hydrographs are shown from figure 5.14 to figure 5.20.

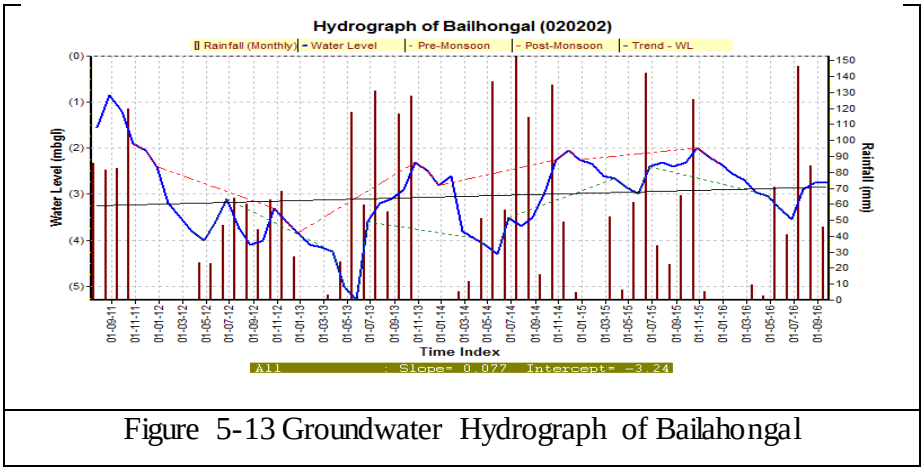

Figure 5-13 Groundwater Hydrograph of Bailahongal

One of the striking feature observed in the bore wells drilled in metagreywackes shows a falling trend in groundwater levels. Rainfall pattern analysis carried out for the

particular site indicated that the groundwater level is mainly dependent on rainfall and irrigation return flow characteristics. An investigation carried out during the study period substantiated that, there was a lower recharge due to less rainfall as well as a change in cropping pattern due to non-availability of sufficient water. This resulted in declining trend of groundwater level.

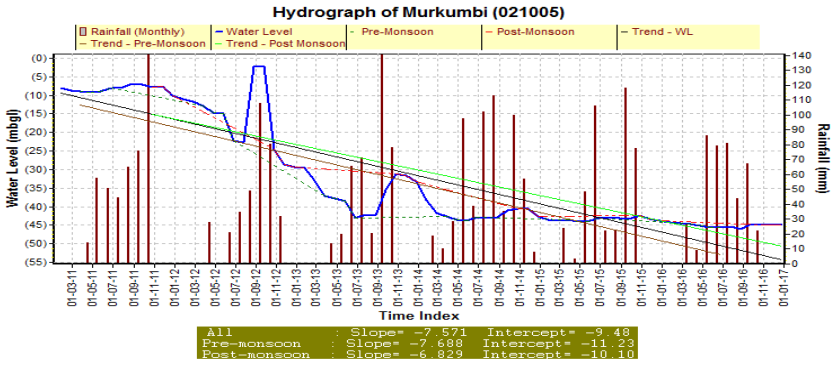

Figure 5-14 Groundwater Hydrograph of Murkumbi

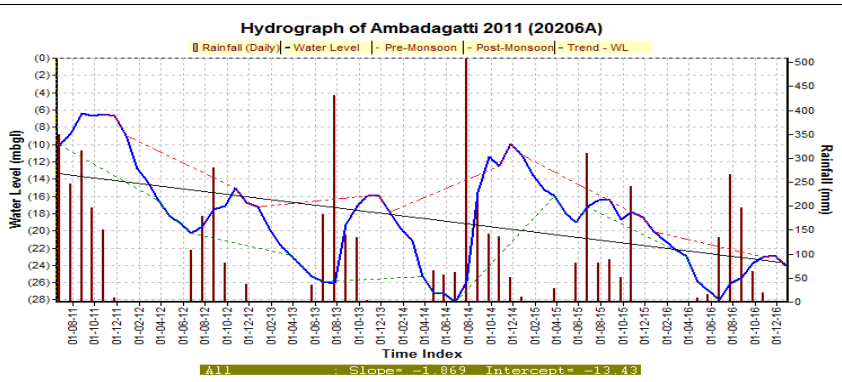

Figure 5-15 Groundwater Hydrograph of Ambadagatti

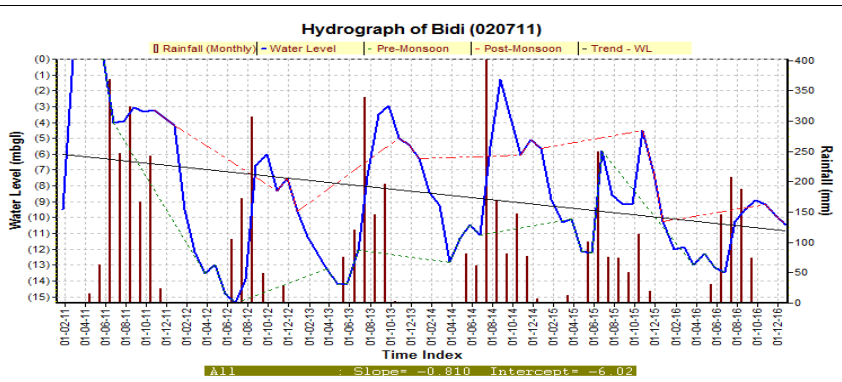

Figure 5-16 Groundwater Hydrograph of Beedi

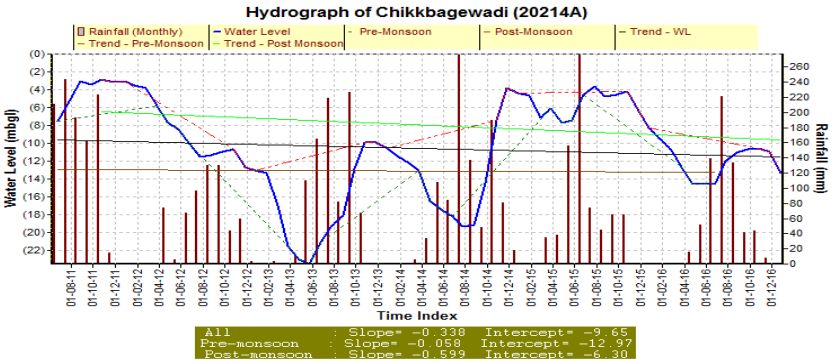

Figure 5-17 Groundwater Hydrograph of Chikkabagewadi

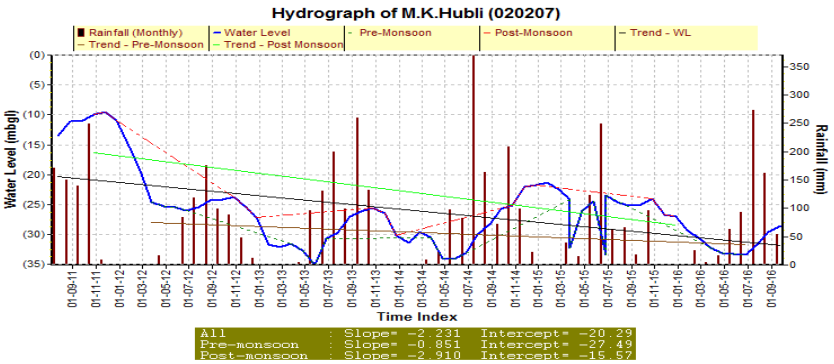

Figure 5-18 Groundwater Hydrograph of M.K.Hubli

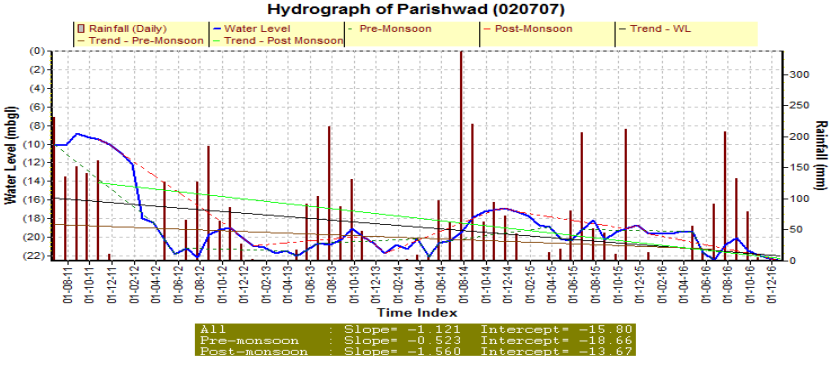

Figure 5-19 Groundwater Hydrograph of Parishwad

5.6.3 Conglomerate, arenite and shale

Nearly eight percent of the total catchment is covered by conglomerate, arenite and shale which are located in the Eastern part of the catchment. There are two observation wells (Katakol and Korkoppa) which showed shows minimum average water level of 6.04 and maximum water level of 12 m with the fluctuation of 6.96 m. The shale present below conglomerate beds restricts deeper percolation. The Hydrographs are shown from figure 5.21 to figure 5.22

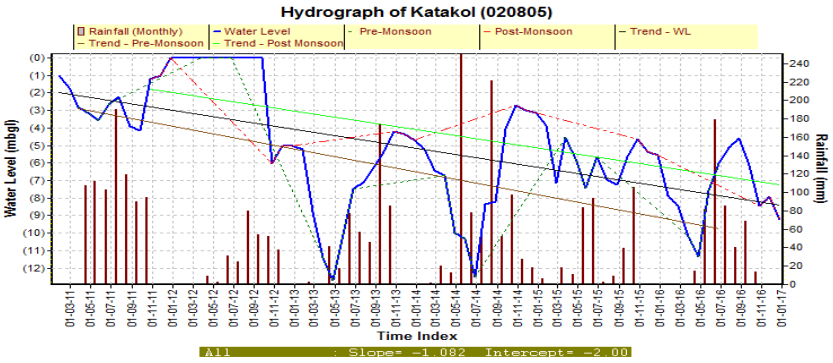

Figure 5-20 Groundwater Hydrograph of Katkol

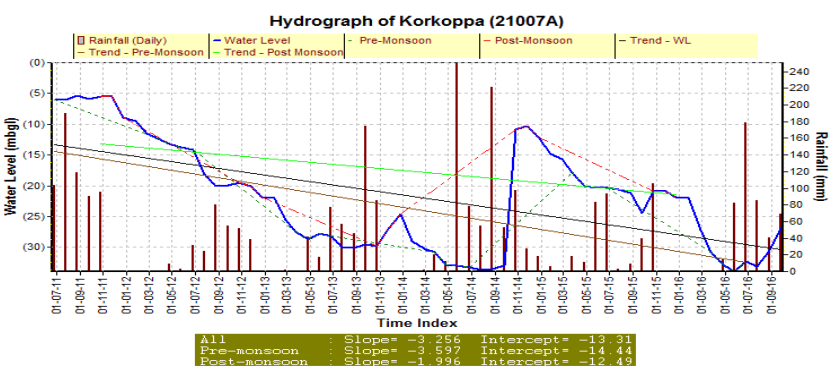

Figure 5-21 Groundwater Hydrograph of Korkoppa

5.6.4 Argillite, quarzite and conglomerate

Nearly eight percent of the total catchment is covered by argillite, quartzite and conglomerate which are located in the eastern part of the catchment. There is one observation wells (Gondi) shows minimum water level of 5.2 m and the maximum water level of 13.08m with a fluctuation of 8 meters. The wells with in this zone has good horizontal conductivity. The Hydrographs are shown from figure 5.23

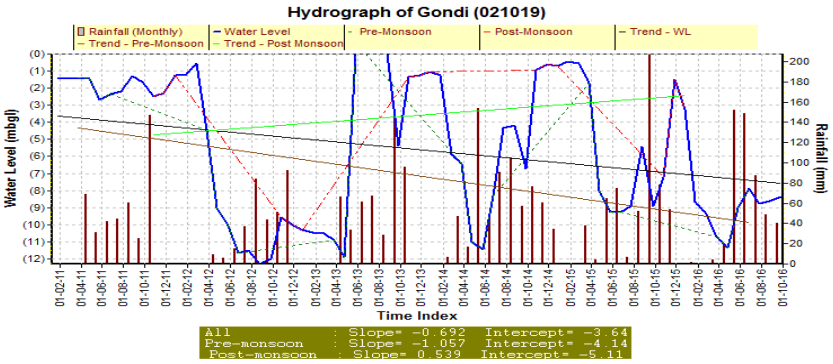

Figure 5-22 Groundwater Hydrograph of Gondi

5.6.5 Basalts

Twenty the total catchment is covered by argillite, quartzite and conglomerate which are located in the Northern part of the catchment and making the higher ridges in the northern watershed boundary. There is one observation wells (K.Chandargi) shows the minimum water level of 6.07m and the maximum water level of 10.5 m with the average fluctuation ranges from 4.53 m. The Hydrographs are shown from figure 5.24

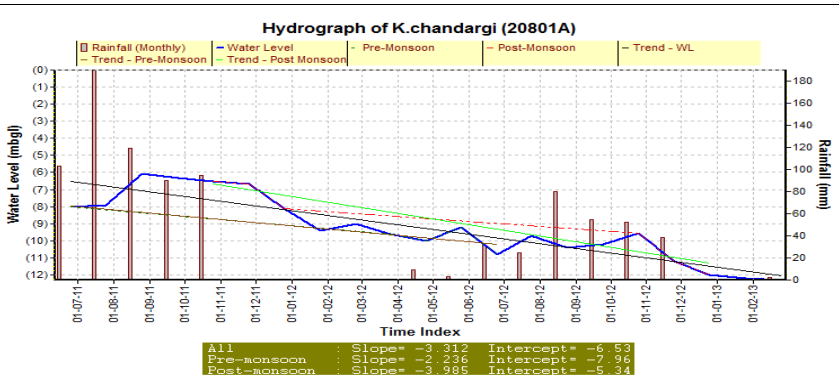

Figure 5-23 Groundwater Hydrograph of K.Chandargi

5.7 Groundwater Recharge Estimation using Empirical Methods

The annual groundwater recharge is estimated using the empirical methods as discussed in the section 4.8 and the results are compared and placed in table 5.9

Table 5-9 Comparison of Groundwater recharge by Empirical Methods

Average % of Groundwater Recharge		18.64	18.92	18.33	18.42	17.71	13.03	11.45	15.13	16.75	16.49	17.06	18.65	16.89	18.46	18.92	17.07	18.03
Kumar & Sethapathi (GW recharge in mm)	$R_g = 0.63 (P-15.29)^{0.76}$	8.63	13.1	7.61	7.87	6.38	2.95	2.37	3.98	5.22	4.97	5.54	8.67	5.35	7.99	10.6	5.55	6.94
GW recharge %		29.7	26.3	30.4	30.3	31.1	28.4	26.2	30.5	31.2	31.2	31.3	29.7	31.3	30.2	28.2	31.3	30.8
Sehgal (GW recharge in mm)	$R_g = 2.5 (P-16)^{0.5}$	13.8	18.3	12.6	12.9	11.2	6.43	5.43	8.02	9.73	9.4	10.2	13.8	9.91	13.1	15.8	10.2	11.9
Krishna Rao (GW recharge in mm)		7.95	16	6.27	6.69	5.08	1.37	0.99	2.64	3.85	3.6	4.18	8	3.99	6.88	11.3	4.19	5.69
GW recharge %		17	14.1	17.7	17.5	18.6	19.8	19.3	19.9	19.4	19.5	19.2	17	19.3	17.5	15.7	19.2	18.2
Bhattach- arjee (GW recharge in mm)	$Rg = 3.47(P - 38)^{0.4}$	20	24.9	18.7	19.1	17.1	11.4	10.2	13.3	15.3	15	15.8	20	15.6	19.2	22.3	15.9	17.8
GW recharge %		16.3	14.4	16.7	16.6	17.2	16.5	15.6	17.3	17.4	17.4	17.4	16.3	17.4	16.6	15.4	17.4	17
UPRI (GW recharge in mm)	$1.35(P - 14)^{0.5}$	7.6	10	7	7.1	6.2	3.7	3.2	4.5	5.4	5.3	5.6	7.6	5.5	7.2	8.7	5.7	6.6
GW recharge %		17.1	14.3	17.9	17.7	18.8	19.9	19.4	20.1	19.5	19.7	19.3	17.1	19.5	17.6	15.8	19.3	18.4
Chaturvedi (GW recharge in mm)	2(P-15)e0.4	7.9	9.9	7.4	7.6	6.8	4.5	4	5.3	6.1	5.9	6.3	8	6.2	7.6	8.8	6.3	7.1
Average Rainfall in mm		1176.7	1763.4	1055.4	1085.8	915.76	574.35	526.33	667.98	791.06	765.58	824.75	1180.4	805.18	1099.6	1422.7	825.95	978.17
year		1980	1981	1982	1983	1984	1985	1986	1987	1988	1989	1990	1991	1992	1993	1994	1995	1996

1997	1083.2	7.6	17.7	7.1	16.6	19	17.6	6.66	12.9	30.3	7.85	18.41
1998	777.75	6	19.6	5.3	17.4	15.1	19.5	3.72	9.56	31.2	5.09	16.62
1999	966.33	7	18.4	6.5	17	17.7	18.3	5.57	11.7	30.9	6.84	17.97
2000	845.81	6.4	19.2	5.8	17.3	16.1	19.1	4.39	10.4	31.2	5.74	17.23
2001	633.97	5	20.1	4.3	17.1	12.7	20	2.3	7.48	30	3.61	14.48
2002	716.55	5.6	19.9	4.9	17.4	14.2	19.8	3.12	8.74	31	4.48	15.88
2003	709.89	5.6	19.9	4.9	17.4	14.1	19.8	3.05	8.64	30.9	4.41	15.79
2004	879.33	6.6	19	6	17.3	16.6	18.9	4.72	10.8	31.2	6.05	17.48
2005	1397.6	8.8	15.9	8.5	15.5	22.1	15.8	11	15.6	28.4	10.4	18.9
2006	1199.6	8	17	7.7	16.2	20.2	16.9	8.26	14	29.6	8.82	18.68
2007	1425.6	8.8	15.8	8.7	15.4	22.3	15.6	11.4	15.8	28.2	10.6	18.92
2008	1187.7	8	17.1	7.6	16.3	20.1	16.9	8.1	13.9	29.7	8.72	18.66
2009	1395.3	8.7	15.9	8.5	15.5	22	15.8	11	15.6	28.4	10.4	18.9
2010	1144.6	7.8	17.3	7.4	16.4	19.7	17.2	7.5	13.5	29.9	8.37	18.57
2011	1263.3	8.3	16.6	8	16	20.8	16.5	9.14	14.5	29.2	9.34	18.78
2012	690.34	5.4	20	4.7	17.3	13.7	19.9	2.86	8.36	30.8	4.21	15.49
2013	690.34	5.4	20	4.7	17.3	13.7	19.9	2.86	8.36	30.8	4.21	15.49
2014	1201.9	8	17	7.7	16.2	20.2	16.8	8.29	14	29.6	8.84	18.68
2015	782.43	6	19.6	5.4	17.4	15.2	19.4	3.76	9.62	31.2	5.13	16.66
2016	811.03	6.2	19.4	5.6	17.4	15.6	19.3	4.05	9.98	31.3	5.41	16.94

5.7.1.1 Chaturvedhi formula (1936)

According to this formula the highest rainfall recharge is observed is 20.1 % in the year 2001 and lowest rainfall is observed in 14.25 %in the year 1981. The mean recharge of 18.28 % is observed in last 30 years.

5.7.1.2 Up Irrigation Research Institute Formula

Based on this formula the estimated groundwater recharge ranges from 17.43 % in the year 1981 and 14.25 1981 The mean recharge of 16.69% is observed in the study period.

5.7.1.3 Bhattacharjee Formula (1954)

The estimated lowest groundwater recharge (14.14) is noticed in 1981 and highest (19.28) is noticed in 1986. The average rainfall induced recharge of 18.1 is observed in between the year 1980 to 2016.

5.7.1.4 Krishna Rao Formula (1970)

According to this formula Groundwater recharge is varies between 29.22 % (Year 2001) to 31.97% (Year 2006). The 30.84% of mean recharge is observed in last 20 years.

5.7.1.5 Sehgal Formula (1973)

According to Sehgal formulae the groundwater recharge varies in between 28.18 % to 40.08 % for the year 2001 and 2006 respectively. The average recharge of 34.27% is observed in 1996 to 2015.

5.7.1.6 Kumar and Seethapathi (2002)

Based on above formulae groundwater recharge ranges from 15.69% to 17.56 % for the year 2001 and 2006 respectively. The average recharge of 16.57% is observed in 1996 to 2015.

5.8 Comparison of Empirical Formulas

The calculated Groundwater recharge percentages were compared and are shown in Figure 5.25. Among these methods, Chaturvedi, Bhattacharjee, UPRI are coinciding and are suitbale for our study area.

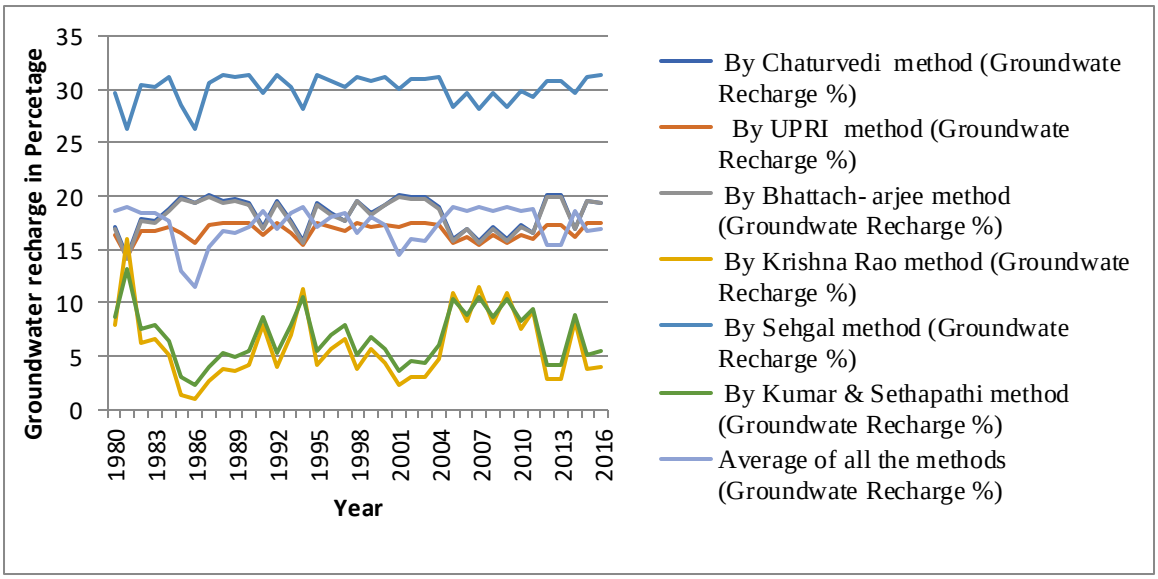

Figure 5-24 Comparitive Graph of Groundwater recharge Estimation by various empirical methods

5.9 Correlation Analysis of Empirical Methods for Groundwater Recharge Estimation

Inter Correlation Matrix of Annual rainfall Recharge shows Chaturvedi formulae is more positively correlated with UPRI formulae and Kumar and Sethapathi formulae and very less positively correlated with Bhattacharjee formulae. Chaturvedi formula is more negatively correlated with Krishna Rao and Sehgal formuale. It indicates Chaturvedi, UPRI and Kumar and Sethapathi formulas are nearly same.

5.10 Groundwater Resources Estimation

5.10.1 Dynamic Groundwater Resource Estimation by Groundwater Estimation committee norms (GEC-2015)

The dynamic groundwater resources were calculated as per the GEC-2015 norms. The Malaprabha sub-basin comprises of non-command (Karnataka state watershed code 4D7C9) and command (4D7C8) covering an area of 290863.00 Ha. The Groundwater Estimation has been carried out separately for two watersheds (4D7C8 and 4D7C9).

5.10.2 Groundwater Resource Estimation of 4D7C9(Non-Command):

This watershed is in the upper catchment of the sub-basin covering an area of 119700 Ha. For the estimation purpose the rocky area of 3997 is eliminated as there is less recharge or no recharge from the area. Hence the groundwater resources are calculated for the area 115703 Ha. The watershed covers mainly Khanapur, Belagavi and Bailahongal talukas.

The calculations are done as per the Groundwater Estimation Committee norms and are placed in Annexure -I

The Groundwater resources estimated by rainfall infiltration method is 42635.12 Ham and by Groundwater fluctuation method is 41686.94. In order to find the suitability of methodology percent difference is calculated by difference obtained from the two methods over the recharge obtained by rainfall infiltration factor method. The ratio is multiplied to get the percent difference (PD). For this watershed the PD is -2.22 and is less than +/- 20 % hence the Groundwater fluctuation method is adopted.

The gross recharge from rainfall infiltration and return recharge from all the surface water sources is 48821.82 Ham. The net Groundwater draft which includes irrigation, domestic and

Industrial use is 27940.5 Ham. The percentage against draft to net groundwater recharge is 57.22%. Hence this water shed is categorised as Safe for Groundwater exploitation.

5.10.3 Groundwater Resource Estimation of 4D7C8(Command and Non-Command):

This watershed is in the Lower catchment of the sub-basin covering an area of 111075 Ha of Non-Command area and 53092.93 of Command area (Both Lift irrigation and Malaprabha left bank canal command below the reservoir. For the estimation purpose the rocky area of 8080 Ha in non-command area and 7065.75 Ha is eliminated as there is less recharge or no recharge from the area. Hence the groundwater resources are calculated for the area 102995 Ha non-command area and 46025 Ha of command area. The watershed covers mainly Bailahongal, Savadatti, Ramdurga talukas.

The calculations are done as per the Groundwater Estimation Committee norms and are placed in Annexure -II.

The Groundwater resources estimated by rainfall infiltration method is 18150 Ham and by Groundwater fluctuation method is 19600.37Ham. In order to find the suitability of methodology percent difference is calculated by difference obtained from the two methods over the recharge obtained by rainfall infiltration factor method. The ratio is multiplied with 100 to get the percent difference (PD). For this watershed the PD is 7.99 % and is less than +/- 20 % hence the Groundwater fluctuation method is adopted.

The gross recharge from rainfall infiltration and return recharge from all the surface water sources is 24379 Ham. The net Groundwater draft which includes irrigation, domestic and Industrial use is 14101 Ham. The percentage against draft to net groundwater recharge is 57.84%. Hence this water shed is categorised as Safe for Groundwater exploitation.

5.11 Geophysical Studies

Electrical resistivity technique has been widely employed in groundwater exploration, depth to bedrock determination and basement rock characterization (Zohdy *et al.*, 1974; Beck, 1981; Olorunfemi and Okhue, 1992).Geoelectric investigation of Malaprabha sub basin was carried out with a view of understanding the subsurface lithology and hydrogeological setting to characterize the groundwater potentials.

5.11.1 Data acquisition and interpretation:

In this study, a total of sixteen VES (Vertical Electrical Sounding) stations were carried out. Resistivity meter was used for the geophysical survey. The apparent resistivity values were obtained using the product of apparent resistance and geometric factor. For the manual data interpretation, apparent resistivity values were plotted against half current electrode separation (AB/2) on a log-log graph. Partial curve-matching was performed using the Schlumberger array master curve and auxiliary curves to determine the layer resistivity values and thicknesses.

The results of the electrical soundings carried out in this study area are presented in figures from .Sixteen locations sounded at the Malaprabha catchment were used to characterize the subsurface lithology to a depth of about 100-120m. Based on the interpretation of the VES resistivity data, the inferred geo-electric sections revealed the thickness of the various formations in the study area.

Quantitative Interpretation

Quantitative interpretation allows getting the real numbers of layers, their resistivities and thicknesses. The 4 different types of curves for a three-layered surface are explained below.

A Type: (p1< p2 <p3) 'A' type curves are obtained in typical hard rock terrain with thin topsoil and hence the resistivity of layers increase continuously with depth.

Q Type: (p1> p2> p3) A resistivity curve with a continuously decreasing resistivity is called 'Q' type curves. This kind of is very common in the study area

H Type: (p1> p2 <p3) Seen generally in hard rock terrains consisting of top soil of high resistivity followed by either a water saturated or weathered layer of low resistivity and then a compact hard rock of very high resistivity at the bottom.

K type: (p1< p2> p3) Seen usually in basaltic areas such the 'K' type curves show a peak with values lowering towards the sides. Also present in coastal areas where freshwater aquifer occurs between clayey layer at the top and a saline zone in the bottom.

A simple linear graphs were drawn to show the variation of resistivity with depth. Figures 5.25 to 5.28.

5.11.2 VES Curves of Grainitic Terrain

VES soundings obtained for a grainitic terrain in Khanapur taluk is shown in figure 5.25. Significant variation in the type curves are observed. Granite one and 3 show similar trend as that of A type curve, however in granite 3 a water saturated zone is found at a depth between 60-80m whereas in the case of granite one there is no water bearing zone up to the observed depth.

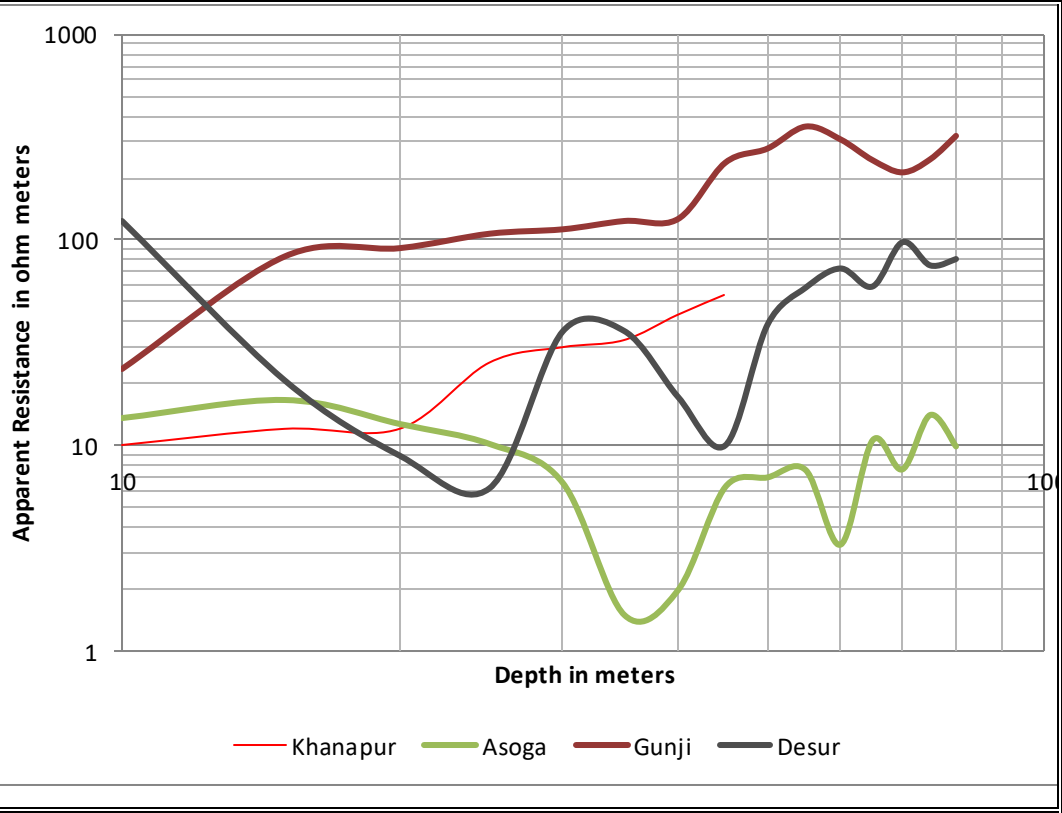

Figure 5-25 Vertical Electrical Soundings carried out in the Granitic terrain

In the case of granite 2 and 4 lower values are observed which is attributed to the presence of clay content. The granites continuously exposed to heavy rains causing the kaolinization. This is clearly indicated in the existing clay mines in and around Khanapur. These clay zones acts as impervious zones forming the perched aquifers. Hence the groundwater occurs mainly in the unconfined zones. The bore wells in this

zones are low yielding .(800-1200 Gallons Per Hour) since because of clay zones have less permeability. Table 5.10 shows the field observed resistivity values.

Table 5-10 The Apparent resistivity values obtained from various locations of the granitic terrain

S.No	AB/2	Khanapur	Asoga	Gunji	Desur
	Depth in meters	Apparent Resistivity in ohm-m	Apparent Resistivity in ohm-m	Apparent Resistivity in ohm-m	Apparent Resistivity in ohm-m
1	10	10.00	13.60	23.71	124.34
2	15	12.00	16.65	83.59	20.86
3	20	12.00	12.72	91.80	8.95
4	25	25.27	10.18	107.86	6.22
5	30	30.14	6.60	113.30	36.02
6	35	32.64	1.50	124.40	36.20
7	40	43.33	1.98	127.21	17.32
8	45	54.40	6.28	238.85	10.05
9	50		7.00	280.02	38.89
10	55		7.60	358.41	58.94
11	60		3.30	310.14	73.04
12	65		10.62	245.58	59.73
13	70		7.66	214.48	98.00
14	75		14.07	248.00	75.63
15	80		9.90	322.74	81.18

5.11.3 Basaltic formation

The resistivity curves obtained in the basaltic rock formation (figure 5.26) of the sub basin ranges between 35 to 100 ohm-m. Because of the presence of mafic minerals in basalts the electrical conductivity is less compared to the other type of rocks such as meta-greywacke, granite and quartzite. In between the basaltic lava flows the red bole bed is observed throughout the sub-basin. The resistivity values suddenly drops where

ever these bole beds are encountered. The sudden fall and small rise in the resistivity curves indicates presence of groundwater in basaltic flows. All the curves exhibited similar characteristics except in the case of series 4 which shows an undulating curve indicating the occurrence of groundwater in the unconfined state.

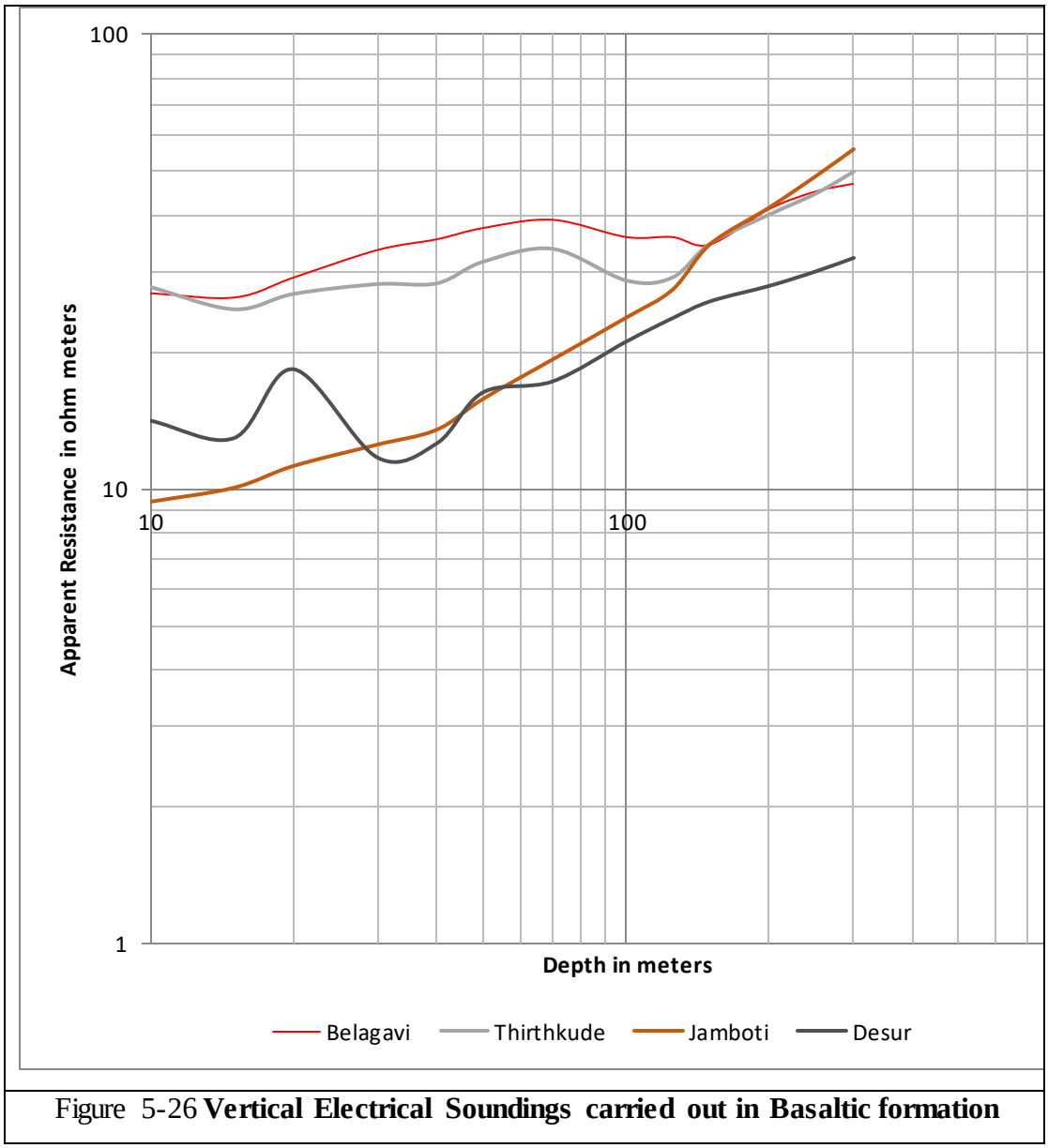

Figure 5-26 **Vertical Electrical Soundings carried out in Basaltic formation**

Table 5-11shows the resistivity variations along the profile of a subsurface horizon.

From the observations it is evident that the range of resistivity values are narrow and typically characterizes the weathered zone of basalt found in the study area.

Table 5-11 The Apparent resistivity values obtained from various locations of basin in basalt formation

S.No	AB/2	Belagavi	Thirthkude	Jamboti	Desur	K.Chandargi

	Depth in meters	Apparent Resistivity in ohm-m	Apparent Resistivity in ohm-m	Apparent Resistivity in ohm-m	Apparent Resistivity in ohm-m	Apparent Resistivity in ohm-m
1	2.5	91.09	65.64	41.99	120.03	75.04
2	5	40.2	32.26	14.62	20.18	27.23
3	7	31.77	31.1	10.53	5.5	19.99
4	10	26.93	27.82	9.38	14.1	16.05
5	15	26.37	24.84	10.07	12.9	13.7
6	20	29.18	26.86	11.24	18.33	14.6
7	30	33.5	28.23	12.52	11.68	15.47
8	40	35.36	28.34	13.5	12.56	17.04
9	50	37.405	31.63	15.77	16.29	19.75
10	70	38.99	33.77	19.25	17.23	23.04
11	100	35.75	28.75	23.79	21.12	25.77
12	125	35.75	29.21	27.4	23.79	28.78
13	150	34.42	34.73	34.47	25.93	33.5
14	200	41.16	40.25	41.54	28.07	40.866
15	250	44.93	44.76	48.61	30.21	48.232
16	300	46.733	50	55.68	32.35	55.598

5.11.4 Metagreywackes

Figure 5.27 shows the typical graph representing resistivity with depth. In general, the curve follows 'A' type curve where the resistivity shows an increasing trend. Though there are exception at shallow depths which is presumed due to the change in moisture conditions and soil type.

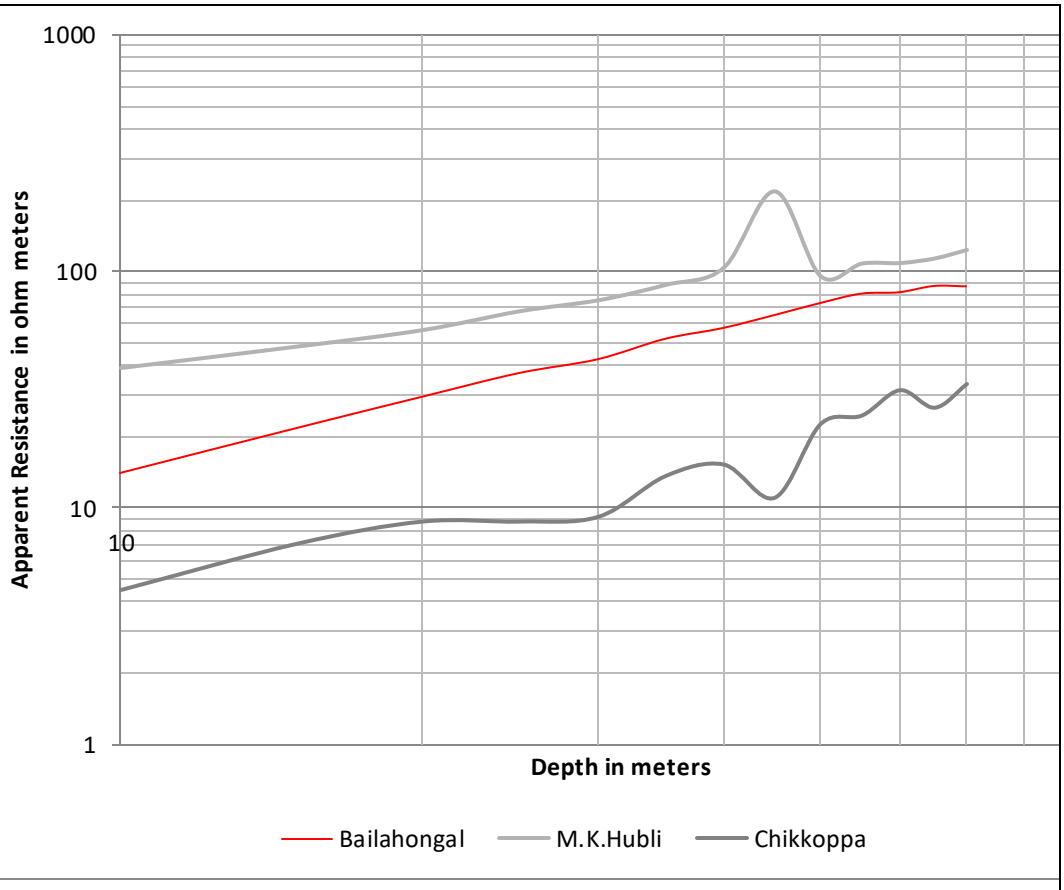

Figure 5-27 Vertical Electrical Soundings carried out in Meta Greywacke formation.

From Table 5.12 it is evident that the resistivity value indicates a gradual increase except at few depths. Such minor variations are very common in the study sites.

Table 5-12 The Apparent resistivity values obtained from various locations of basin in Meta Greywackes

S.No	AB/2	Bailahongal	M.K.Hubli	Chikkoppa
	Depth in meters	Apparent Resistivity in ohm-m	Apparent Resistivity in ohm-m	Apparent Resistivity in ohm-m
1	10	13.96	38.7	4.49
2	15	21.62	47.7	7.04
3	20	29.29	56	8.73
4	25	36.91	67.3	8.73
5	30	42.28	75	9.15
6	35	51.54	87.1	13.59
7	40	57.29	102.9	15.2
8	45	64.94	217.1	11.01
9	50	73.04	94.8	22.53
10	55	80.11	107.3	24.48
11	60	81.19	107.8	31.29
12	65	86.32	112.8	26.4
13	70	86.01	122.5	33.25
14	75	104.42	247.8	62.61

5.11.5 Quarztie Formation

From the figure 5.28, it is evident that both massive and water bearing formation are found in the downstream part of the study area. It is also noticed that the groundwater availability is restricted to depths below 120 m.

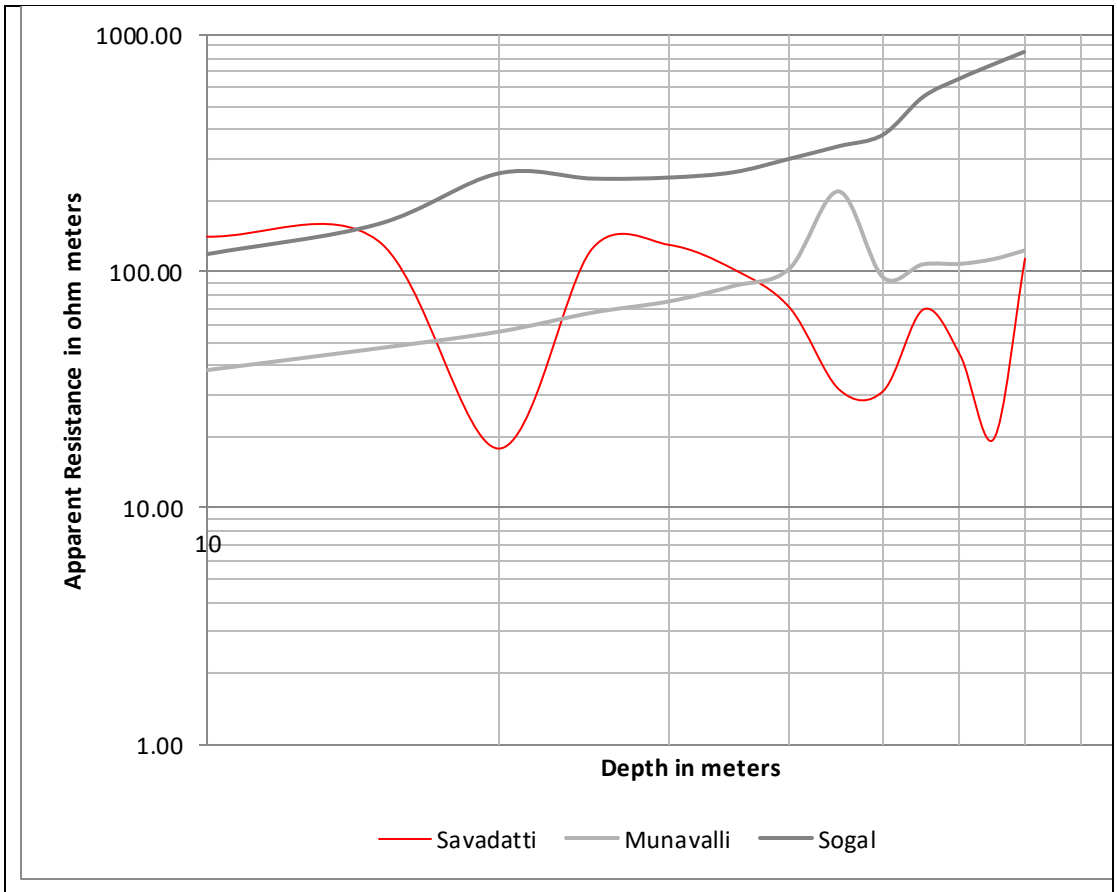

Figure 5-28 Vertical Electrical Soundings carried out in Quarzitic formation

Table 5.13 represent the observed resistivity in quartzite formation of Malaprabha sub basin. It is found that the resistivity values are relatively higher in the quartzite formation as compared to all other formation discussed above.

Table 5-13 The Apparent resistivity values obtained from various locations of basin in Quartzites

S.No	AB/2	Savadatti	Munavalli	Sogal
	Depth in meters	Apparent Resistivity in ohm-m	Apparent Resistivity in ohm-m	Apparent Resistivity in ohm-m
1	10	140.00	38.70	118.50
2	15	135.13	47.70	158.49
3	20	17.68	56.00	259.69
4	25	124.46	67.30	246.96
5	30	129.25	75.00	249.40
6	35	101.83	87.10	262.65
7	40	69.90	102.90	299.31
8	45	31.43	217.10	338.40
9	50	31.11	94.80	378.38
10	55	68.85	107.30	546.00
11	60	43.96	107.80	653.00
12	65	19.43	112.80	750.00
13	70	113.04	122.50	847.00
14	75	237.46	247.80	944.00
15	80	69.30	373.10	1041.00
16	85	89.01	498.40	1138.00
17	90	98.00	623.70	1235.00
18	95	111.00	749.00	1332.00
19	100	120.00	874.30	1429.00
20	105		999.60	1526.00
21	110		1124.90	1623.00
22	115		1250.20	1720.00
23	120		1375.50	1817.00
24	125		1500.80	1914.00

5.12 Groundwater Hydraulics

Estimation of Transmissivity using Geophysical data

The aquifer performance of any hydrogeological formation is based on two parameters, i.e. transmissivity and hydraulic conductivity. Generally, the aquifer parameters are estimated by using pumping test data analysis methods. In the present study, the transmissivity T value was determined by using the analytical relation between Transmissivity and Dar Zarrouk parameters, i.e. longitudinal conductance and transverse resistance. The transmissivity (T) of the aquifer is related to the field hydraulic conductivity (K by the equation as:

$T = Kb$ ---------- (5.1)

Hence, $K = T\, b^{-1}$

According to Niwas and Singhal (1981) in a porous medium, the Transmissivity (Tc) is defined as:

$Tc = K\, R\, \rho^{-1}$

$= KS\, \rho$ ----------(5.2)

Where Tc = calculated Transmissivity (m2/day) from VES

R= Total Transverse Resistance (Ohm-m2)

(resistivity *aquifer thickness)

S= Total longitudinal conductance (ohm-1)

P = resistivity of the saturated layer (potential aquifer zone) (ohm-m).

According to Froulich and Kelly observations, the transverse resistance ® is the dominant parameter for the layer in which current tends to flow perpendicular to conductance (S), observed in H type of curves. The estimated hydraulic characteristic parameters of the study area including transmissivity values and corresponding static water level are shown in Table 5.14. Data was also compared with the data collected from CGWB, Bengaluru

Table 5-14 Formation wise Pumping details of Malaprabha sub basin

Sl.NO.	Location	Topo sheet No	Depth drilled meters below Ground level	Lithology	Depth of Groundwater Occurrence mgbl	Discharge in lps	Drawdown (m)	Transmissivity (m2/day)	Static Water Level (mbgl)
1	Belgaum		40.65	Deccan trap	21.3-22.3	0.13			9.17
2	Kasabachandargi		26.15	Deccan trap	11.15-12.15	0.30			6.43
3	Agasge	48I-1B	80.00	Deccan trap	31-32, 43-44	0.50	0.775.	80.00	33.17
4	Jamboti	48I-2B	80.00	Deccan trap	13-14, 28-29	0.50	16.02	-	9.09
5	Murkatnal	47P-4A	200.00	Deccan trap	15-16	0.60	11.24	2.00	6.72
6	Belwadi junction	48I-2D	80.00	Granite	26-27, 29-34, 45-46	1.05	4.20	131.00	10.04
7	Londa	48I-3B	80.00	Granite	22-23. 43-44	0.30	22.14	-	10.50
8	Khanapur		40.65	Granite	22.35	0.30			8.84
9	Desur	8I-2C	80.00	Granitic gneises	26-27, 36-38, 50-51	0.40	26.20	-	5.33
10	Khanapur	48I-2C	88.00	Granitic gneises	22-24, 28-29, 33-34, 69	1.00	12.58	1.00	20.47
11	Kittur	48M-1B	57.60	Granitic gneisses	30-31	4.40	7.84	54.00	7.74
12	Suriban	48M-1B		Granitic gneisses	11-18, 21-28, 31-34, 49-51	4.80	6.39	155.00	5.94
13	Suriban	48M-1B	77.00	Granitic gneisses	23-24, 40-41, 74-75	2.00	11.46	57.00	5.79
14	Yadwad	47P-4A	80.00	Limestone		Negl			1.10
15	Tigadi	48I-1C	80.00	Meta Greywacke	27-29, 49-50	1.14	1.87	67.00	17.37
16	Itagi	48I-2C	82.00	Meta Greywacke	39-40, 57-58	Negl		-	24.61
17	Kittur	48M-1B	62.00	Meta Greywacke	34-35	0.60	13.72	1.00	7.95
18	Yargatti		40.65	Meta Greywacke		DRY			
19	Murgod		40.00	Meta Greywacke	34.5-35.5	-			28.04
20	Bailhongala		40.65	Meta Greywacke		DRY			
21	M-k-hubli		40.65	Meta Greywacke		0.75			22.06
22	Bidi		35.00	Phyllite		-			4.61
23	Manoli	48M-1A	32.45	Quartizite	20-22, 23-25, 26-32	4.20	2.42	96.00	8.59

24	Murgod	48I-1D	60.00	Quartizite	39-41, 50-52	0.40	1.00	25.00	17.00
25	Ramdurga		28.45	Quartzite	14.2-15.2, 16.25-17.25, 19.3-20.3, 22.35-23.35, 25.4-26.4	2.70	0.44		7.66
26	Savadatti		40.65	Quartzite/Granite	35.5-35.7	1.05	6.07	11.00	16.74

Chapter 6

Groundwater Modelling

6.1 Introduction

Optimum management of the available surface and subsurface water resources with respect to quantity and quality is an urgent need in view of increasing demand, declining groundwater levels and water logging problems. Efficient water management is one of the key elements in successful operation of irrigation schemes in arid and semi-arid regions. New technologies and improvement of on-farm water management are essential to solve the problems of rising/falling water tables and soil salinity. At the same time, it is equally important to develop regional water management policies, which may enable irrigation managers/planners to optimally manage the scarce available water resources. Therefore, regional solutions, based on integrated approach for ground and surface water management along with improved on-farm water management, have to be found. The groundwater model can be used as a regional model to study the effect of net recharge on water table behaviour in the area. The net recharge to the aquifer is the linking factor between the water balance of the unsaturated zone and the groundwater balance. This net recharge constitutes various recharge and discharge components, viz: rainfall, seepage from irrigation conveyance system, field irrigation losses, capillary rise from water tables and pumping from tube wells. In the present investigation and modelling, the net recharge from different sources from rainfall and other hydrological processes are calculated using both conventional and modelling approach. However, the major limitation is the non-representation of exact field conditions due to the use of general norms and also it does not help in studying the effect of different interventions from unsaturated part of the hydrologic cycle on the water table behaviour in the area so that the remedial measures can be taken. Therefore, it is necessary to simultaneously estimate the aquifer parameters and the recharge factors which requires field data for a period of one or more years. Presently, the quantitative assessment of groundwater, is done with the help of periodic measurements of water levels at observation wells, particularly during pre and post monsoon seasons.

Accordingly in the present study, with a basic objective of groundwater modelling of Malaprabha sub-basin, both SWAT model and Groundwater Modeling System (MODFLOW package) models were applied to simulate both surface and subsurface

flow processes, thereby enabling detailed description of watershed processes such as runoff, infiltration, in-streamflow, three-dimensional groundwater flow in a heterogeneous aquifer system with sources and sinks (e.g. pumping, seepage to subsurface drains), and spatially-variable surface and groundwater exchange. Model obtained results were also compared with the conventional estimation groundwater recharge and field observations.

6.2 Application of swat model

The Soil Water Analysis Tool which is widely known as SWAT model is a semi-distributed basin-scale model developed by the United States Department of Agriculture (USDA). In the present study, the SWAT interface for ArcGIS (Winchell *et al.* 2007) has been used to predict the impacts of land use and agricultural management on water (Arnold *et al.* 1998). The model considers multiple hydrological processes occurring in the soil: infiltration, evapotranspiration, percolation into a deeper aquifer and water losses by runoff, as well as lateral and deep percolation (groundwater recharge). The SWAT model has been calibrated and validated through the comparison of observed and simulated stream flow data, as well as nutrient and sediment loads at watershed outlets.

6.2.1 Input data for SWAT

Kumar (2013) explains that a large amount of information and a complete description of the flow system are required to make the most efficient use of the models. In situations where only rough estimates of the flow system are needed, the input requirements of models may not justify the use. The credibility of any model depends on the availability of wide range of data and proper incorporation of this data into the model. Higher the extent of detailed input data, higher will be the accuracy of the model. The model inputs required for the SWAT and MODFLOW models are discussed briefly below:

a) *Digital Elevation Model (DEM)*: The DEM for the study is obtained from BHUVAN portal of the Indian Space Research Organization (ISRO). The DEM available for the areas were CARTOSAT-1 with a spatial resolution of 30 meters. The ground surface elevations for the areas were obtained from DEM. Also, these were pre-processed using ArcGIS before being used in ArcSWAT for watershed delineation process.

b) *Land use maps*: The land use maps preapared by the Karnataka Space Application center with 1:50000 scale map is used for the present study. The detailed map and the geographical extents of the units are presented in Table 3.5 and is shown in figure 3.9

c) *Soil maps*: The global soil map prepared by the Food and Agricultural Organization (FAO) called as 'Harmonized World Soil Database (HWSD)' was used in this study. The HWSD can be freely downloaded from the official FAO website. Additionally, the database is also available at the website www.waterbase.org and www.swat.tamu.edu. Apart from the FAO soil map, the detailed soil and lithology map for the study area were obtained from the Karnataka State Water Resource Department.

d) *Meteorological data*: The gridded dataset of the meteorological data for the entire India for a period of 30 years from 1975 to 2005 is available as the 'Indian Meteorological Department (IMD) weather generator database'. It was presented at the 2012 International SWAT conference held at New Delhi and was developed specifically for the SWAT users to incorporate the weather parameters conveniently in the model database. The rainfall data obtained from 19 Rain gauge stations with in the study area are taken for the study.

e) *Hydrogeological data*: In order to accurately represent the real-world condition in the mathematical model, it is very essential to have sound knowledge and adequate dataset regarding the hydrogeological system of the study area. The data regarding the basic hydrogeology of the study areas was obtained from previous reports based on the field studies conducted by NIH, Belgaum. The 2012 report titled 'Aquifer systems of Karnataka' published by Central Groundwater Board, Bangalore imparted sufficient idea regarding the formations and geology of the study areas as well as value ranges for the basic soil parameters.

The SWAT model was applied to Malaprabha sub-basin for the estimation of recharge and evapotranspiration. The model was set up in a GIS environment and run for a simulation period of 14 years from 1980 to 1993, with the help of land use, soil and

elevation maps. Weather parameters such as daily precipitation and temperature were used as an input to the model, and other parameters (relative humidity, solar radiation and wind speed) were simulated using IMD weather generator database. The model was then calibrated for a period of nine years from 1980 to 1988 using observed daily runoff data at the Khanapur gauging station. The catchment considered for the calibration is up to the first gauging site of Malaprabha catchment.

Initially in the SWAT the model divided the catchments into number of sub-units and further classified the sub-units into HRU's based on soil, land use and slope characteristics (Figure).

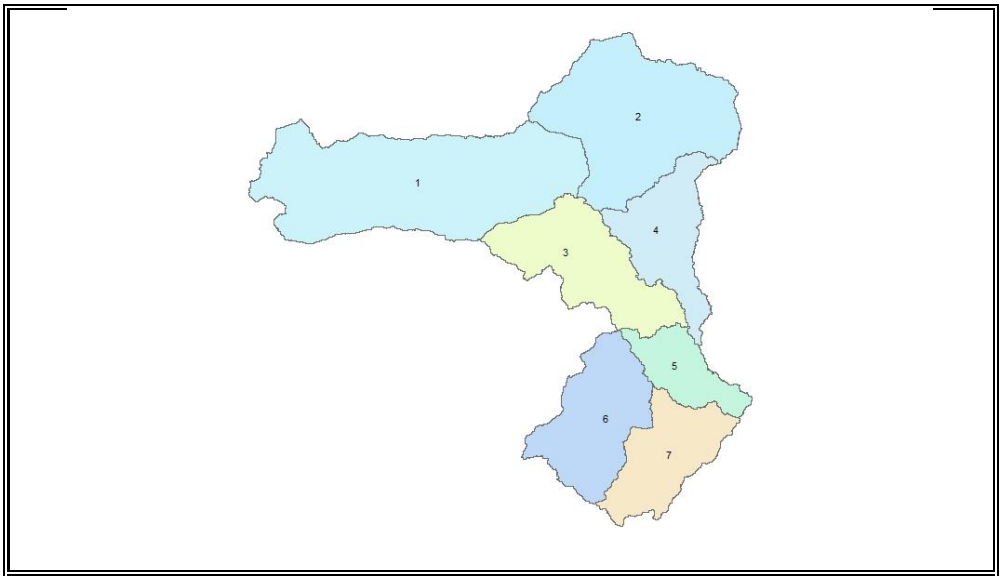

Figure 6-1 Malaprabha catchment demarcated into sub-units by using SWAT model

6.2.2 Calibration and Validation of the SWAT model

The calibration of a model includes the determination of the spatially distributed value of certain input parameters of which no exact information is available. Therefore, the value of different parameters is varied within a pre-set range. Model results obtained with the input parameters are compared with observed results and the parameters giving the best match of calculations with observations are fixed for further model applications. The adjustments of the value of parameters are a matter of professional guessing based on the logic of the water balance. The validation of the model includes the determination of the reliability of predictions made through the model for circumstances, which differs from those for which the model was calibrated.

The whole simulation was performed with a daily time step; the first 4 years (1986–1989) were excluded from the results since they were used as a warm-up period.

First, a sensitivity analysis was carried out in order to identify calibration parameters. Then, by manual calibration, the parameters were adjusted. River discharge was calibrated at the outlet of the Malaprabha sub basin at Khanapur discharge point with the observed daily discharge of Khanapur gauging station for a period of 9 years (1980-1988) by using SWAT. The results obtained from the calibrated model is shown in figure 6.2.

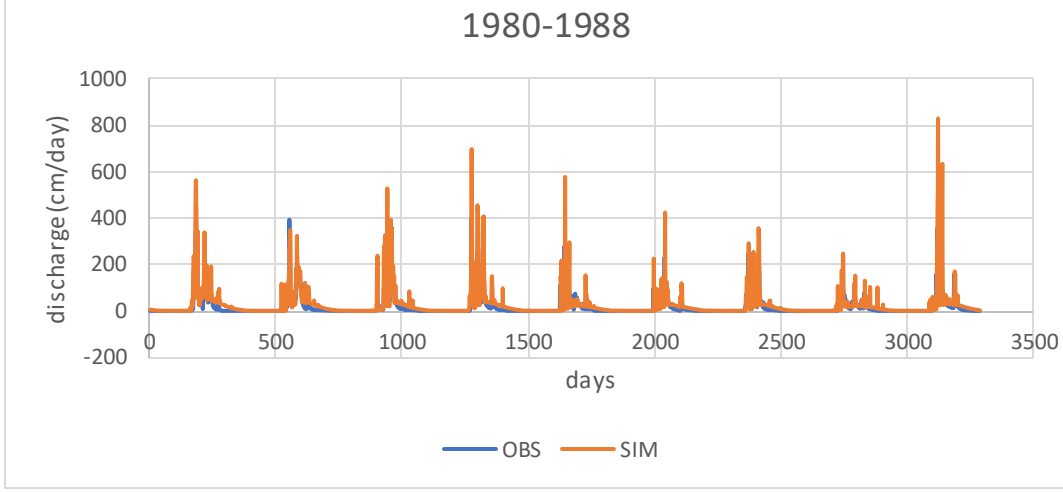

Figure 6-2 Observed and simulated discharge values for the calibration period

The calibrated parameters for the Malaprabha sub-basin is presented in Table 6.1

. Table 6-1 Fitted values of the parameters as obtained after the calibration

S. No.	Parameter Name	Fitted Value	Minimum value	Maximum value
1	R__CN2.mgt	-0.140000	-0.200000	0.200000
2	V__ALPHA_BF.gw	0.550000	0.000000	1.000000
3	V__GW_DELAY.gw	51.000000	30.000000	450.000000
4	V__GWQMN.gw	0.500000	0.000000	2.000000

•

Here, the parameters refer to the following:

CN2 = Initial SCS runoff curve number for moisture condition II

ALPHA_BF = Baseflow alpha factor

GW_DELAY = Groundwater delay (days)

GWQMN = Threshold depth of water in the shallow aquifer for return flow to occur (mm H_2O)

Additional information about the various parameters in SWAT model can be obtained in the official SWAT documentation. It can be downloaded from www.swat.tamu.edu.

6.2.3 Validation of the Model

The model was validated for the remaining five years i.e. 1989 to 1993. The graph plotted between the observed and simulated daily runoff values for the year 1993 is as follows:

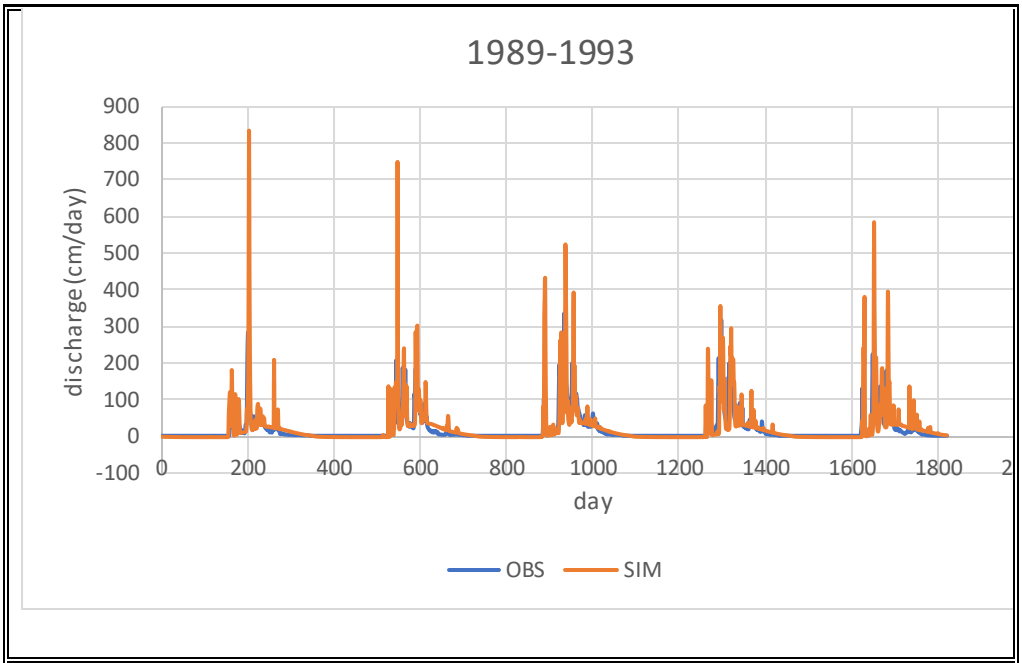

Figure 6-3 Observed and simulated discharge values for the validation period

6.2.4 Surface and Groundwater Interactions:

The total catchment area of the study area is 2800 sq km which is a part of the Sub-Catchment (Watershed Atlas of Karnataka) of Malaprabha sub basin. In the SWAT model, the sub-catchment is separated into sub-watersheds and are linked through a river channel. These hydrological boundaries are further sub-divided into hydrologic response units (HRUs) with overlay of soils, land uses, slope parameters in different ratios and combinations (Borah et al., 2006). The average curve number for the watershed is 82.01. The above variables which are simulated are routed through the

river network up to the mouth of the catchment. The water budget is computed as the difference in soil water content which is equal to the difference between precipitation, LULC water requirement and Surface run-off, base flow, lateral flow, percolation, evaporation and transpiration. SCS curve number method along with several other APEX algorithms are used in the computations of average curve number for the watershed. The yield in different stretches of the river is calculated using exponential functions considering lag co-efficient. Penman-Monteith, Priestly-Taylor, and Hargreaves are incorporated in the model to compute PET. Flows are added from different HRUs in order of flow direction to the sub –catchment scale and Muskingum method is used for routing the flows in the river to the catchment outlet.

Model delineated a total of 217 HRUs in the sub basin. The hydrological balance output from the SWAT model simulated according to respective HRUs includes major water balance components such as precipitation, evaporation and transpiration, percolation to shallow aquifer, surface run-off, lateral flows, return flow to the streams, recharge to deep aquifer, evaporation from shallow aquifer.

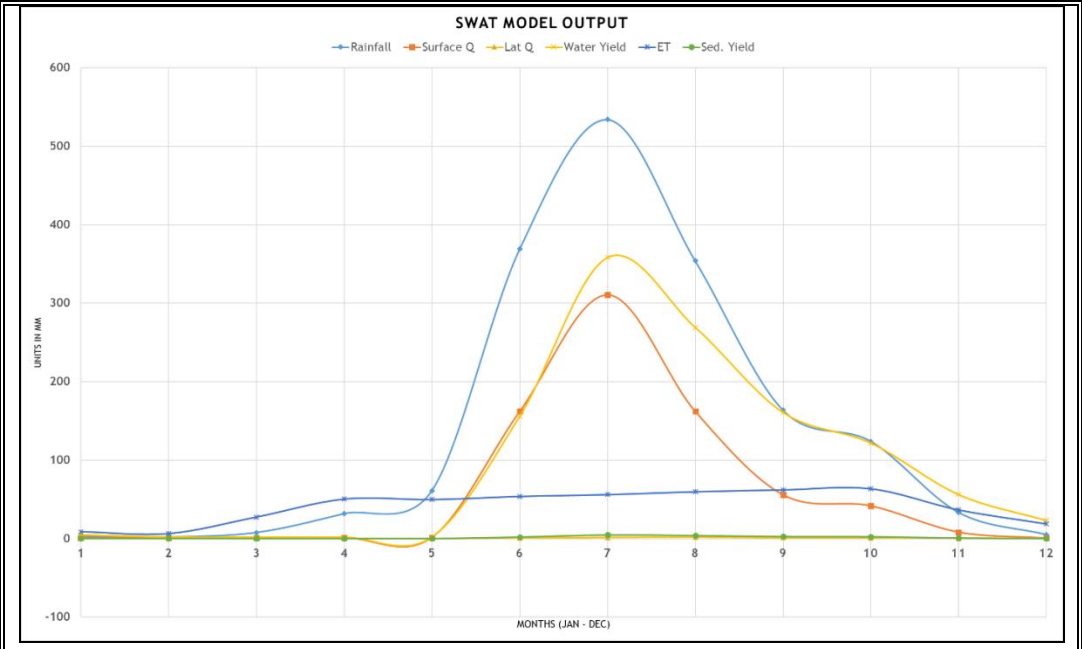

Figure 6-4 Water balance components obtained through SWAT model

The exponential base flow recession governs the Groundwater simulation in the model. The processes simulated in SWAT model is on monthly basis and performed the model run at the HRU level. The simulation run for 37 years with a warm-up period of 5 years provides the analysis results as the precipitation to be 1688.54 mm, the surface run-off

is 746.72 mm, Evaporation and Transpiration amounting to 494.53 mm, Return flow is 383.79 mm, Percolation to shallow aquifer is 439.68 mm, lateral flow is 7.36 mm, evaporation from shallow aquifer is 33.67mm and recharge to deep aquifer is 21.98 mm.

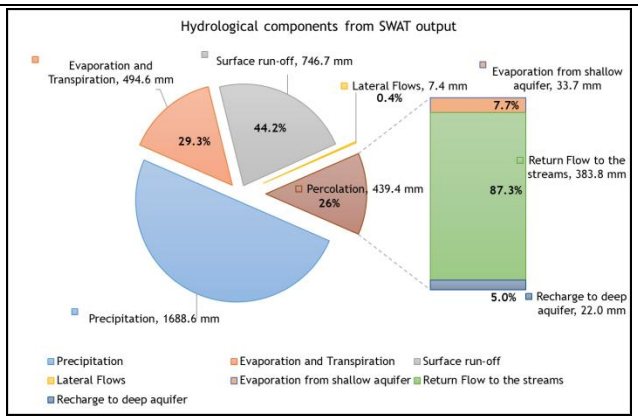

Figure 6-5 Water balance obtained from the Soil Water Assessment tool

Monthly rainfall, surface runoff lateral flow, water yield to the basin, Evapotranspiration and Sediment yield and potential evapotranspiration are shown in the Table 6.1

Table 6-2 Water balance components estimated using the SWAT Model

Month	Rainfall mm	Surface Q mm	Lat Q mm	Water Yield mm	ET mm	Sediment. Yield g/cc	PET mm
1	2.74	0.83	0.19	4.99	8.83	0.16	154.44
2	2.04	0.83	0.11	2.26	6.44	0.23	173.31
3	7.76	0.95	0.1	2.12	27.55	0.13	198.15
4	31.81	1.22	0.11	2.12	50.54	0.13	181.85
5	61.26	1.45	0.16	2.27	49.88	0.05	177.32
6	369.04	162.1	0.67	156	53.91	2.1	93.68
7	534.09	310.85	1.48	358.17	56.18	4.87	77.47
8	353.96	162.25	1.7	269.29	59.88	3.99	83.32
9	163.64	55.78	1.14	160.97	62.24	2.76	114.69
10	123.92	41.68	0.87	121.94	63.67	2.54	135.27
11	33.28	8.19	0.52	56.32	36.67	0.77	141.4
12	5	0.59	0.31	23.16	18.74	0.05	151.06
Total	1688.54	746.72	7.36	1159.61	494.53	17.78	1681.96

6.3 Conceptual Frame work of the Study Area

The hard rocks such as granites, basalts, metaquartzites or gneisses are of igneous or metamorphic origin with negligible primary porosity and permeability (Clark, 1985; Gustafson and Krásný, 1994). The crystalline outcrops are exposed in various locations of the study area. The storage capacity and well yield depends primarily on thickness,

degree of weathering and extent of the weathered zone. The massive hard rocks found beneath 70 m are devoid of any kind of fracture for the transport of water. However, in certain pockets of the study area due to stresses occurred during different geological periods added with physical and geochemical properties of the rock and paleo-climatic conditions resulted in the development of a network of joints and fractures. In the basaltic terrain, the thickness of the interflow bole bed varies widely from few centimetres to few meters and acts as an indicator to demarcate the flow occurred during different geological period. The lithological variations is shown in the form of fence diagram (figure 6.7).

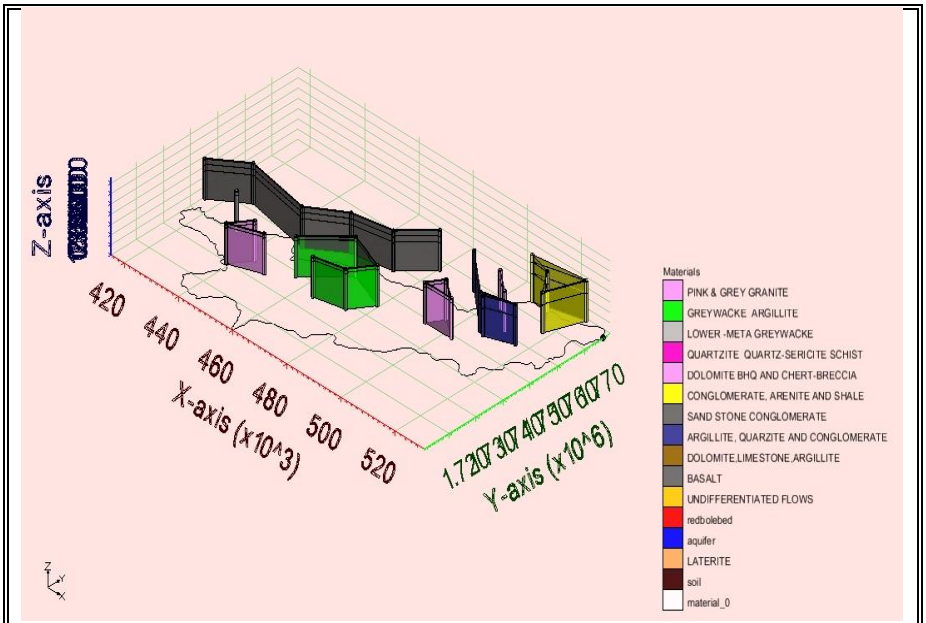

Figure 6-6 Fence diagram of the Borewells in the Malaprabha sub basin

Malaprabha river is an ephemeral river and become affluent and influent depending on the flow variations and surrounding groundwater fluctuations. Therefore, a river package embedded in the model was used. Leakage in to the fractured zone from the overlying weathered zone is also taken into consideration. Aquifer system may also show certain outflow and also receive water from the surface water bodies and streams through seepage as evidenced by studies conducted by various researchers. The delay in recharge to the aquifer is inappreciable, and the hydrogeological parameters do not change during the period for which the aquifer is simulated.

Basic assumptions made for the purpose of modelling based on field observations are listed below.

1. There are eleven lithological units with varying hydraulic properties
2. Spatial variation in hydraulic properties is significantly high

3. Groundwater Recharge is mainly due to Rainfall.

4. Ground water in the unsaturated zone is restricted to 15-17 m thickness.

5. Unsaturated zone is underlain by a thin layer of semipermeable/impermeable zone completely obstructing the ground water flow to the deeper aquifer

6. The groundwater in the deeper aquifer is only through fracture and joints

7. An overlying regolith (unconsolidated material derived from prolonged in-situ decomposition of bedrock.), with a thickness from negligible to a couple of tens of meters.

8. Weathering is more rapid in the semi-arid zone whereas in the arid areas and higher elevations the rate of weathering is low in comparison with that of erosion.

9. The regolith usually has a high porosity and a low permeability (due to clay-rich material)

10. The porosity of the weathered profile generally decreases with depth, along with clay content, until fresh rock is reached.

The schematic representation of the conceptualized model is shown in figure 6.7 The study area forms a part of isoclinal synclonorium with a wide variety of rock types dominantly granitic rocks as the basement above which sedimentary rocks such as greywackes, sandstones meta greywackes and quartzites. These are rocks are overlaid by the basaltic volcanic flows.

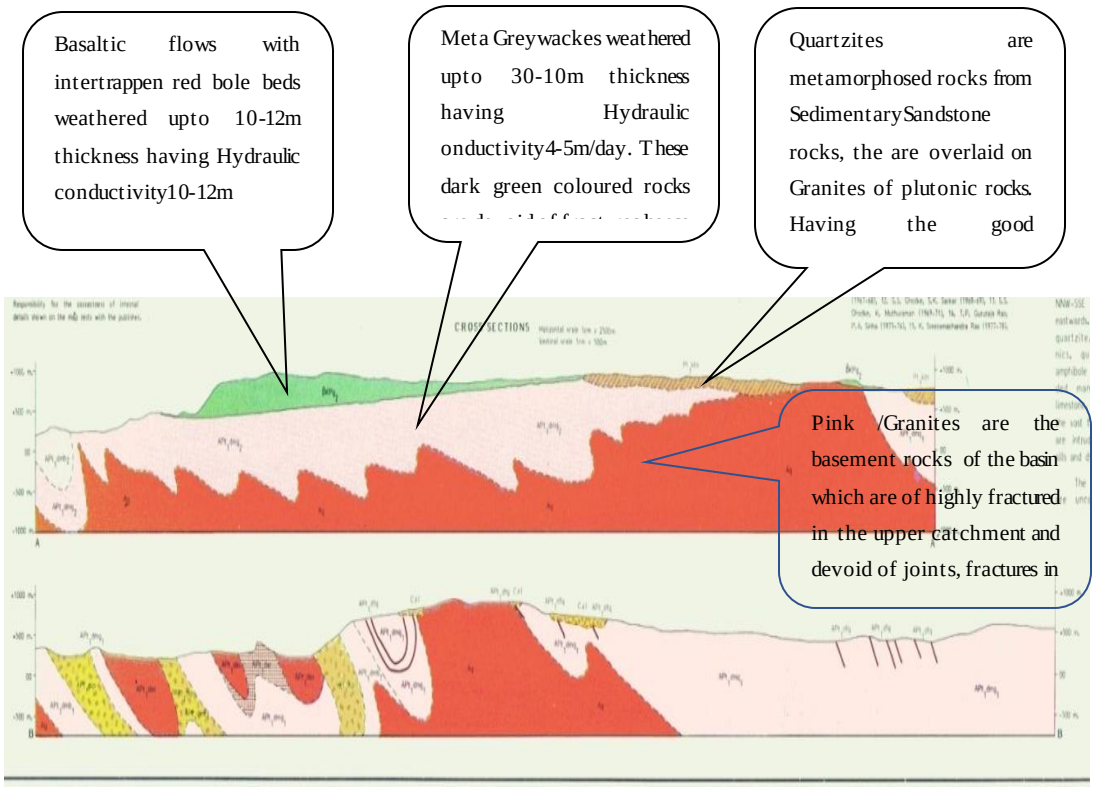

Figure 6-7 The Conceptualized Model of the Malaprabha sub-basin

6.3.1 Model Design

In the present study, three dimensional, numerical time dependent flow model of finite difference GMS program was applied to understand the hydrologic response of aquifers due to various kinds of stresses occurred due to cropping pattern followed during different seasons. An attempt is made to simulate a two-layer groundwater flow model through the defined conditions establishing of the boundary conditions. The above conceptual model (figure 6.6) was transformed to a form, suitable for mathematical modeling. The most important activities of model design include the design of spatial domain, selection of initial conditions and setting the boundary conditions.

6.3.2 Horizontal extent

The horizontal extent of the model domain is 120 km bounded by 41430 to 534304 m UTM East 1710425 to 1780425 m UTM north. The basin is bounded with in these co-ordinates. The area outside the basin is considered as no flow boundary and the area with in the boundary covers an area of 2800 square kilometers.

6.3.3 Vertical extent

Model layers, which are considered in the discretized domain, depends on the hydrogeological stratification of the system. Based on the geologic and geophysical

logs and well completion data, two layers of which unconfined layer of thickness 40 m and Semi confined (Leaky) aquifer of thickness 80 m is considered to model the Malaprabha Sub basin. The top and bottom elevations of the aquifer system are defined based on the lithological logs and the DEM extracted from the BHUVAN CARTOSAT image.

6.3.4 Discretization

In numerical models, the continuous natural phenomenon is replaced by a discretized domain, the so called grid. Grid size depends on hydraulic gradient, degree of aquifer heterogeneity, size of the model area, level of detail required and availability of data. Selecting the size of the nodal spacing is a critical step in grid design (Anderson & Woessner, 1992). The size of the nodal spacing in horizontal dimension is a function of the expected curvature in the water table or potentiometric surfaces. Finer nodal spacing is required to define highly curved surfaces. A grid with a smaller number of nodes is preferred in order to minimize data handling, computer storage and computation time. Yet, it is desirable to use a large number of nodes to represent the system accurately. By making simplifications and assumptions of the actual field condition, the model area is discretized to two layers with a regular grid of (1000 m by 1000 m, 70 rows by 120 columns) consisting of 19304 active cells.

6.3.5 Boundary Conditions

No flow boundary occurs across catchment as these boundaries coincide approximately with groundwater divides.

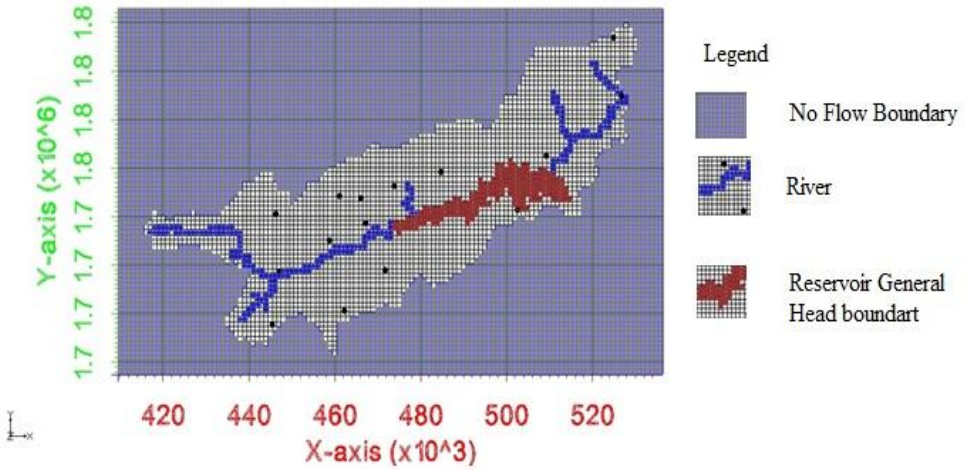

Figure 6-8 Boundary conditions

6.3.6 Initial conditions

The initial conditions in numerical groundwater models are initial head distributions and have only to be entered to fulfill the convergence criteria of the numerical scheme. If the hydraulic gradient between heads of boundary elements and non-boundary elements become too large, many computer codes will fail in their calculations by numeric instabilities. So for steady state models initial heads should be only in the range with the values of the hydraulic head conditions at the boundary element of the model. For the present case, the static water level records of the wells are interpolated within the model to obtain the initial hydraulic heads for the entire model (figure 6.9).

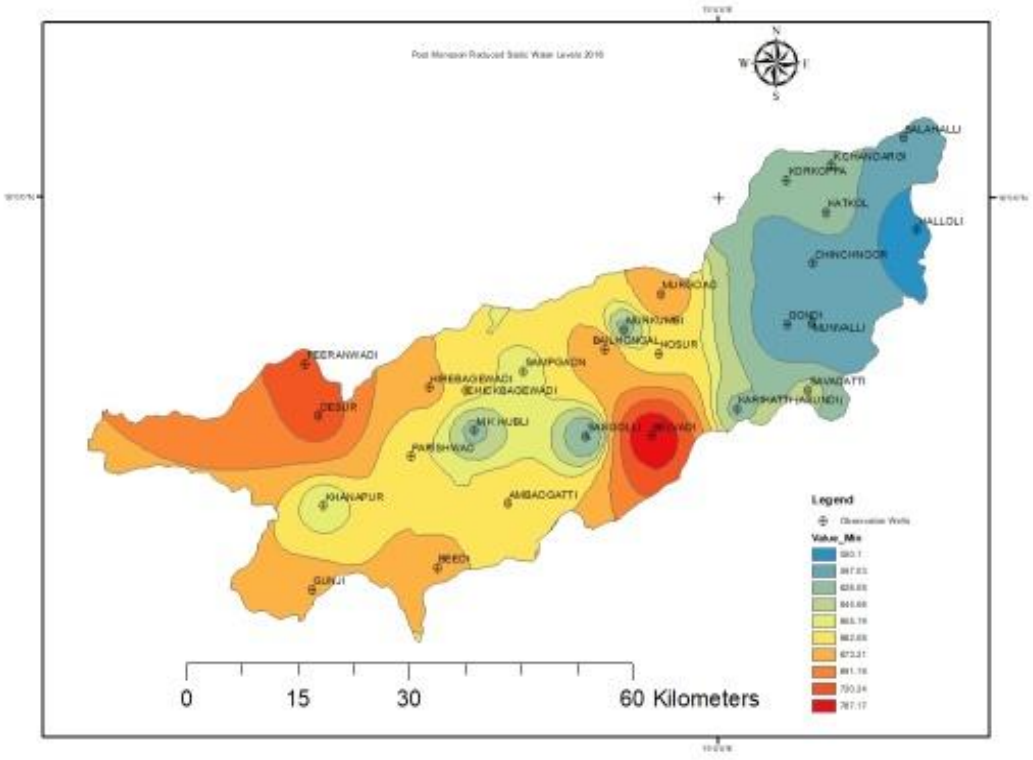

Figure 6-9 Starting heads (Groundwater levels)

6.3.7 Estimation of Groundwater Recharge using Infiltration Parameter:

Double ring infiltrometer and Disc permeameter were used to determine the infiltration parameters at identified sites based on land use, hydrogeology and soil characteristics. The rates of infiltration observed were converted into recharge components which is shown in figure 6.10

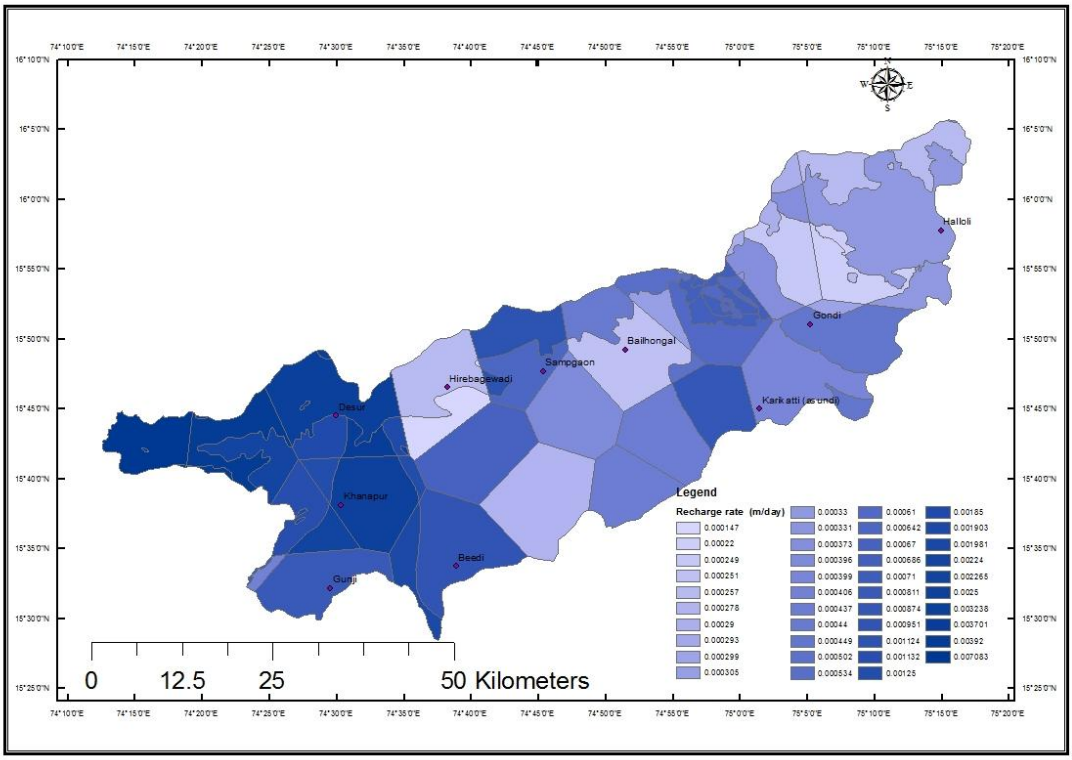

Figure 6-10 Recharge rates for Groundwater Modeling

6.3.8 Horizontal and Vertical Conductivity:

Hydraulic conductivities estimated from pumping tests were used as initial values for the steady state simulation. Since due to lack of adequate facilities only limited experiments were conducted for the determination of hydraulic conductivity and therefore a zonal pattern was adopted rather than nodal interpolation. The hydraulic conductivity values ranged between 1.8 m/d and 3.6 m/d and is shown in Fig. 6.11. The storage coefficient of 0.0002 for the basaltic terrain and 0.00028 for granitic terrain was assumed, based on earlier studies (Limaye 2010). Further, by trial and error calibration, the horizontal hydraulic conductivity was adjusted during many sequential model runs until the match between the observed and simulated heads were obtained. Also minor adjustments were done on the boundary conditions that were firstly used in the initial runs. Vertical conductivity is considered as $1/10^{th}$ of the horizontal conductivity.

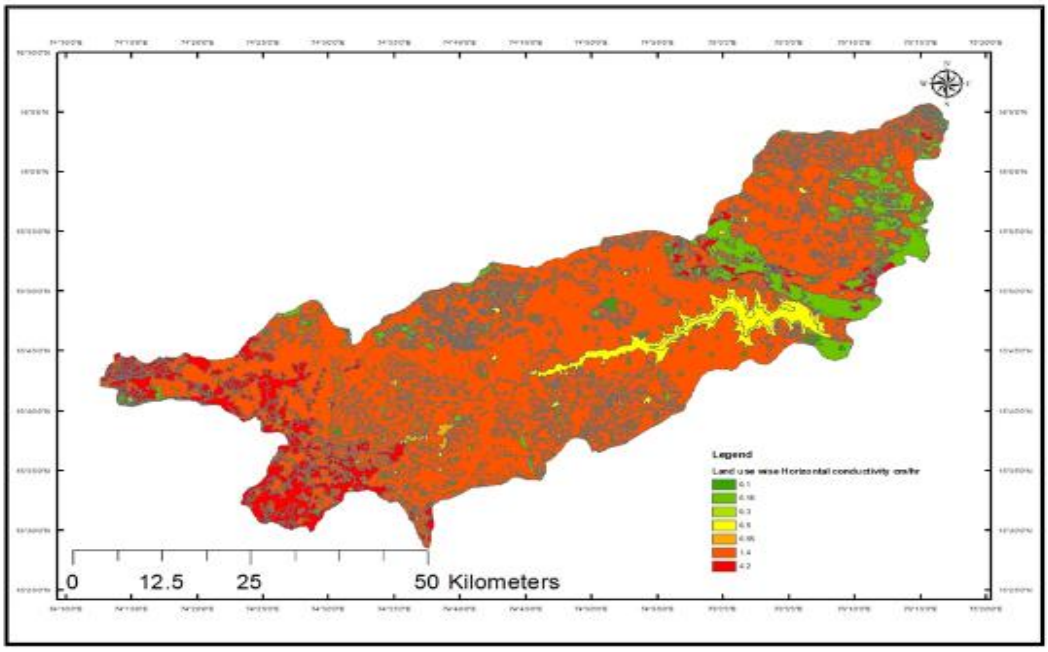

Figure 6-11 Distribution of hydraulic conductivity

The transmissivity values were taken from pumping test data. Lithologs were collected from Central Ground Water Board (CGWB), and Karnataka State Ground Water Department (KSGWD). The estimated transmissivity of the fractured granites ranges between 7 and 290 m^2/day and the specific yield of phreatic aquifer ranged between 0.01 and 0.04. The transmissivity range of vesicular basalts varied from less than 1 to approximately 198 m2/day. The average specific yield of the weathered basalt and laterite was 0.01 and 0.02, respectively. (Table 6.3).

Table 6-3 Hydraulic conductivity, Vertical Hydraulic conductivity, Specific yield taken into the model

Lithologic unit	Horizontal conductivity	Vertical conductivity	Horizontal anisotropy	Vertical anisotropy	Specific yeild
Granite	0.56	0.06	1.00	3.00	0.02
Meta greywacke	0.54	0.05	1.00	3.00	0.03
Dolomite bhq and chert-breccia	0.21	0.02	1.00	3.00	0.03
Conglomerate, arenite and shale	0.37	0.04	1.00	3.00	0.03
Sand stone conglomerate	0.37	0.04	1.00	3.00	0.03
Argillite, quarzite and conglomerate	0.37	0.04	1.00	3.00	0.03
Dolomite,limestone,argillite	0.37	0.04	1.00	3.00	0.03
Basalt	0.34	0.03	1.00	3.00	0.02
Undifferentiated flows	0.34	0.03	1.00	3.00	0.02
Laterite	0.54	0.05	1.00	3.00	0.02

Evapotranspiration (ET) of groundwater may occur when the water table is near or above the ground surface (top of layer 1). ET values were obtained from the SWAT model and used as an input to the model.

6.4 Estimation of Groundwater Draft:

The study area is primarily dependent on groundwater for its irrigation because of scanty rainfall and fewer surface water resources. The well draft data is a point source data. The there are 18950 groundwater abstraction structures with in the study area.The draft of the individual well varies from 11 m^3 to 22 m^3 per day. The taluka wise summarized draft per day is placed in Table 6.3

Table 6-4 Groundwater draft

Taluka	Total Number of Dugwells/ Borewells	Total Draft in m^3/day
Bailhongal	4460	71360
Belgaum	2516	40256
Khanapur	3299	52784
Ramadurg	3259	52144
Savadatti	5416	86656
Grand	18950	303200

6.4.1 Steady state calibration

The steady state condition is a condition that existed in the aquifer before any development had occurred. Matching the initial heads observed for the aquifer with the hydraulic heads simulated by Modflow is called steady state calibration. It is done by sequential adjustment of the model parameters. The groundwater flow model has been constructed for computation of hydraulic head distribution. As minor fluctuation is observed in groundwater level in the area, this indicates that hydraulic gradients do not change significantly with time (Hani et al., 2007). Thus groundwater flow was assumed to be under steady state condition represented by groundwater condition of June, 2015. For steady state simulation, 10 observation wells were included on the calculated versus observed heads graph (Figure 6.12). The groundwater levels measured during June 2015 were used as initial water level configuration for the groundwater flow model. The groundwater head in the aquifer model was computed by using GMS. In this case, the changes brought in every cell is below the set of convergence tolerance (here 0.01 m). The groundwater flow model has converged after 17 iterations. The purpose of the

calibration of a groundwater flow model is to demonstrate that the model can response field measured heads and flows. A trial and error calibration technique has been used. The flow model was calibrated by adjusting several parameters (Hydraulic conductivity, recharge, river and drain bottom conductance) within a narrow range of values until the best fit was obtained between the observed heads and simulated heads.

6.4.2 Model calibration

In order to get satisfactory results with maximum accuracy, all possible data have been collected based on observations, field experiments and also by laboratory analysis. The model was calibrated based on the observed heads obtained from the observation wells. In GMS Parameter Estimation Test (PEST) module is run to calibrate the model. For the calibration purpose the targeted hydraulic parameters are given negative key values in the model. The Model automatically recognizes the negative key values targeted for the simulation. The minimum and maximum values of the parameters range have to be entered in the Parameterization dialogue box. And the model was run. The model took several iterations and adjust the parameter values based on the Mass balance.

6.4.3 Calibration target and uncertainty

Prior to the calibration process, parameter setting is required. to derive calibration value and its associated errors. In the present case, hydraulic heads obtained from groundwater level monitored data during the study period and static water level was considered based on drilling time observation of June 2015. Water level measurements from some of the wells (Ambadagtti, Parishwad, Hirebagewadi) are erratic and are believed as outliers due to large measurement errors and are left out during calibration. The observation well data obtained from the 11 Observation wells with in the basin is considered as the target for the Model calibration.

S.NO	Observation Well Name	UTM E	UTM N	Altitude In m above MSL	Layer No	Observed Head in M above MSL
1	Bailhongal	484711.7	1749186	691.00	1	688.6
2	Beedi	462265.1	1720574	682.00	2	676.2
3	Desur	446288.3	1740487	739.00	1	738.25
4	Gondi	509250	1752499	615.00	1	605.75
5	Gunji	445460.3	1717691	700.00	1	699.3
6	Halloli	526693.7	1764896	569.00	1	566.6
7	Hirebagewadi	461142.7	1744205	708.00	2	694.55
8	Karikatti (asundi)	502531.7	1741345	638.00	1	636.3
9	Khanapur	447004.5	1728717	670.00	2	663.65
10	Sampgaon	473821.1	1746278	675.00	1	670.6

6.4.4 Trial and error calibration

Trial and error calibration is the process of manual adjustment of input parameters until the model produce field measured heads within the range of the error criteria. The model was calibrated for natural steady-state conditions with varying horizontal and vertical hydraulic conductivity values (Table 6.5)

Table 6-5 Estimated Hydraulic conductivity (HK), Vertical Conductivity(VK) and the Model predicted values of HK and VK.

S.No	Lithologic Unit	HK input	Model Predicted HK	VK input	Model Predicted VK
1	Granite	0.56	0.03	0.06	0.05
2	Meta greywacke	0.54	0.10	0.05	0.05
3	Conglomerate, arenite and shale	0.37	2.74	0.04	0.03
4	Sand stone conglomerate	0.37	0.03	0.04	0.03
5	Dolomite,limestone,argillite	0.37	0.30	0.04	0.03
6	Basalt	0.34	0.22	0.03	0.03
7	Undifferentiated flows	0.34	0.01	0.03	0.03
8	Laterite	0.54	0.73	0.05	0.05

The best fit results were achieved when the study area was divided into regions with different Hydraulic conductivity zones. The Hydraulic conductivity values applied during the calibration ranges from 0.21 to 0.56 m day^{-1}. The Hydraulic conductivity values attained during the calibration process are by little higher than the input Hydraulic conductivity from previous studies. The procedure followed during the trial and error method of calibration is indicated in Figure 6.2.

6.4.5 Sensitivity analysis

Sensitivity analysis is an essential step in all modeling applications. As discussed by Anderson & Woessner (1992), the purpose of a sensitivity analysis is to quantify the sensitivity of the model simulations in the calibrated model caused by uncertainty in the estimates of aquifer parameters, stress and boundary conditions. Sensitivity analysis provides information on which model parameters are most important to the simulated system. Sensitivity analysis is also inherently part of model calibration. The most sensitive parameters will be the most important parameters for matching the model result with the observed values.

To assess the sensitivity of the simulations in the calibrated model, Automatic PEST is applied and the model has increased some of the Hydraulic conductivity values and decreased Recharge values in order to maintain the mass balance and to reach the Calibration target.

The sensitivities of the Hydraulic conductivities are shown in the figure 6.16

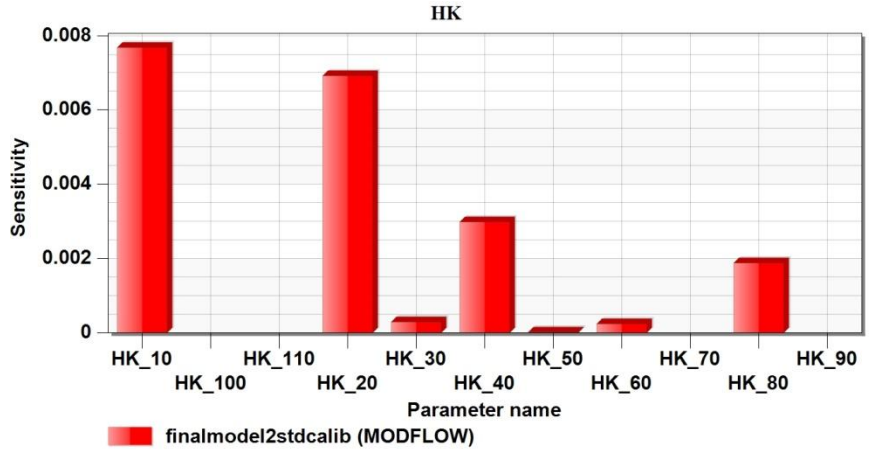

Figure 6-12 Hydraulic conductivity sensitivity

6.4.6 Recharge

Recharge to the groundwater regime resulting from monsoon rainfall, seepage from

surface water bodies, and irrigation return seepage from fields contribute as inputs to the aquifer system. The outflow occurs primarily through groundwater withdrawal from wells for irrigation and evapotranspiration, and acts as output. The groundwater recharge values were calculated lithologic unit use by considering the Infiltration factors obtained from the field studies. The weighted average of recharge values for the month of June-2015 were prepared by constructing the Theissen polygons and same are incorporated into the model. The sensitivities of the Recharge rates are shown in the figure 6.13

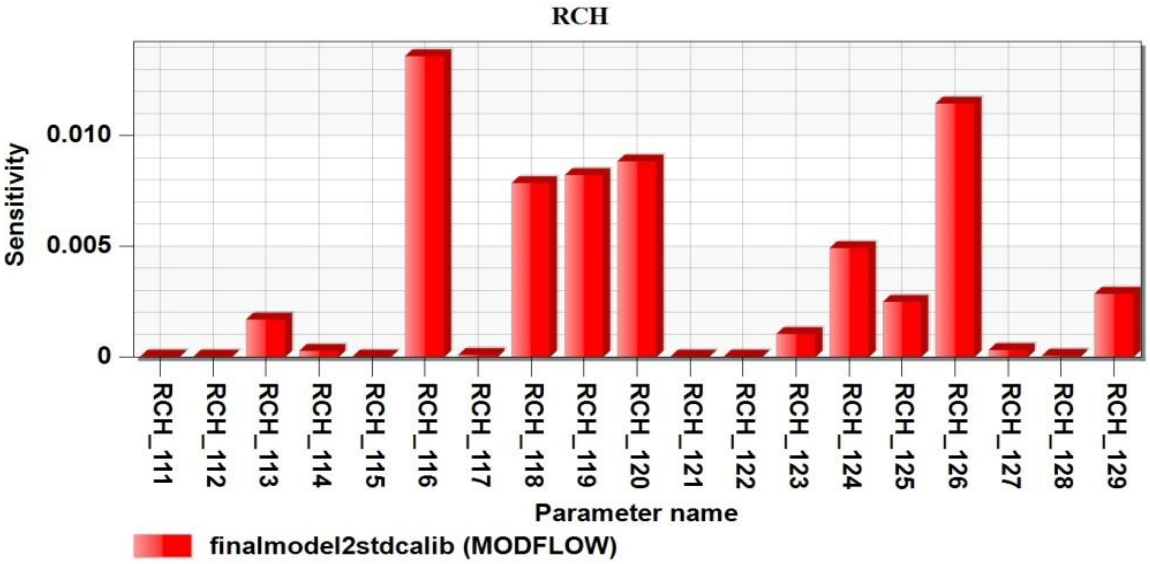

Figure 6-13 The sensitivities of the Recharge rates

Table shows the observed and computed heads before calibration. It is noticed that there is a significant variation between observed and computed heads. Variations are conspicuous particularly in the case of dug wells in comparison to bore wells. Maximum head estimated before calibration was -27.99m and minimum at Hirebagewadi borewell.

Table 6-6 Observed and calculated heads Before Calibration

Name	UTM X co-ordinate	UTM Y co-ordinate	Elevation in (m) above msl	Observed head in (m)	Computed Head (m)	Residual (m)
Bailhongal	484712	1749186	691	688.6	692.77	-4.17
Beedi	462265	1720574	682	676.2	674.47	1.73
Desur	446288	1740487	739	738.25	736.24	2.01

Gondi	509250	1752499	615	605.75	607.73	-1.98
Gunji	445460	1717691	700	699.3	698.8	0.5
Halloli	526694	1764896	569	566.6	569.41	-2.81
Hirebagewadi	461143	1744205	708	694.55	694.7	-0.15
Karikatti (asundi)	502532	1741345	638	636.3	635.88	0.42
Khanapur	447004	1728717	670	663.65	660.99	2.66
Sampgaon	473821	1746278	675	670.6	674.95	-4.35

The results of the model before (figure 6.14) calibration is presented. Comparison between contour maps of measured and simulated heads provides a visual qualitative measure of the similarity between patterns and also indicates the water table conditions of the study area.

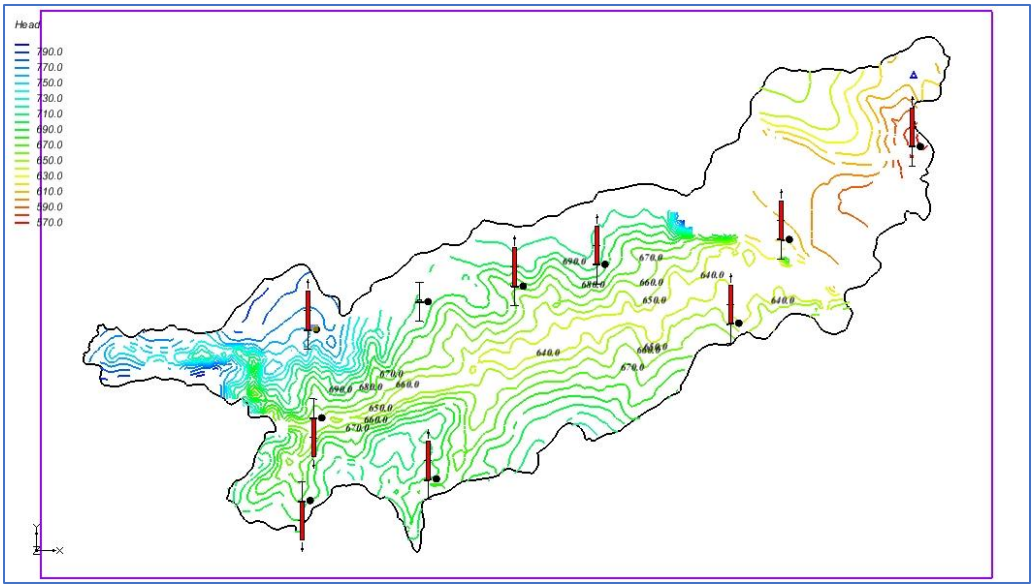

Figure 6-14 Contour map of simulated heads before the Calibration

Table 6.6 shows the relationship between observed and computed heads after calibration. The results of the calibration is quite appreciable in most of the wells except in the case of Gondi where the difference of groundwater level showed a wide variation (8.89 m) which indicates the hydrological variability in the particular part of the study area. Therefore, this can be considered as an outlier for practical purposes.

Table 6-7 Observed and calculated heads After Calibration

Obsevation well	UTM X co-ordinate	UTM Y co-ordinate	Elevation in (m) above msl	Observed head in (m)	Computed Head (m)	Residual (m)
Bailhongal	484711	1749185	691	688.60	688.59	0.01
Beedi	462265	17205745	682	676.20	676.28	-0.08
Desur	446288	17404878	739	738.25	739.13	-0.88
Gunji	445460	1717690	700	699.30	698.77	0.53
Halloli	526693	1764895	569	566.60	566.34	0.26
Hirebagewadi	461142	1744204	708	694.55	694.79	-0.24
Khanapur	447004	1728716	670	663.65	663.70	-0.05
Sampgaon	473821	1746277	675	670.60	670.62	-0.02

Simulated heads after calibration is presented below (figure6.15). There is a balanced distribution of residuals around zero and most of the residual heads are located between 0.01 and −2.89m. It is clear that the distribution of the head is almost normal around zero However, the calibration has brought down the computed head significantly which clearly indicates the sensitivity of the model application.

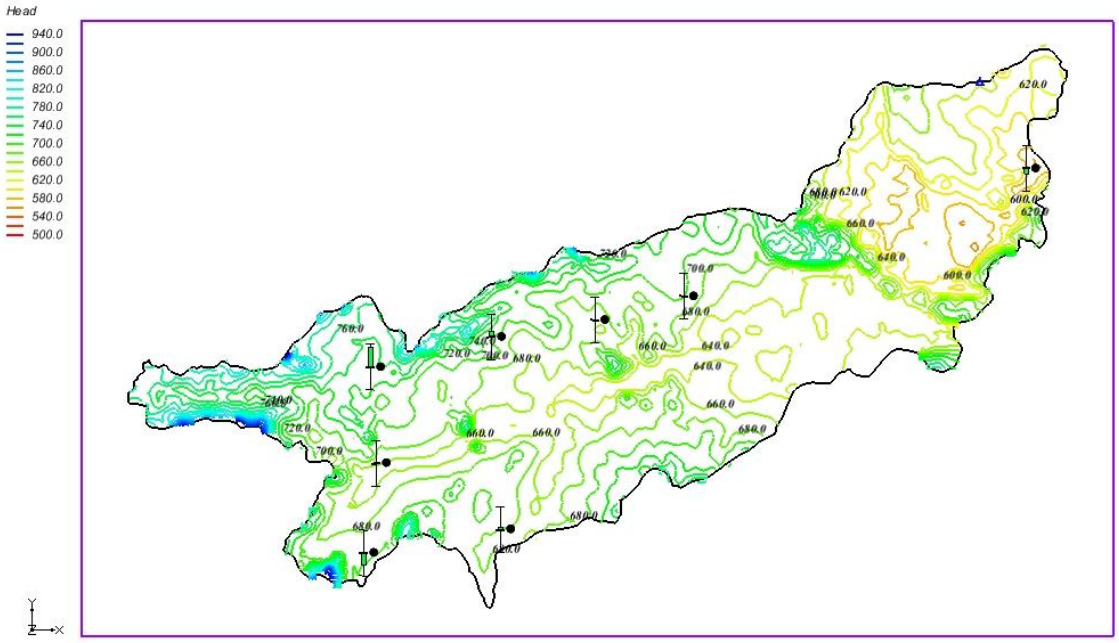

Figure 6-15 Contour map of simulated heads after the Calibration

6.4.7 Evaluation of calibration

The calibrated model was evaluated qualitatively and quantitatively as suggested by

Anderson and woessner(1992). Accordingly, hydraulic head distributions have been used as quantitative calibration targets whereas flow directions have been used as qualitative calibration targets. Qualitatively, the contour maps of the simulated heads were analyzed to see whether the results are comparable with the actual field condition. Flow direction was determined based on the simulated head distribution and comparison is made with the flow direction determined in the conceptual model. A scatter plot of measured against simulated heads is shown in figure 6.4 The scatter plots are visually examined whether points in a plot deviated from the straight line in a random distribution. Deviation of points from the straight line should be randomly distributed.

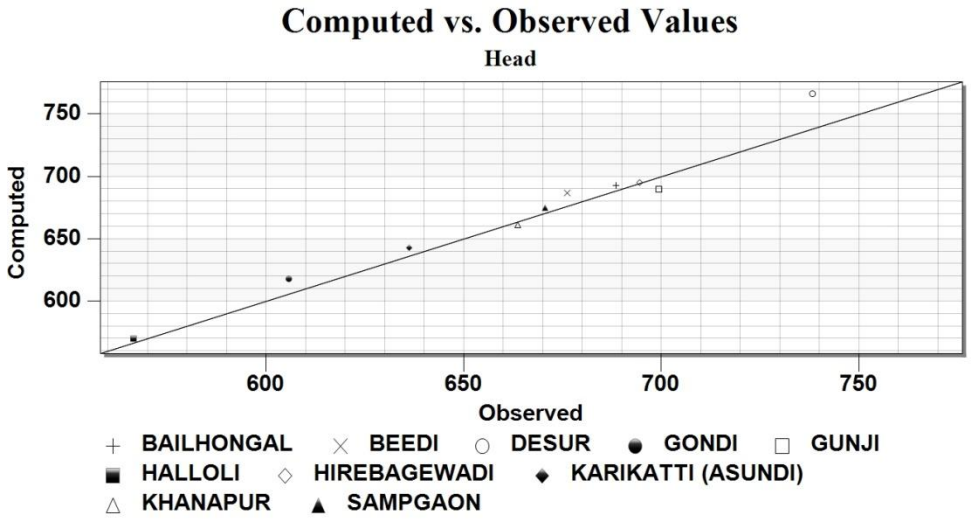

Figure 6-16 The Scatter plot before Calibraiton

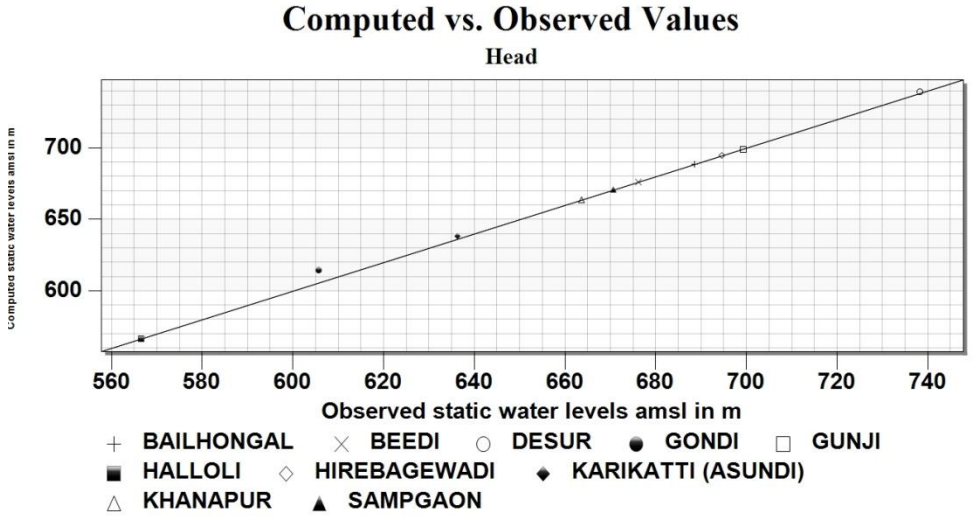

Figure 6-17 The Scatter plot after Calibraiton

The evaluation of the calibrated model result shows that most of the simulated heads are within the pre-established calibration target. Water balance discrepancy was zero

(Appendix 7). The overall results of the groundwater model are comparable with the measured well data and in agreement with conceptual model. The measure of errors evaluated by ME, MAE and RMSE are in the acceptable range according to the pre-determined error criteria. Table 6.3 indicates the model errors before and after calibration.

Table 6.3. Errors of the model before calibration and the rectified error after calibration

Error Description	Error Before Calibration	Error After Calibration
Mean Residual (Head)	-5.61	-1.15
Mean Absolute Residual (Head)	8.05	1.31
Root Mean Squared Residual (Head)	11.03	2.91
Mean Residual (Flow)	0	0
Absolute Residual (Flow)	0	0
Root Mean Squared Residual (Flow)	0	0
Mean Weighted Residual (Head+Flow)	-11	0
Root Mean Squared Weighted Residual (Head+Flow)	26.52	0
Sum of Squared Weighted Residual (Head+Flow)	4675.87	325.74
Displayed Precision	2	2

Though the overall result of the model was comparable with the measured well data, few observations which are not uniformly distributed over the model domain are utilised in the calibration process. Ideally calibration values should be measured at a large number of points uniformly distributed over the model domains. Thus it is not possible to conclude that the calibration is accurate by only quantifying the errors using ME, MAE and RMSE without considering the distribution of the residuals.

6.4.8 Model Validation

The uncertainties observed in the estimation of the aquifer parameters, stresses, and boundary conditions in the calibration, it is essential to apply the validation technique to make the model prediction more realistic. In model validation, the normal procedure is to define a set of measurements or observations of system variables, where part is used for model calibration and the remaining part is used for model validation. Here the steady state model for the month of June-2015 is calibrated and the same model is validated for the period June-2015 to May 2016. The Model shows satisfactory results and matches with the observed value. The following figure shows the Time series graph between observed and computed values of observation wells. Four locations, viz. Beedi, Desur, Parishwad and Sampgaon (dug and bore well) for which parameters such

as hydraulic conductivity and transmissivity were determined through field experiments and groundwater level data was monitored in order to obtain close proximity with the ground truth information. The observed and computed heads obtained during the process of validation for each individual well are shown in figures 6.18 to 6.22

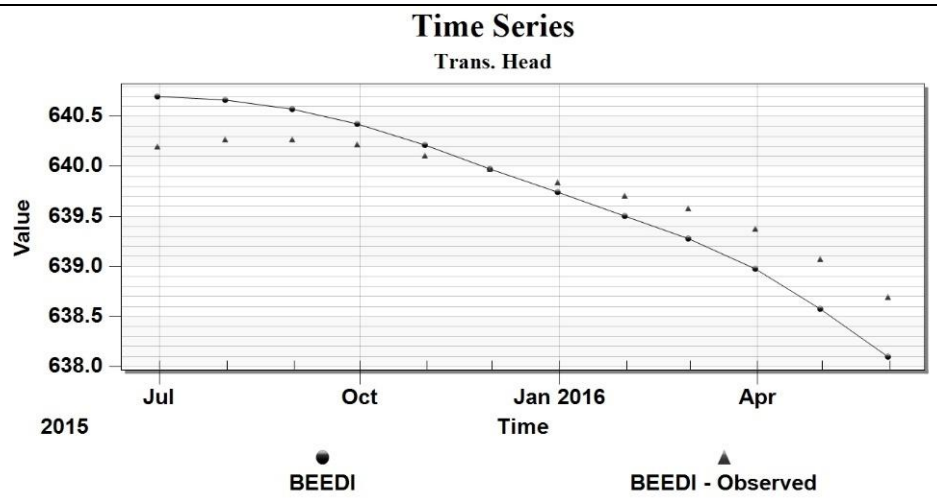

Figure 6-18 Computed V/S Observed Groundwater heads for Beedi observation well

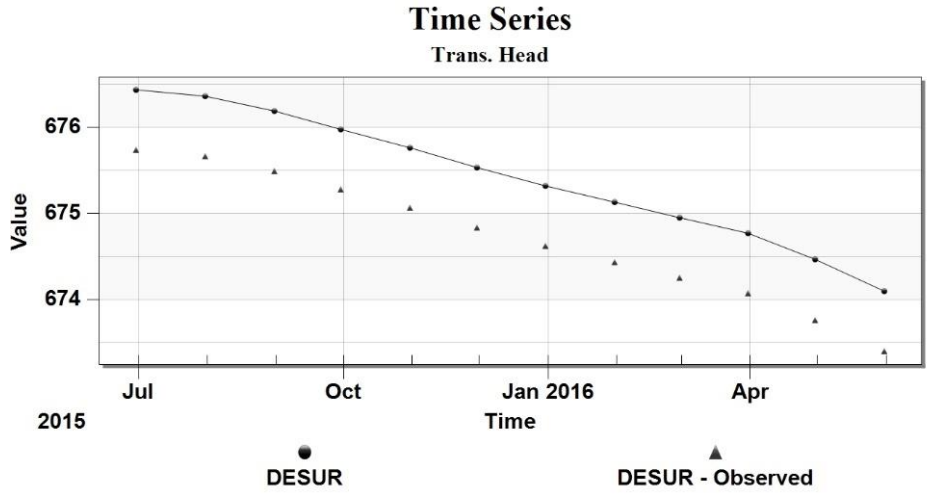

Figure 6-19 Computed V/S Observed Groundwater heads for Desur observation well

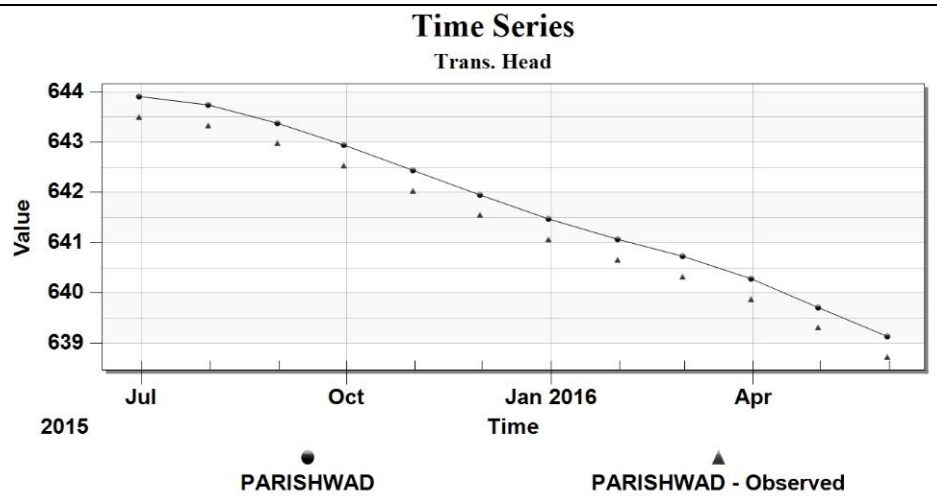

Figure 6-20 Computed V/S Observed Groundwater heads for Parishwad observation well

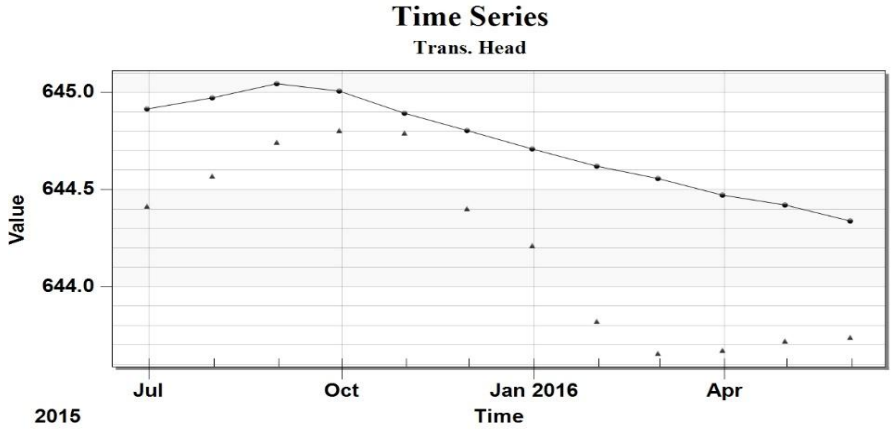

Figure 6-21 Computed V/S Observed Groundwater heads for Bailahongal observation well

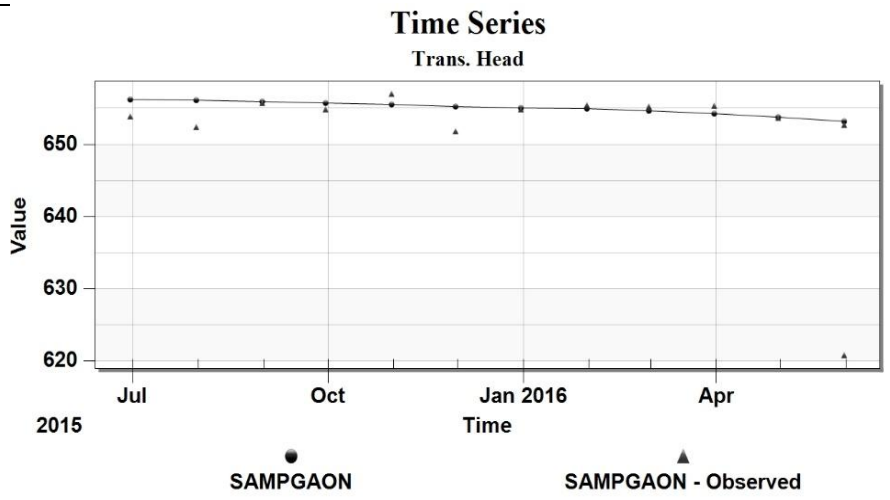

Figure 6-22 Computed V/S Observed Groundwater heads for Sampgaon observation well

6.4.9 The Flow budget

The groundwater flow budget estimated by the model for the entire sub basin is shown in Table 6.8.

Table 6-8 Groundwater flow budget for the steady state flow.

Sources/sinks	IN (m^3 day^{-1})	OUT (m^3 day^{-1})
Constant head	0	0
Wells	0	340222
Drains	0	927754
River leakage	2,264	914712
Head dep bounds	691,847	821,502
Recharge	2,309,968	0
Total source/sink	3,004,080	3004191
Summary	In - Out	% difference
	111.38	-.003707721

The groundwater recharge due to precipitation is computed as 2,309,968 m3/ day with a groundwater draft of 340222 m3 /day in the month of the June-2015. The contribution of drainage system to the basin is about 927754m3 /day. The river recharge to the groundwater is 914712 m3/day and river receive 914712 m3/day from groundwater. The reservoir contribution to the groundwater is 821,502 m3/ day whereas the contribution of groundwater to the reservoir 691,847 m3/ day.

6.5 Transient Model

Three stress periods for an year is considered for groundwater simulation

1. Kharif Season(June-Sep)
2. Rabi Season(Oct- Jan)
3. Summer Season(Feb-May)

6.5.1.1 **Kharif Season(June-Sep):**

This is the monsoon season hence the water consumed for agriculture practice is less hence in this season the draft is about 20 % of the total draft and the reservoir stage is 629 m above mean sea level, River stage is considered based on the river gauging near Khanapur. The recharge is calculated for accumulated months of June, July, August, September. The Observation well measured from the observation well are used for the calibration.

Table 6-9 Flow Budget for Kharif Season(June-Sep)

Flow term	IN (m^3 day^{-1})	OUT (m^3 day^{-1})
STORAGE	0.00	0.00
Constant head	0.00	0.00
Wells	0.00	289800.00
Drains	0.00	384929.70
River leakage	1348.67	204864.90
Head dep bounds	626180.80	698020.90
Recharge	950085.50	0.00
Total	1577615.00	1577615.00
IN - OUT		-0.48
Percent Discrepancy		-0.00003

The simulated groundwater heads for the kharif season are shown in the figure: 6.17

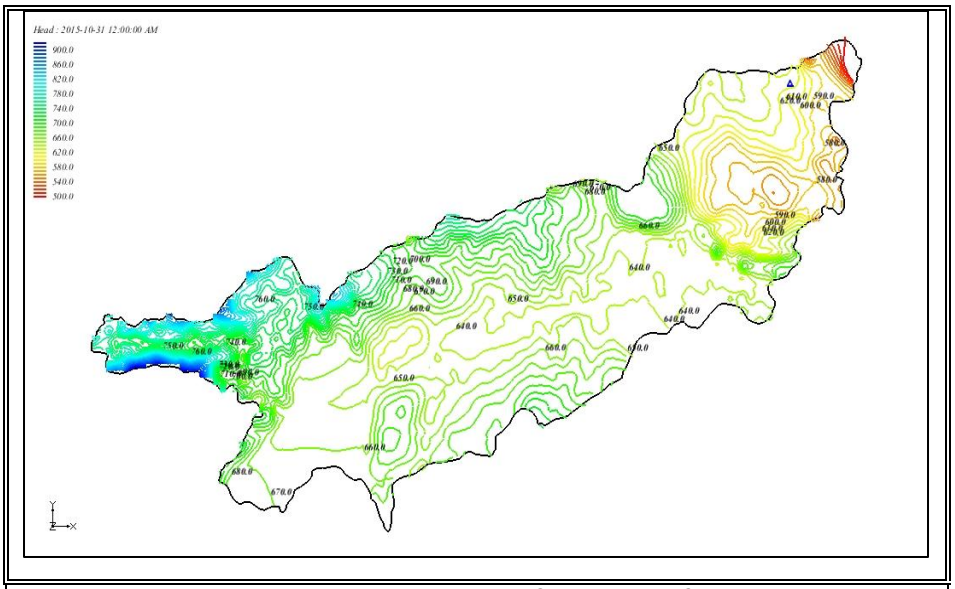

Figure 6-23 Simulated Groundwater heads for the Kharif Seaon(June to Sep)

6.5.1.2 Rabi Season (Oct- Jan)):

This is season is after the monsoon season hence the water consumed for agriculture practice is maximum for the crops like sugarcane, cotton, maize etc hence in this season the draft is about 60 % of the total draft and the reservoir stage is 622 m above mean sea level, River stage is is considered based on the river gauging near Khanapur. The recharge is calculated for rainfall accumulated months of Oct, Nov, Dec, Jan. The Observation well data are used for the modeling.

Table 6-10 Flow budget for Rabi season (Oct - Jan)

Flow term	IN (m^3 day^{-1})	OUT (m^3 day^{-1})
Storage	400437.10	0.00
Constant head	0.00	0.00
Wells	0.00	289800.00
Drains	0.00	231117.50
River leakage	1780.80	147313.30
Head dep bounds	634328.70	680452.70
Recharge	312012.00	0.00
Total	1348559.00	1348684.00
IN - OUT		-124.98180
Percent Discrepancy		-0.00927

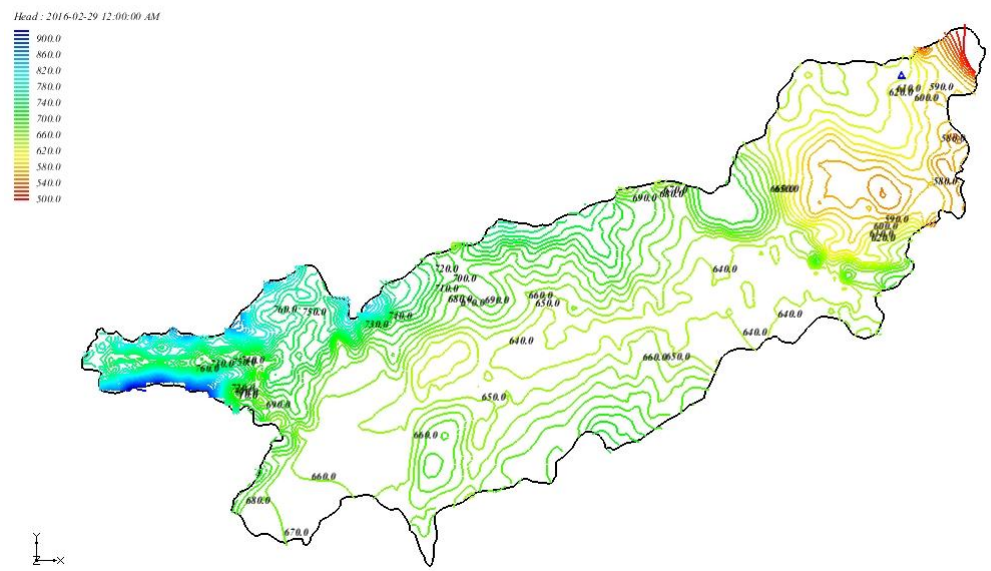

Figure 6-24 Simulated Groundwater Heads for Rabi season

6.5.1.3 Summer Season ((Feb- May)):

During the Summer season the water is required for the perennial crops like Sugar cane and the yield in the bore wells decreases hence 20% is considered from the draft for well draft. The reservoir reaches to minimum level 619 m above mean sea level, River stage is is considered based on the river gauging near Khanapur gauging station. The recharge is calculated for rainfall accumulated months of Feb, March, April, May. The Observation well measured from observation well are used for the calibration.

Table 6-11 Flow budget for Summer season (Oct - Jan)

Flow term	IN (m^3 day^{-1})	OUT (m^3 day^{-1})
Storage	380460.70	9.08

Constant head	0.00	0.00
Wells	0.00	289800.00
Drains	0.00	182791.40
River leakage	1844.24	135251.90
Head dep bounds	636469.10	679106.90
Recharge	268051.60	0.00
Total	1286826.00	1286959.00
IN - OUT		-133.5969
Percent Discrepancy		-0.0104

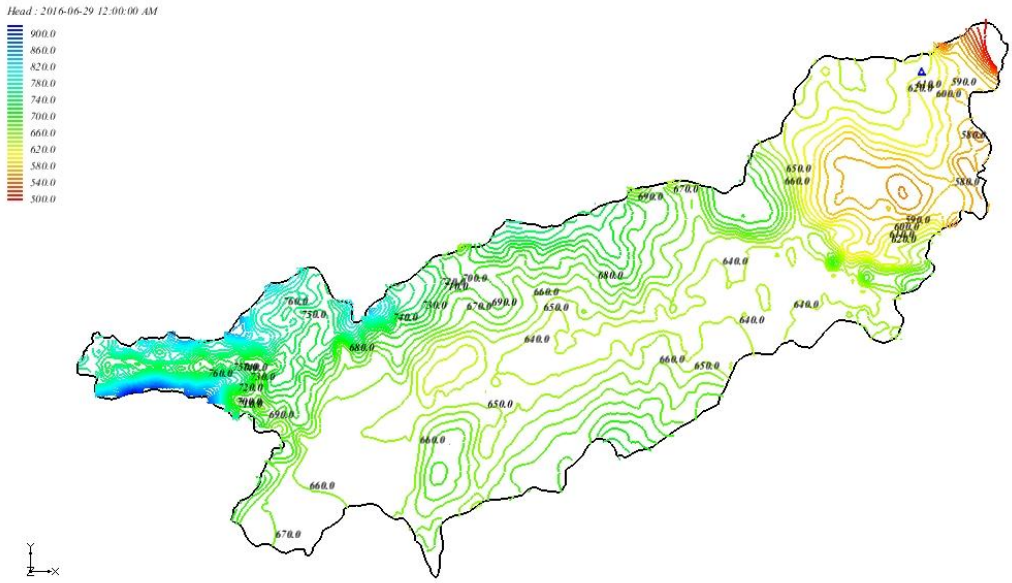

Figure 6-25 Simulated Groundwater Heads for Summer season

Chapter 7

7.1 Conclusions and Scope for future work

As a logical culmination to the aquifer modeling studies, it is natural to know the aquifer response in the future by increasing, decreasing, and continuing the existing draft. The calibrated model and the information on the likely patterns of recharge and discharge can be used to estimate the futuristic aquifer response.

The Co efficient of Variation of the rainfall over the basin as a whole is 30 %, whereas the C.V. of the individual stations for their long-term data varies from 21.63 % to 43.38 %. The coefficient of Skewness of the rainfall over the basin as a whole is -0.0774, whereas the coefficient of Skewness of the individual stations for their long-term data varies from -0.8779 to 1.16%. The Standard deviation of the rainfall over the basin as a whole is 332.74, whereas the Standard deviation of the individual stations for their long-term data varies from 105.80 to 1462.86.

Individual rain gauge station Trend analysis carried out by Mann Kendell Test (Test Z) statistical method. The values of test Z varies from -1.91 to 3.78. The rain gauge stations Desur, Hulikatti, Kankumbi,Khanapur,Murugod,Neginahal are showing the negative Test Z values indicating the decrease in Annual rainfall. Whereas Asoga, Bailahongal, Belawadi, Bidi, Gunji, Hirebagewadi, Kadasagatti, Katkol, M.K.Hubli, Savadatti, Tigadi, Yargatti are showing positive Test Z values indicating no decrease in rainfall trend.

The extreme variation in the spatial distribution of groundwater has led to non-consistency of groundwater availability. The various geological formations along the river course has low infiltration capacities hence the availability of ground water resources in the confined aquifers is less compared to lower basin. The change in Land use and land cover has major contribution in the depletion of groundwater resources. i.e increase in sugarcane growing, degradation of forest cover.

Infiltration and hydraulic properties of soil showed wide variation in upstream part of the basin where the forest percentage is due to which, infiltration rate is much higher than the downstream region where there is large rock exposures are seen.

Based on hydrogeological and geophysical analysis eleven aquifer units have been identified which showed significant variation in groundwater levels.

SWAT MODEL CONCLUSIONS: Impact of land use land cover showed considerable variation in water yield during the study period.

The seasonal variations of groundwater system in the whole area, the groundwater head increases during the wet seasons (June to September) and decreases during the rabi and dry seasons (October to May). This is because the aquifer has a positive change in storage during the wet seasons and a negative change during the dry seasons. Furthermore, the seasonal variation of groundwater head is determined by the state of aquifer water exchange. For example, the water absorption rate of aquifer in May is higher than that in other months, leading to the fastest groundwater head rise in the year, while the groundwater head has no significant decrease in October because the release rate of aquifer is close to zero. It is important to note that aquifer can regulate hydrological processes like a sponge. It absorbs and stores the abundant infiltration of storm water during wet seasons and releases the stored water in the dry months to maintain groundwater discharge. The state of aquifer water exchange is mainly affected by the net groundwater recharge. Generally, the aquifer absorbs more water when there is adequate recharge and releases more water in dry months with little rainfall. In addition, the rate of aquifer water exchange is also affected by the antecedent dry period. For example, although the net groundwater recharge rates in May and October are nearly the same (0.6 million m3/day), the water absorption rate of aquifer in May is 0.13 million m3/day more than that in October. This can be explained by the greater storage capacity of aquifer in May due to the continuous water release in former dry seasons. Due to the "buffer" function of the aquifer, the seasonal change in groundwater discharge appears a relatively small fluctuation relative to the rainfall variations, ranging from **0.32 million m3/month during the dry months to 0.55 million m3/month during the wet seasons**

The Net recharge rate during the Kharif season is 0.95 million m^3/day and during the Rabi season the net recharge is 0.31 m^3/day and for the summer seaon 0.2 m/day. Due

to the "buffer" function of the aquifer, the seasonal change in groundwater discharge appears a relatively small fluctuation relative to the rainfall variations, ranging from 0.2 million m3 (Feb-May)during the summer dry months to 0.95 million m3 (June to September) during the wet seasons.

7.2 Recommendations

7.2.1 Management approaches need to be relooked in the following directions

- If surplus water generated through water saving measures upstream could be stored and conveyed to downstream farmers using infrastructure that had lower water loss than for surface water there would be a greater potential for trades.

- Water saving measures upstream that increase groundwater recharge in an aquifer shared with command area users would be such a case. In effect, aquifers environmental service would be in water conveyance and storage at lower loss rates than could be achieved by man-made canals or pipes. However, a case must then be made for the extent of aquifers.
- Crop yields and crop distribution must be similar between the upstream providers and downstream beneficiaries.

7.2.2 Scope for further work

- The study area has complex Lithology, varied spatial distribution of rainfall, recharge, Cropping pattern with considering these variables this research work has carried out at regional scale to know the response of sub basin to Hydro meteorological changes.
- Hence further detailed work has to be carried out microwatershed level
- There is lot of inadequacy in data availability for Modeling hence much focus has to be thrown on data generation.
- The real world models will help in knowing the recharge and discharge and Groundwater budget in a nutshell.
- As per the SWAT(Soil Water Assesment Tool) model there are **18** Hydrological responsive Units and hence these units are to be considered for future Modeling of the basin
- In the Hard rock terrain the occurrence is not uniform hence Primary and Secondary structures are to be mapped in Large scale
- The detailed Aquifer map has to be prepared by considering lithological, Geophysical aspects.
- The Inventory of existing Irrigation bore wells and drinking water wells gives lot of information for detailed aquifer mapping
- To begin with regulatory system for cropping pattern, optimization procedures must be adopted based on water availability.

- The Unscientific way of Groundwater exploitation and poor Groundwater management has led to over exploitation of the area.

References

Abdulla, F. & Al-Assa'D, T. J Earth Syst Sci (2006) 115: 289. https://doi.org/10.1007/BF02702043

Abdulla, M. A. Al-Khatib, and Z. D. Al-Ghazzawi, "Development of groundwater Modelling for the Azraq Basin, Jordan," *Environmental Geology*, vol. 40, no. 1-2, pp. 11–18, 2000.

Ahmad, Rubina Kausar, Iftikhar Ahmad (2010), Implications of depletion of groundwater levels in three layered aquifers and its management to optimize the supply demand in the urban settlement near Kahota Industrial Triangle area, Islamabad, Pakistan Environmental Monitoring and Assessment, 2010, Volume 166, Number 1-4, Page 41

Ahmed S, Maréchal J, Ledoux E, de Marsily G (2008) Groundwater flow modelling in hard-rock terrain in semi-arid areas: experience from India. In: Hydrological modelling in arid and semi-arid areas. Cambridge University Press, Cambridge, UK, pp 157–190.

Ahmed, Izrar & Umar, Rashid. (2009). Groundwater flow modelling of Yamuna-Krishni interstream, a part of central Ganga Plain Uttar Pradesh. Journal of Earth System Science. 118. 507-523. 10.1007/s12040-009-0050-5.

Aigler, B. V., & Ge, S. (2012). Evaluation of groundwater withdrawal from a mountain watershed, Colorado, USA. *Environmental Earth Sciences*, *69*(6), 1901–1913. doi: 10.1007/s12665-012-2022-3

Al-Dousari, Ahmad & Milewski, Adam & Uddin, Saif & Ahmed, Mohamed. (2010). Remote sensing inputs to SWAT model for groundwater recharge estimates in Kuwait. Advances in Natural and Applied Sciences. 4. 71-77.

Anderson, M. P., & Woessner, W. W. (1992). Applied groundwater modeling : simulation of flow and advective transport. San Diego Academic Press

Ankeny M.D., M. Ahmed, T.C. Kaspar and R. Horton, Simple field method for determining hydraulic conductivity. Soil Sci. Soc. Am. J., 55, pp.467-470, 1991.

Ankeny M.D., M. Ahmed, T.C. Kaspar and R. Horton, Simple field method for determining hydraulic conductivity. Soil Sci. Soc. Am. J., 55, pp.467-470, 1991.

Arnold JG, Allen PM (1999) Automated methods for estimating baseflow and ground water recharge from streamflow records. JAWRA J Am Water Resour Assoc 35:411–424

Awasthi, Manoj & Sharma, Shailesh & Hardaha, Mahesh & Nema, Rajendra. (2018). Ground Water Flow Modelling Using MODFLOW –A Review. International Journal of Current Microbiology and Applied Sciences. 7. 83-88. 10.20546/ijcmas.2018.702.011.

Ayenew, Tenalem & Demlie, Molla & Wohnlich, Stefan. (2008). Application of Numerical Modeling for Groundwater Flow System Analysis in the Akaki Catchment, Central Ethiopia. Mathematical Geosciences. 40. 887-906. 10.1007/s11004-008-9144-x.

B. B. S. Singhal and R. P. Gupta, *Applied hydrogeology of fractured rocks*. New York: Springer, 2014.

B. B. S. Singhal and R. P. Gupta, *Applied hydrogeology of fractured rocks*. New York: Springer, 2010 Netherlands: Springer, 2010. ISBN: 978-90-481-8798-0

Baharuddin, M. F. T., et al. "Simulation of Sub-Drains Performance Using Visual MODFLOW for Slope Water Seepage Problem." IOP Conference Series: Materials Science and Engineering. Vol. 136. No. 1. IOP Publishing, 2016.

Banks, D. 1998:Predictin g the probability distribution of yield from multiple boreholes in crystalline bedrock.Ground Water 36,2,269-2 74.

Bejranonda, Werapol & Koontanakulvong, Sucharit. (2007). Surface and groundwater dynamic interactions in the Upper Great Chao Phraya Plain of Thailand: semi-coupling of SWAT and MODFLOW.

Beltrán, Guillermina Gómez, et al. "Application of the Visual Modflow Model for the Evaluation of the Hydrodynamics of Underlying Aquifer to an Urban Solid Waste Sinter." *International Journal of Environmental Pollution* 29 (2013): 119-126.

Byragi Reddy, t.b., & aregai, m. (2011). Effects of land cover dynamics and the relative response to water resources in middle highland tigray, ethiopia: the case of areas around laelay -koraro.

Calderón Palma, Heyddy and Bentley, Laurence R. (2007) A regional-scale groundwater flow model for the Leon-Chinandega aquifer, Nicaragua. Hydrogeology Journal, 15 (8). pp. 1457-1472.

Clark L (1985) Groundwater abstraction from Crystalline Complex areas of Africa. Q. J. Eng. Geol. 18 25-34.

Clothier, B.E., White, I., 1981. Measurement of sorptivity and soil water diffusivity in the field. Soil Science Society of America Journal 45, 241-245.

Clothier, B.E., White, I., 1981. Measurement of sorptivity and soil water diffusivity in the field. Soil Science Society of America Journal 45, 241-245.

Collection in a Mountain Watershed" Ground Water Monitoring & Remediation, 27(1), pp 75–83.

Da (2011)

Dams, Jef & Woldeamlak, S. & Batelaan, Okke. (2008). Predicting land-use change and its impact on the groundwater system of the Kleine Nete catchment, Belgium. Hydrology and Earth System Sciences. 12. 10.5194/hess-12-1369-2008.

de Condappa, Devaraj & Chaponnière, Anne & Lemoalle, Jacques. (2009). Decision-tool for water allocation in the Volta Basin. Water International - WATER INT. 34. 71-87. 10.1080/02508060802677861.

Ebrahim, G.Y., Villholth, K.G. & Boulos, M. Hydrogeol J (2019) 27: 965. https://doi.org/10.1007/s10040-019-01957-6

Ehsan Shirkhani et al (2013)

Faghihi, N & Kave, F & Babazadeh, Hossein. (2010). Prediction of aquifer reaction to different hydrological and management scenarios using visual MODFLOW model-Case study of Qazvin plain. JOURNAL OF WATER SCIENCES RESEARCH (JWSR).

Fei (2008)

Feng, Juan, Guan Qun Liu, and Quan Sheng Zhao. 2010"Application of Visual MODFLOW to the dynamic change and simulation of deep groundwater in Dezhou City, China." Advanced Materials Research. Vol. 113. Trans Tech Publications.

Fetter CW (1988) Applied Hydrogeology, 2nd ed., Merrill Publ. Co., Columbus, p. 592.

Fetter CW (1993) Contaminant Hydrogeology. Macmillan Publishing Company, New York, p. 458.

Fouepe, Alain & Kuitcha, D. & Fantong, Wilson & Ewodo Mboudou, Guillaume & Khan, Haris & ISSA, No first name & Ohba, Takeshi. (2013). Assessing Groundwater Nitrate Pollution in Yaoundé, Cameroon: Modelling Approach. World Applied Sciences Journal. World Appl. Sci. J.. 10.5829/idosi.wasj.2013.23.03.321.

Gburek, W.J & Folmar, G.J. (1999). Flow and Chemical Contributions to Streamflow in an Upland Watershed: A Baseflow Survey. Journal of Hydrology. 217. 1-18. 10.1016/S0022-1694(98)00282-0.

Guo, C.-Y & Cui, Y.-L & Liu, W.-N & Cui, X.-X & Fei, Y.-H. (2018). Research on numerical simulation of the groundwater funnels restoration in Shijiazhuang. Journal of Groundwater Science and Engineering. 6. 126-135. 10.19637/j.cnki.2305-7068.2018.02.006.

Haque, M. & Jahan, Chowdhury & Mazumder, Q. & Nawaz, S. & Mirdha, G. & Mamud, P. & Adham, Md. (2012). Hydrogeological condition and assessment of groundwater resource using Visual MODFLOW modeling, Rajshahi city aquifer, Bangladesh. Journal of the Geological Society of India. 79. 10.1007/s12594-012-0001-7.

Haque, M., Jahan, C., Mazumder, Q., Nawaz, S., Mirdha, G., Mamud, P., & Adham, M. (2012). Hydrogeological Condition and Assessment of Groundwater Resource Using Visual Modflow Modeling, Rajshahi City Aquifer, Bangladesh. *Geological Society Of India*, *79*(1), 77-84. Retrieved from http://www.geosocindia.org/index.php/jgsi/article/view/57687

Hani A, Djorfi S, Lamouroux C, Lallahem S (2007) Impact of the industrial rejections on water of Annaba aquifer (Algeria). Eur Water 19(20):3–14

Hariharan, V & Shankar, Uma. (2017). A review of visual MODFLOW applications in groundwater modelling. IOP Conference Series: Materials Science and Engineering. 263. 032025. 10.1088/1757-899X/263/3/032025.

Horton RE (1932) Drainage basin characteristics. Trans Amer Geophys Union 13:350–361CrossRefGoogle Scholar

Hu, Yi, et al. 2006 "Visual Modflow and Its application problems in groundwater simulation." Journal of Nanhua University (Science and Technology) 2.

Idrysy, Houcyne & Smedt, Florimond. (2006). Modelling groundwater flow of the Trifa aquifer, Morocco. Hydrogeology Journal. 14. 1265-1276. 10.1007/s10040-006-0080-x.

Ismail, wan zamri & Yusoff, Ismail & A. Rahim, Bahaa-edlin. (2012). Simulation of horizontal well performance using Visual MODFLOW. Environmental Earth Sciences. 68. 10.1007/s12665-012-1813-x.

J.L. Shao, Z.Z. Zhao, Y.L. Cui, R. Wang, C.Q. Li, Q.Q. YangApplication of groundwater modeling system to the evaluation of groundwater resources in North China plain Resources Science, 313 (2009), pp. 361-367

Jia, Jin-sheng, and Chang-ming Liu.2002 "Groundwater dynamic drift and response to different exploitation in the North China Plain: A case study of Luancheng County, Hebei Province." ACTA GEOGRAPHICA SINICA-CHINESE EDITION- 57.2 p 201-209.

Johnson, R.H. (2007) "Ground Water Flow Modeling with Sensitivity Analyses to Guide Field Data

Johnson, R.H. (2007) "Ground Water Flow Modeling with Sensitivity Analyses to Guide Field Data Collection in a Mountain Watershed" Ground Water Monitoring & Remediation, 27(1), pp 75–83.

Jovanovic, Nebo & Israel, Sumaya & Tredoux, Gideon & Soltau, Louise & Le Maitre, David & Rusinga, F & Rozanov, Andrei & van der Merwe, Nikolaas. (2009). Nitrogen dynamics in land cleared of alien vegetation (Acacia saligna) and impacts on groundwater at Riverlands Nature Reserve (Western Cape, South Africa). Water SA. 35,. 10.4314/wsa.v35i1.76653.

Kilb, N. "Groundwater Mapping." GEO 305: Field Geology Course Work. SUNY at Stony Brook, New York. September 2005.

Kim, Man-Kyu. (2003). Development of the GIS Based Pre- and Post-Processing Tool for the Visual MODFLOW Groundwater Flow Modeling. Journal of the Korean Association of Geographic Information Studies. 6.

Kim, Nam & Chung, Il-Moon & Won, Yoo & Arnold, Jeff. (2008). Development and application of the integrated SWAT-MODFLOW model. Journal of Hydrology. 356. 1-16. 10.1016/j.jhydrol.2008.02.024.

Kiss, R., 2004, Determination of drainage network in digital elevation model, utilities and limitations Journal of Hungarian Geomathematics, vol.2, p.16-29.

Kittu N (1990) High yielding bore wells in basaltic terrain at Yerangaon, Nagpur district, Maharashtra. Bhu-Jal News, 5(4), Coverstory.

Kittu N, Mehta M (1990) Numerical technique for evaluation of aquifer parameters on large diameter wells in hard rocks. Proc. All India Seminar on Modern Techniques of Rain Water Harvesting, Water Conservation and Artificial Recharge for Drinking Water, Pune, pp. 259–62.

KrasnY,J.1996a: Hydr ogeological environment in hard rocks :an attempt at its schematizing and terminol ogical con siderat ions.In:KrasnY,J.& Mls, J. (eds.): First Workshop on "Hard rock hydr og eolog y of th e Boh emi an Massif" 1994,Acta Universitatis Carolinae Geologica, 40, 2, 115-122 .

Krishnaswamy, The groundwater recharge response and hydrologic services of tropical humid forest ecosystems to use and reforestation: Support for the “Infiltration-evapotranspiration trade-off Hypothesis Journal of Hydrology 2013/08/01 VL - 498

Kuchling K, Chorley D, Zawadzki W (2000) Hydrogeological modelling of mining operations at the Diavik Diamonds Project. In: Proceedings, 6th International symposium on environmental issues and waste management in energy and mineral production, Univ of Calgary, Calgary AB, Canada

Kumar, S., Halder, S., & Singhal, D. (2011). Groundwater Resources Management through Flow Modeling in Lower Part of Bhagirathi - Jalangi Interfluve, Nadia,

West Bengal. *Geological Society Of India, 78*(6), 587-598. Retrieved from http://www.geosocindia.org/index.php/jgsi/article/view/58366

Li etal, Xiaolong, et al. "Study on groundwater using visual MODFLOW in the Manas River Basin, China." Water Policy (2016): wp2016180

Limaye, S. D. (2010). "Groundwater development and management in the deccan traps (basalts) of western India." Hydrogeol. J., 18(3), 543–558.

M. Albhaisi, L. Brendonck, and O. Batelaan, "Predicted impacts of land use change on groundwater recharge of the upper Berg catchment, South Africa," *Water SA*, vol. 39, no. 2, 2013.

Maréchal J, Dewandel B, Subrahmanyam K (2004) Use of hydraulic tests at different scales to characterize fracture network properties in the weathered-fractured layer of a hard rock aquifer. Water Resour Res 40(11). https://doi.org/10.1029/2004WR003137

Massuel, S., George, B.A., Gaur, A. and Rajesh, N. (2007). "GroundWater Modelling for Substantial Resource management in the Musi catchment, India". International Congress on Modelling and Simulation (MODSIM 2007) by the University of Canterbury, Newzealand, Vol.11, No.8, pp.1429-1435

Mazurek, M. 2000: Geolog ical and hyd raulic properties of water-conducting features in cry stalline rock s. In: Stober, I. & Bucher, K. (ed s.): Hydrogeology of crystalline rocks,Kluwer Acad em ic Publishers, 3-26.

Meriano, Mandy & Eyles, Nick. (2003). Groundwater flow through Pleistocene glacial deposits in the rapidly urbanizing Rouge River–Highland Creek watershed, City of Scarborough, southern Ontario, Canada. Hydrogeology Journal. 11. 288-303. 10.1007/s10040-002-0226-4.

Miller VC (1953) A quantitative geomorphic study of drainage basin characteristics in the clinch mountain area. Virginia and Tennessee. In: Technical Report. 3. Office of Naval Research. Department of Geology. Columbia University

Mirudhula K., 2014, "Impact of lined/unlined canal on groundwater recharge in the lower Bhavani basin", *International Journal of engineering research and technology, Volume 3, No. 9, September 2014*.

Mondal N. C., Singh V. P., Sankaran S., 2011, "Groundwater model for a tannery belt in Southern India", *Journal of Water Resources and Protection, Volume.3, page 85-97, 2011*

Mondal, N. C., Singh, V. P., and Sankaran, S. (2011). "Groundwater flow model for a tannery belt in southern India." J. Water Resour. Protect., 3, 85–97.

Mondal, NC & Singh, V.. (2009). Mass transport modeling of an industrial belt using visual MODFLOW and MODPATH: A case study. J. Geogr. Reg. Plan. 2.

Narasimha Reddy, T., Prakasam, P., Subrahmanyam, G.V., Prakash Goud, P.V., Gurunatha Rao, V.V.S., and Guptha, C.P., (1994), "Characterization of Groundwater Recharge in a Crystalline Watershed through Recharge Process and Groundwater Flow Models", Proc.of Seminar on Groundwater hydrology, held during July 17-18, NIH, Roorkee, Vol.II, pp.7-22.

National Institute of Hydrology, Roorkee, India (1997), Groundwater Modelling of Ghataprabha sub basin Research article. CS/AR-31 96-97

Needhidasan S., Nallanathel M., 2013, "Application of Visual MODFLOW and GIS in groundwater Modelling", *International Journal of Civil Engineering , Volume 2, No. 3, 41-50, July 2013.*

Olorunfemi, M.O. and E.T. Okhue, 1992. Hydrogeologic and geologic significance of a geoelectric survey in Ile Ife, Southwesten Nigeria. J. Min. Geol., 28: 221-229.

Owen, Richard & Dahlin, Torleif. (2010). Inherited drainage - paleochannels and preferential groundwater flow. Hydrogeology Journal. 18. 893-903. 10.1007/s10040-010-0588-y.

P. C. Trescott, "Documentation of finite-difference model for simulation of three-dimensional groundwater flow," Open-File Report, 1975.

Parameswari, K., B. V. Mudgal, and Prakash Nelliyat. "Evaluation of groundwater contamination and its impact: an interdisciplinary approach." *Environment, development and sustainability* 14.5 (2012): 725-744.

Park, Haeyong, Myounghak Oh, and Osoon Kwon. "Analysis on Contaminant Transport according to the Embedded Depth of Vertical Barrier of Offshore Landfill." Journal of the Korean Geoenvironmental Society 17.8 (2016): 29-37.

Patil, N., & Chetan, N. (2017). Groundwater Modeling of Hiranyakeshi Watershed of Ghataprabha Sub-Basin. *Geological Society Of India, 90*(3), 357-361. doi:10.1007/s12594-017-0724-6.

Perroux K.M. and I. White, Designs for disc permeameters. Soil Sci. Soc. Am. J., 52, pp. 1205-1214, 1988

Perroux K.M. and I. White, Designs for disc permeameters. Soil Sci. Soc. Am. J., 52, pp. 1205-1214, 1988

Persson, Joakim, and Niklas Andersson. "Modeling groundwater flow and PFOS transport: A case study at the old fire drill site of Bromma Stockholm Airport." (2016).

Pradeep Kumar G. N., Kumar A. P., (2014), "Development of groundwater flow model using Visual MODFLOW", *International Journal of Advanced Research, Volume 2, No. 6, pp. 649-656, 2014.*

Purandara, B. K., Venkatesh, B., Choubey, V.K. (2010). Estimation of groundwater recharge under various land covers in parts of westrn ghat, Karnataka, India. *RMZ-materials and geoenvironment, letnik 57, številka 2, str. 181-194*. URN:NBN:SI:DOC-CAKWSIJC from http://www.dlib.si

Putty et al., (2000)

R. A. Freeze and P. A. Witherspoon, "Theoretical analysis of regional groundwater flow: 1. Analytical and numerical solutions to the mathematical model," Water Resources Research, vol. 2, no. 4, pp. 641–656, 1966.

Rajamanickam and S.Nagan "Groundwater Quality Modelling of Amaravathi River Basin of Karur District, Tamil Nadu, Using Visual Modflow" *International Journal Of Environmental Sciences* Volume 1, No1,2010

Rajamanickam, R. "Groundwater quality modeling of Amaravathi river basin of Karur district,Tamil nadu, using visual Modflow." (2013).

Rao, G. Tamma, et al. "Assessment of groundwater contamination from a hazardous dump site in Ranipet, Tamil Nadu, India." *Hydrogeology Journal*19.8 (2011): 1587-1598.

Regional Aquifer-System Analysis Program of the US Geological Survey; bibliography, 1978-86," 1987.

Rejani, R., et al 2008. "Simulation modeling for efficient groundwater management in Balasore coastal basin, India." Water Resources Management 22.1 p23-50.

Roadcap, George S., and Steven D. Wilson.2001 The impact of emergency pumpage at the Decatur wellfields on the Mahomet Aquifer: Model review and recommendations. Illinois State Water Survey

Saghravani, Seyed Reza & Mustapha, Saari & Ibrahim, Sharharin & Yusoff, Mohd & Saghravani, Seyed Fazlolah. (2011). Phosphorus migration in an unconfined aquifer using MODFLOW and MT3DMS. Journal of Environmental Engineering and Landscape Management. 19. 271-277. 10.3846/16486897.2011.634053.

Sarada.M, (2006). "Ground water flow model of Upper Musi Basin Andhra Pradesh" M.Tech Thesis submitted to Centre for Water Resourrces, IST, JNTUH, 96p

Saravanan, R., et al. 2011 "Groundwater modeling and demarcation of groundwater protection zones for Tirupur Basin–A case study." *Journal of Hydro-environment Research* 5.3 : p197-212.

Schumm SA (1963) Sinuosity of alluvial river on the great plains. Bull Geol Soc Amer 74:1089–1100

Shi, Weifang & Zeng, Weihua & Chen, Bin. (2010). Application of Visual MODFLOW to assess the Sewage Plant accident pool leakage impact on groundwater in the Guanting Reservoir area of Beijing. Frontiers of Earth Science in China. 4. 320-325. 10.1007/s11707-010-0118-1.

Singh P, Arora M and Goel N K. 2006. Effect of climate changeon runoff of a glaciarized Himalayan basin. HydrologicalProcesses 20 (9): 1 979–92

Singh S, Singh MC (1997) Morphometric analysis of Kanhar River Basin. Natl Geogr J India 43(1):31–43

Singhal BBS (1973) Some observations on the occurrence, utilisation and management of groundwater in the Deccan trap areas of Central Maharashtra, India, Proc. Int. Symp. on Development of Ground Water Resources, Vol. 3, Madras, India, pp. 75–81.

Smettem K.R.J. and B.E. Clothier, Measuring unsaturated sorptivity and hydraulicc conductivity using multiple disc permeameters. J. Soil Sci., 40, pp. 563-568, 1989.

Smettem K.R.J. and B.E. Clothier, Measuring unsaturated sorptivity and hydraulicc conductivity using multiple disc permeameters. J. Soil Sci., 40, pp. 563-568, 1989.

Smith KG (1950) Standards for grading texture of erosional topography. Am J Sci 248:655–668

Stearns HT (1942) Hydrology of volcanic terraines, in Hydrology (Meinzer OE ed.), Dover Publ., Inc., New York, pp. 678–703

Steiakakis, E., et al. "Drought impacts on the fresh water potential of a karst aquifer in Crete, Greece." *Environmental Earth Sciences* 75.6 (2016): 1-19.

Surinaidu1 "Application of MODFLOW for groundwater Seepage Problems in the Subsurface Tunnels" *Journal of Indian Geophysical Union*', Volume 9

Thangarajan, M., Linn, F., Uhl, V. et al. Environmental Geology (1999) 38: 285. https://doi.org/10.1007/s002540050426

Titus R, Beekman H, Adams S, Strachan L (2009) The basement aquifers of southern Africa. Water Research Commission report no. TT 428- 09, Water Research Commission, Pretoria, South Africa, 183 pp

Tiwary, Rahul & Dhakate, Ratnakar & Rao, V. & Singh, V.. (2005). Assessment and prediction of contaminant migration in ground water from chromite waste dump. Environmental Geology. 48. 420-429. 10.1007/s00254-005-1233-2.

Tóth, "A theoretical analysis of groundwater flow in small drainage basins," Journal of Geophysical Research, vol. 68, no. 16, pp. 4795–4812, 1963.

Vandecasteele, Ine & Nyssen, Jan & Clymans, Wim & Moeyersons, Jan & Martens, Kristine & Van Camp, Marc & Gebreyohannes, Tesfamichael & Desmedt, Florimond & Deckers, Jozef & Walraevens, Kristine. (2011). Hydrogeology and groundwater flow in a basalt-capped Mesozoic sedimentary series of the Ethiopian highlands. Hydrogeology Journal. 19. 641-650. 10.1007/s10040-010-0667-0.

Varalakshmi, V., et al. "Groundwater flow modeling of a hard rock aquifer: case study." *Journal of Hydrologic Engineering* 19.5 (2012): 877-886.

Vijay, Ritesh, and P. K. Mohapatra. "Hydrodynamic assessment of coastal aquifer against saltwater intrusion for city water supply of Puri, India." Environmental Earth Sciences 75.7 (2016): 1-8.

Vikrant Vishal "Estimation of Groundwater recharge in National capital territory, Delhi using Groundwater modelling", *Journal of Indian Water Resources Society, Vol 34, No.1, January, 2014, Sudhir Kumar and D.C.Singhal*

Villholth K, Tøttrup C, Stendel M, Maherry A (2013) Integrated mapping of groundwater drought risk in the southern African development community (SADC) region. Hydrogeol J 21:863–885

Wake (2008)

WANG, Qing-yong, et al.2007 "Visual MODFLOW and its application to groundwater simulation [J]." *Journal of Water Resources and Water Engineering* p 25.

White I. and M.J. Sully, Macroscopic and microscopic capillary length and time scales from field infiltration. Water Resour. Res., 23, pp. 1514- 1522, 1987. [15]

White I. and M.J. Sully, Macroscopic and microscopic capillary length and time scales from field infiltration. Water Resour. Res., 23, pp. 1514- 1522, 1987. [15]

Winchell M, Srinivasan R, Di Luzio M, Arnold JG (2007) ArcSWAT interface for SWAT2005: user's guide. USDA-ARS Blackland Research Center, Texas Agricultural Experiment Station, and Grassland, Soil and Water Research Laboratory, Temple Google Scholar

Wooding R.A., Steady infiltration from a shallow circular pond Water Resour. Res., 4, pp. 1514-1522, 1968.

Wooding R.A., Steady infiltration from a shallow circular pond Water Resour. Res., 4, pp. 1514-1522, 1968.

Yizhong (2007)

Youssef, T.. (2012). Assessment of Groundwater Resources Management in Wadi ElFarigh Area Using MODFLOW. IOSR Journal of Engineering. 02. 69-78. 10.9790/3021-021016978.

Yugen (2011)

Zare, M.. (2016). Using ANN and ANFIS Models for simulating and predicting Groundwater Level Fluctuations in the Miandarband Plain, Iran. Qadir, Anwar, et al. "A spatio-temporal three-dimensional conceptualization and simulation of Dera Ismail Khan alluvial aquifer in visual MODFLOW: a case study from Pakistan." Arabian Journal of Geosciences 9.2 (2016): 1-9.

Zohdy, A.A.R., G.P. Eaton and D.R. Mabey, 1974. Application of Surface Geophysics to Ground-Water Investigations. 1st Edn., Chapter Book 2, USGS Publication, USA., pp: 116.

Zume, Joseph & Tarhule, Aondover. (2008). Simulating the Impacts of Groundwater Pumping on Stream-Aquifer Dynamics in Semiarid Northwestern Oklahoma, USA. Hydrogeology Journal. 16. 797-810. 10.1007/s10040-007-0268-8.

Annexure-I

DYNAMIC GROUNDWATER RESOURCE ESTIMATION WATERSHED CODE 4D7C9 BY GROUNDWATER ESTIMATION COMMITTEE METHODOLOGY (GEC-2015)

S.No		Units	Non command
1.	Geographical area	Ha	119700.00
2.	Massive rock area	Ha	3997.00
3.	Area having > 20% slope	Ha	0.00
4.	Poor quality area	Ha	0.00
5.	Aquifer area	Ha	115703.00
6.	Rain guage stations		Asoga
			Bidi
			Desur
			Gunji
			Hirebagewadi
			Hulikatti
			Jamboti
7.	Observation wells	Dug wells (No's)	Desur
			Gunji
		Borewells (No's)	Ambadgatti
			Beedi
			Chickbagewadi
			Hirebagewadi
			Khanapur

			M k hubli Parishwad

STATIC GROUNDWATER LEVEL DATA ANALYSIS

Units: water level meters below groundlevel (mbgl)

Village	Jan	Feb	Mar	Apr	May	Jun	Jul	Aug	Sep	Oct	Nov	Dec	Average	Fluctuation
Desur	4.03	4.75	4.88	5.59	6.91	3.66	2.24	1.33	1.36	1.91	2.58	3.45	3.56	6.32
Gunji	1.45	2.06	2.08	2.1	1.95	1.25	1.11	0.89	0.85	0.91	0.99	1.26	1.41	2.09
	2.74	3.40	3.48	3.845	4.43	2.45	1.65	1.11	1.10	1.41	1.785	2.35	2.48	4.20

NORMAL RAINFALL DATA (1980-2016)

Units: Rainfall in mm (millimeters)

Rain gauges	Jan	Feb	Mar	Apr	May	Jun	Jul	Aug	Sep	Oct	Nov	Dec	Total	Normal monsoon	Normal non monsoon
Asoga			25.20	7.40	40.35	253.00	513.62	379.00	122.60	76.16	21.80	12.73	1405.38	1268.22	137.16
Bidi					80.69	164.54	255.64	190.02	109.03	103.11	30.31	4.31	987.34	719.23	268.11
Desur		4.7	7.07	9.42	84.30	202.50	263.72	150.12	66.40	92.35	32.90	12.70	864.42	682.74	181.68
Gunji			44.90	24.40	58.48	411.25	743.95	415.68	155.73	104.20	34.05	6.40	1561.48	1381.28	180.20
Hirebagewadi					86.71	153.21	225.96	157.70	92.50	90.00	25.62	4.83	836.52	629.37	207.16
Hulikatti				37.32	83.28	130.34	197.72	140.47	95.55	86.52	24.29	4.55	800.05	564.08	235.97
Jamboti			29.00	7.80	67.53	352.03	532.90	356.75	200.33	64.40	25.27	4.40	1589.35	1153.60	117.88
Kankumbi	12.4	0.4	112.00	16.58	95.15	983.75	1811.17	1388.19	557.31	245.64	24.87	18.85	5124.53	4740.42	384.10
Khanapur	0.3	7.65	28.05	12.43	66.64	278.86	527.20	344.72	119.92	71.18	20.90	19.00	1456.74	1270.70	186.04

Mkhubli		25.2	17.90	14.76	76.42	130.26	206.48	132.64	99.90	111.56	54.00	15.98	832.98	569.28	263.70
Monthly average	6.35	8.38	29.77	17.61	74.65	302.82	523.23	364.67	161.25	105.63	28.70	9.37	1545.88	1297.89	216.20

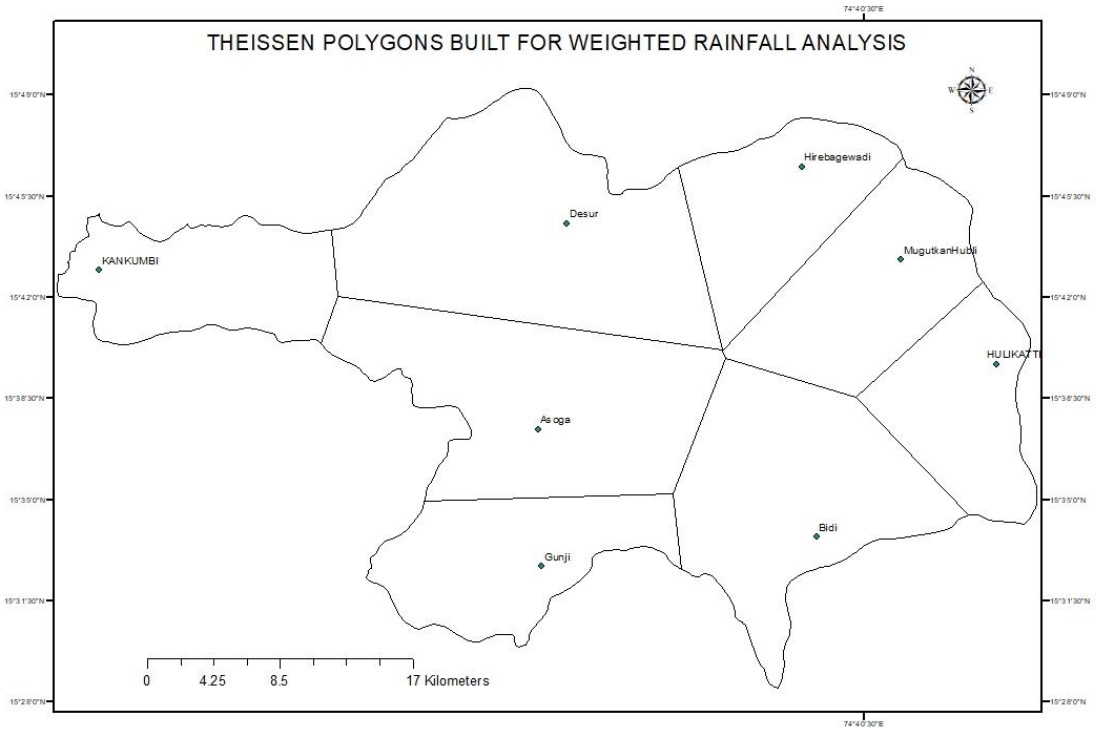

Calculation of Weighted Average Rainfall using Theissen Polygon Mehtod

Rain gauges	Theissen polygon area	Total watershed area	Fraction	Normal mon	Weighted rainfall	Normal non	Weighted rainfall	Actual m rf	Weighted rainfall	Actual non monsoon	Weighted rainfall
	Ha	Ha		(mm)	(mm)	(mm)	(mm)	(mm)	(mm)	(mm)	(mm)
Asoga	7675.56	118296	0.06	1561.84	101.34	181.18	11.76	1268.22	82.29	137.16	8.90
Bagevadi	9576.03	118296	0.08	886.81	71.79	255.95	20.72	629.37	50.95	207.16	16.77
Bidi	16927.50	118296	0.14	1034.27	148.00	170.13	24.35	719.23	102.92	268.11	38.36
Desur	17681.50	118296	0.15	1623.53	242.67	157.19	23.49	682.74	102.05	181.68	27.16
Gunji	10770.10	118296	0.09	723.94	65.91	201.90	18.38	1381.28	125.76	180.20	16.41
Hulikatti	9069.51	118296	0.08	653.18	50.08	235.66	18.07	564.08	43.25	235.97	18.09
Jamboti	12314.70	118296	0.10	1787.23	186.05	181.47	18.89	1153.60	120.09	117.88	12.27
Kankumbi	7002.11	118296	0.06	5035.86	298.08	373.28	22.10	4740.42	280.59	384.10	22.74

Khanapur	13447.60	118296	0.11	1617.49	183.87	249.81	28.40	1270.70	144.45	186.04	21.15
Mugutkhan hubli	12684.50	118296	0.11	604.64	64.83	238.59	25.58	569.28	61.04	263.70	28.28
Tigadi	1114.86	118296	0.01	492.42	4.64	334.56	3.15	1659.62	15.64	237.54	2.24
Average					1417.26		214.88		1129.02		212.36

For all assessments of recharge components, cropping seasons are classified into monsoon and non monsoon seasons and crops are classified into Paddy and non paddy. Standard crop water requirement are applied for assessment in case local study data are unavailable. All other factors such as seepage are to be applied as per GEC 2016 recommendations

Ground water draft for irrigation (Unit draft method)			
	Total No's	Unit draft in (Ham)	Total draft
Borewells& dugcumborewell	1731	1.1	1904.1
Dugwells	4039	0.6	2423.4
		Total draft for irrigation	4327.5

Gound water draft for domestic and industrial purposes	
60 lts per person per day	Non command
Total population	449101
Population using surface sources	0
Population using G.W sources(20016)	449101
Domestic & Industrial Draft (Ham)	= Population using G.W sourcesx365x60/1000/10000
	983.53

R gw (Return recharge from ground water irrigation)			
Crops grown area (Ha)			
Monsoon paddy	Non Monsoon paddy	Monsoon non paddy	Non Monsoon non Paddy
a	b	c	d
5100.77	2500	37404.98	18702

CROP WATER DUTY (Ham) per Anum			
Monsoon paddy	Non Monsoon paddy	Monsoon non paddy	Non Monsoon non Paddy
(e)	(f)	(g)	(h)
1.25	1.35	0.2	0.52

IRRIGATION DRAFT (Ham)

Monsoon paddy	Non Monsoon paddy	Monsoon non paddy	Non Monsoon non Paddy
(a x e)= i	(b x f) = j	(c x g)=k	(d x h)=l
6375.9625	3375	7480.996	9725.04

Ground water draft based on Crop water duty

M draft Ham (i+k)	NM draft Ham(J+l)	TOTAL
13856.96	13100.04	26956.99

R gw -Return flow from groundwater irrigation

Mon seep Ham (I x 0.35) +(k x0.15)	N Mon seep Ham (j x 0.35) +(l x0.15)	Total
3353.73	2640.00	5993.73

Rt - Return recharge from Tank storage

Water spread Area (Ha)	Mon no of days	Non mon no of days	M Seepage (q*0.6xrx0.0014) Ham	N Mon Seepage (q*0.6xsx0.0014)	Total recharge from tanks Ham
q	r	s	t	u	v
775	120	60	78.12	12.09	90.21

Return recharge from tank irrigation

M paddy Ha	NM paddy Ha	M non paddy Ha	NM non paddy Ha
x	y	z	Aa
100	100	150	150

M paddy Ha	NM	M non	NM non paddy

	paddy	paddy	
ab	ac	ad	ae
1.25	1.35	0.2	0.52

M paddy Ha (x x ab)	NM paddy (y x ac)	M non paddy (z x ad)	NM non paddy (aa x ae)
125	135	30	78

R sw- Tank irrigation recharge

M paddy ham (af x 0.40)	NM paddy (ag x 0.40)	M non paddy (ah x 0.20)	NM non paddy (ai x 0.20)	Mon seep Ham(aj+al)	N Mon seep Ham
aj	ak	al	am	an	ao
50	54	12	31.2	62	85.2

Rwc-Recharge from Water Consevation Structures

Total number of tanks	No of M fillS	No of NM fillS	Ave. Storage Mcu	Mon seepage Ham (ba x0.6 xbb xbd) /10000	Non mon seepage Ham	Total Seepage Ham
ba	bb	bc	bd	be	bf	bg
100	2	1	2000	24	5.76	29.76

(Rgw+Rwc+Rt+Rsw)-Return recharge from all the sources

Rgw	Rwc	Rt	Rsw	Total

5993.74	29.76	85.2	78	6186.7

Recharge Estimation by Water table fluctuation method

Watershed	Area (Ham)	Water table fluctuation (m)	Specific Yield	+ Gross Monsoon Draft (Ham)	- R. other sources monsoon (Ham)	Recharge during Mon (Ham)
4D7C9	115703	4.2	0.07	13856.96	6186.7	41686.94

Recharge Estimation by Rainfall infiltration factor method

Aquifer Area (Ham)	Normal Monsoon rainfall (mm)	Infiltration factor	Annual Recharge (Ham)
115703	1417.26	0.26	42635.12

Comparison of two methods of monsoon rainfall assessment and finalization of estimate Considering percentage difference (P D)

$$\text{Percentage Difference} = \frac{R_{normal.\ W\ tf} - R_{r\ inf}}{R_{r\ inf}} \times 100$$

= (41686.942-42635.12/42635.12)*100

Percentage difference = -2.22

Gross Annual Recharge

Rgw	Rwc	Rt	Rsw	Total	Recharge due to rainfall	Total recharge
(Ham)	(Ham)	(Ham)	(Ham)	(Ham)	(Ham)	(Ham)
5993.74	29.76	85.2	78	6186.7	42635.12	48821.82

Total Draft

domestic / industrial draft (Ham)	irrigation draft (Ham)	Total (Ham)
983.53	26956.99	27940.5

Stage of development = GW DRAFT/NET ANNUAL RECHARGEX100

=(27940.5/ 48821.82)*100

=57.22%

The Stage of development is 57.22% hence the watershed is categorized as safe

Annexure-II

DYNAMIC GROUNDWATER RESOURCE ESTIMATION OF 4D7C8 WATERSHED BY GROUNDWATER ESTIMATION COMMITTEE METHODOLOGY (GEC-2016)

S.No		Units	Non Command	Command
1.	Geographical area	Ha	111075 Ha	53092.93
2.	Massive rock area	Ha	8080 Ha	7067.75
3.	Area having > 20% slope	Ha		
4.	Poor quality area	Ha		
5.	Aquifer area	Ha	102995	46025
6.	Rain guage stations		Bailahongal	Bailahongal
			Belawadi	Belawadi
			Desur	Desur
			Hoolikatti	Hoolikatti
			Kadasagatti	Kadasagatti
			Mkhubli	Mkhubli
			Murgod	Murgod
			Neginal	Neginal
			Soundatti	Soundatti
			Tigadi	Tigadi
7.	Observation wells	Dug wells	Bailhongal	
			Gondi	
			Salahalli	
			Sampgaon	
			Halloli	
			Karikatti (asundi)	

		Borewells	Katkol	
			Korkoppa	
			Murgoad	
			Murkumbi	
	Tanks water spread area		7680.00	221.76
	Irrigation command			60088

STATIC GROUNDWATER LEVEL DATA ANALYSIS

Unit: meters below Ground level

Village	Jan	Feb	Mar	Apr	May	Jun	Jul	Aug	Sep	Oct	Nov	Dec	Fluctuati	Average
Bailhongal	2.96	3.35	3.52	3.80	3.90	3.23	3.17	3.17	2.98	2.51	2.64	2.87	1.65	3.18
Gondi	4.41	5.37	6.84	10.25	9.96	9.74	9.00	8.57	8.27	5.65	3.81	3.98	9.88	7.15
Halloli	5.04	5.46	5.83	6.43	5.52	5.16	5.56	6.11	5.54	4.85	5.20	5.08	3.15	5.48
Karikatti (asundi)	3.21	3.34	3.68	3.89	4.08	3.94	4.18	3.72	3.73	3.42	2.89	3.04	2.85	3.59
Salahalli	8.61	10.40	10.10	10.20	11.00	10.80	10.50	10.00	8.92	10.02	10.60	10.54	2.84	10.14
Sampgaon	7.55	9.42	9.88	11.02	6.54	7.75	7.23	7.41	9.89	7.82	7.73	8.58	7.58	8.40
Grand average	5.30	6.22	6.64	7.60	6.83	6.77	6.61	6.50	6.56	5.71	5.48	5.68	4.66	6.32

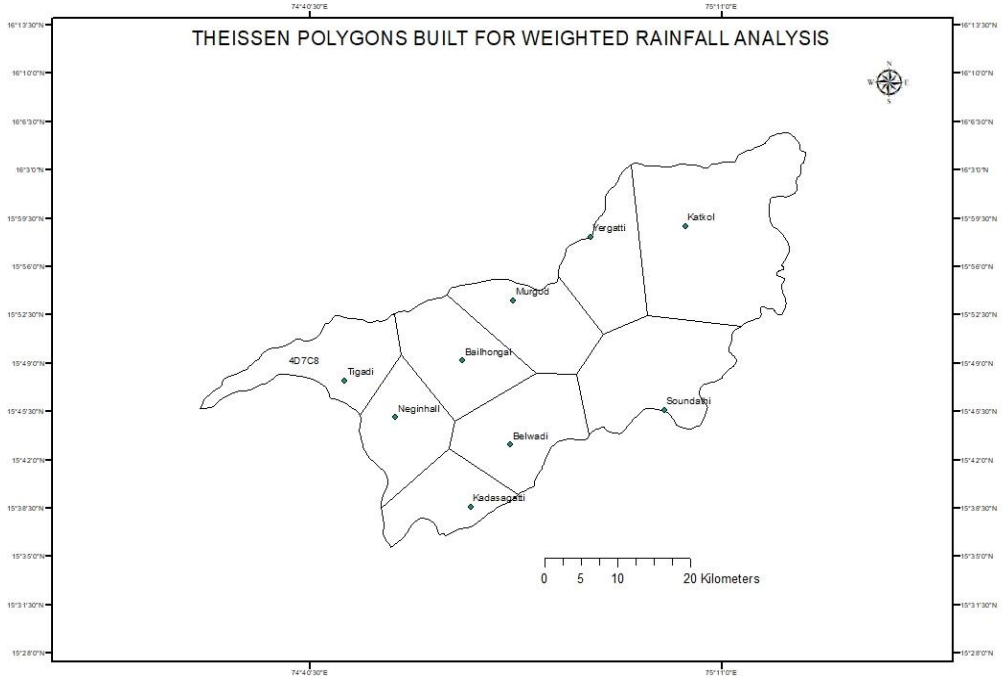

NORMAL RAINFALL DATA (1980-2016)

Units: Rainfall in mm (millimeters)

Rain gauges	Jan	Feb	Mar	Apr	May	Jun	Jul	Aug	Sep	Oct	Nov	Dec	Total	Normal	Normal
Bailahongal	0.89	1.79	9.77	32.09	79.84	57.58	64.71	17.59	88.72	88.59	24.20	4.73	470.49	228.59	241.90
Belawadi		9.20	64.00	28.44	72.60	56.92	109.58	69.32	75.90	96.68	40.53	27.00	577.40	311.72	265.68
Kadasagatti			38.10	27.87	64.63	76.72	139.36	88.85	37.45	83.40	48.65	32.73	542.74	317.12	225.62
Katkol					79.84	57.58	64.71	17.59	88.72	88.59	24.20	4.73	470.49	228.59	241.90
Murgod		19.00	24.00	16.64	65.35	60.76	60.54	49.38	92.78	72.40	34.73	7.07	448.06	263.46	184.60

Neginal		2.40	13.35	24.08	61.88	85.82	138.78	97.70	80.12	124.04	29.25	8.67	642.98	402.42	240.56
Soundatti	0.40	1.36	17.72	8.16	74.08	54.00	36.82	41.22	60.80	59.08	23.32	6.88	383.84	192.84	191.00
Tigadi		2.00	25.75	41.44	104.84	139.40	141.60	116.78	94.64	124.24	37.35	32.90	826.98	492.42	334.56
Yargatti				30.06	83.07	66.52	81.83	25.59	91.32	91.48	19.96	4.22	505.04	265.25	239.79
Monthly average	0.64	3.45	23.62	26.06	76.76	72.81	93.10	57.53	79.88	92.06	30.14	11.62	540.89	300.27	240.62

Weighted Average Rainfall by Theissen Polygon method.

Rain_gauge	Weighted area Ham	Total area Ham	Weighted %	Monsoon rf in mm	Non-monsoon rf in mm	Weighted mon rf in mm	Weighted nonmonrf in mm
Bailhongal	16986	171930	0.10	228.59	241.89	22.58	23.90
Belwadi	17656	171930	0.10	311.72	265.68	32.01	27.28
Kadasagatti	11740	171930	0.07	317.12	225.62	21.65	15.41
Katkol	41937	171930	0.24	228.59	241.89	55.76	59.00
Murgod	15899	171930	0.09	263.46	184.60	24.36	17.07
Neginhall	13898	171930	0.08	402.42	240.56	32.53	19.45
Soundathi	23573	171930	0.14	192.84	191.00	26.44	26.19
Tigadi	15601	171930	0.09	492.42	334.56	44.68	30.36
Yergatti	14640	171930	0.09	265.25	239.79	22.59	20.42
						282.61	239.07

For all assessment of recharge components, cropping seasons are classified into monsoon and non monsoon seasons and crops are classified into Paddy and non paddy. Standard crop water requirement are applied for assessment in case local study data are unavailable. All other factors such as seepage are to be applie as per GEC 2016 recommendations

Ground water draft for irrigation (Unit draft method)					
	Non command (a)	Command (b)	Unit draft in Ham	Total draft Non-command	Total draft
Borewells& dugcumborewell	6614	3525	1.1	7275.4	3877.5
Dugwells	2105	936	0.6	1263	561.6
Total draft for irrigation				8538.4	4439.1

Gound water draft for domestic and industrial purposes		
60 lts per person per day	Non command Ham	Command Ham
Total population	290639	222611
Population using surface sources		111306
Population using G.W sources(20016)	290639	111304
Domestic & Industrial Draft Ham	= Population using G.W sourcesx365x60/1000/10000	
	636.49	

		487.51

R gw (Return recharge from ground water irrigation)			
Crops grown area (Ha)			
Monsoon paddy	Non Monsoon paddy	Monsoon non paddy	Non Monsoon non Paddy
a	b	c	d
1638	0	14743	14743

CROP WATER DUTY (Ham) per Anum			
Monsoon paddy	Non Monsoon paddy	Monsoon non paddy	Non Monsoon non Paddy
(e)	(f)	(g)	(h)
1.25	1.35	0.2	0.52

IRRIGATION DRAFT (Ham)

Monsoon paddy	Non Monsoon paddy	Monsoon non paddy	Non Monsoon non Paddy
(a x e)= i	(b x f) = j	(c x g)=k	(d x h)=l
2047.5	0	2948.6	7666.36

Ground water draft based on Crop water duty

M draft Ham (i+k)	NM draft Ham(J+l)	Total
4996.1	7666.36	12662.46

R gw -Return flow from groundwater irrigation

Mon seep Ham (I x 0.35) +(k x0.15)	N Mon seep Ham (j x 0.35) +(l x0.15)	Total
1158.91	1149.95	2308.87

Rt - Return recharge from Tank storage

Water spread Area (Ha)	Mon no of days	Non mon no of days	M Seepage (q*0.6xrx0.0014) Ham	N Mon Seepage (q*0.6xsx0.0014)	Total recharge from tanks Ham
q	r	s	t	u	v
13556.42	120	60	1366.48	683.24	2049.73

Rsw- Return recharge from tank irrigation

M paddy Ha	NM paddy Ha	M non paddy Ha	NM non paddy Ha
x	y	z	Aa
338.90	0	6439.3	150

M paddy Ha	NM paddy	M non paddy	NM non paddy
ab	ac	ad	ae
1.25	1.35	0.2	0.52

M paddy Ha (x x ab)	NM paddy (y x ac)	M non paddy (z x ad)	NM non paddy (aa x ae)
125	135	30	78

R sw- Tank irrigation recharge

M paddy ham (af x 0.40)	NM paddy (ag x 0.40)	M non paddy (ah x 0.20)	NM non paddy (ai x 0.20)	Mon seep Ham(aj+al)	N Mon seep Ham
aj	ak	al	am	an	ao
50	54	12	31.2	62	85.2

R sw- Lift IRRIGATION

M paddy Ha	NM paddy Ha	M non paddy Ha	NM non paddy Ha
ap	aq	ar	as
0	0	5337.6	8006.4

Crop water duty

M paddy Ha	NM paddy	M non paddy	NM non paddy
at	au	av	aw
1.20	1.35	0.2	0.52

Rsw-Lift Irrigation recharge

Mon water applied Ham(ap x at)	Mon seep Ham(ax x0.4)
ax	az
0	0

Rc -Seepage from canal

Length of the canal km	Wetted perimeter	No of canal flow days	Seepage from canal
206.82	6.25	120	306.59

Rwc-Recharge from Water Consevation Structures

Total	No of	No of	Ave.	Mon seepage	Non mon	Total

nos	M fillS	NM fillS	Storage Mcu	Ham(ba x0.6 xbb xbd) /10000	seepage Ham	Ham
ba	bb	bc	bd	be	bf	bg
56.00	3	4	2000.00	16.80	22.40	39.2

Return recharge from all the sources

(Rgw+Rwc+Rt+Rc+Rsw)

Unit: Ham

Rgw	Rwc	Rt	Rc	Rsw	Total
2308.87	39.2	2049.73	306.59	1524.33	6228.72

Recharge Estimation by Water table fluctuation method

Unit: Ham

Watershed	Area	Water table fluctuation	Specific Yield	+ Gross Monsoon Draft	- R. other sources monsoon	recharge during Mon	Normal Mon rainfall (N)
4D7C8	149020	4.66	0.03	4996.1	6228.72	19600.376	435

Recharge Estimation by Rainfall infiltration factor method

Unit: Ham

Aquifer Area	Normal Monsoon rainfall	Infiltration factor	Annual Recharge

149020	435	0.28	18150.636

Comparison of two methods of monsoon rainfall assessment and finalization of estimate Considering percentage difference (P D)

$$\text{Percentage Difference} = \frac{R_{normal.\ W\ tf} - R_{r\ inf}}{R_{r\ inf}} \times 100$$

= (19600.37-18150.6/18150)*100

= 7.99

Gross Annual Recharge

Rgw	Rwc	Rt	Rc	Rsw	Total	Recharge due to rainfall	Total recharge
2308.87	39.2	2049.73	306.59	1524.33	6228.72	18150.636	24379.356

Total Draft

domestic / industrial draft	irrigation draft	Total
1124	12977.5	14101.5

Stage of development = GW DRAFT/NET ANNUAL RECHARGEX100

=(14101.5/ 24379.35)*100

=57.84%

The Stage of development is 57.84% hence the watershed is categorized as safe

Annexure –III

The Annual average rainfall data of upper catchment (4D7C9)

Year	Asoga	Bidi	Desur	Gunji	Hirebagewadi	Hulikatti	Jamboti	Kankumbi	Khanapur	Mkhubli	Average annual
	(mm)	(mm)	(mm)	(mm)	(mm)	(mm)	(mm)	(mm)	(mm	(mm)	(mm)
1980	2395.60		1512.00	2338.80			2694.80		2273.10	858.60	2012.15
1981	1990.10	1147.20	1414.00	1158.00	977.56	936.99	2081.10	7393.10	1988.20	1273.30	2035.95
1982	1705.60	998.47	1734.30	2265.50	800.38	789.11		1861.20	1959.70	855.40	1441.07
1983	1491.90	1152.47	2534.70	1942.70	1025.66	884.30		2295.90	2082.10	758.90	1574.29
1984	1283.50	872.20	1379.00	1954.10	698.20	662.35		1665.87	1711.70	938.10	1240.56
1985	985.00	893.60		1503.80	746.07	734.39		1650.57	1381.70	565.30	1057.55
1986	877.50	855.74		1123.20	587.72	626.39	1023.80	3951.20	1470.60	729.60	1249.53
1987	913.90	987.48	813.50	959.40	766.84	718.56	1880.30	4280.60	1359.50	775.60	1345.57
1988	1808.90	1430.00	1282.10		1068.51	1059.55	2640.00	5910.00	1692.80	860.00	1972.43
1989	1251.10	995.26	1301.90	1241.10	917.53	830.16	2457.40	5144.70	1417.90	701.70	1625.87
1990	1780.50	1078.79	1263.40	901.00	837.10	834.98	2622.00	6384.50	1661.20	702.60	1806.61
1991	1961.70	1141.06	1476.40	1238.20	1051.60	924.85	2900.20	5678.60	1954.20	1241.10	1956.79
1992	2047.30	1103.31	1851.50	924.00	869.16	812.98	2821.40	6064.20	1967.10	767.70	1922.86
1993	1858.30	1149.99	1566.30	1540.60	957.52	905.82	3115.00	6733.00	2094.70	1011.70	2093.29
1994	2946.40	1152.07	1754.20	3057.90	885.67	883.10	3873.40	8150.80	3149.80	996.00	2684.93
1995	1400.50	1098.28	1732.00	1534.10	873.29	821.64	2476.90	4151.70	1471.30	727.20	1628.69
1996	1407.00	1190.74	1989.00	1047.70	1019.16	923.61	2336.10	4154.40	1699.90	860.40	1662.80
1997	2253.00	1133.52	904.40	2309.30	801.63	782.54	3124.40	6702.00	2373.30	848.70	2123.28
1998	1417.70	1372.59	664.20	1236.80	1144.12	1080.78	2204.60	5774.80	1556.70	533.50	1698.58
1999	1982.10	1121.38	777.60	1640.50	898.54	929.85	2572.50	6868.60	2134.40	771.50	1969.70
2000	1457.00	1468.68	594.50	1870.10	1148.64	1096.03	2077.90	5733.60	1524.50	594.70	1756.56
2001	1199.00	940.45	635.00	1517.70	661.21	723.44	1837.30	4663.60	1185.40	500.90	1386.40
2002	1293.80	969.17	798.70	1460.00	729.11	737.40	1750.20	4669.00	1183.70	588.30	1417.94
2003	1299.80	850.60	814.20	1692.80	662.08	662.77	1679.20	4658.80	1246.30	557.30	1412.38
2004	1511.60	1044.01	939.70	1826.40	810.39	791.63	2127.30	5676.80	1666.90	739.10	1713.38
2005	2798.00	1706.25	1368.30	2863.20	1421.37	1377.48	2952.00	7106.60	2295.90	1136.90	2502.60
2006	2750.90	1403.83	1121.40	2687.50	1233.39	1123.45	2573.10	7775.60	2214.90	872.50	2375.66
2007	2978.30	1752.26	1167.40	3138.10	1403.71	1366.88	2718.60	6516.30	2766.50	1188.90	2499.70
2008	2128.30	1075.21	1046.20	2341.70	739.34	754.02	2130.60	5772.30	2193.40	908.90	1909.00
2009	2281.20	1403.64	1180.80	2091.40	1184.58	1140.27	2139.40	5464.30	3011.90	1061.20	2095.87
2010	1754.50	1664.52	912.40	2140.30	1391.59	1292.06	1551.80	6338.00	2080.60	1041.70	2016.75
2011	2254.60	1049.68	1303.10	2752.50	835.94	790.64	2123.20	7527.70	3036.60	1067.50	2274.15
2012	1194.60	828.89	542.40	1803.10	650.30	665.84	1180.10	5095.70	1206.10	651.90	1381.89
2013	1590.00	1063.27	859.00	2174.00	928.29	877.74		1936.03	1591.00	935.00	1328.26
2014	1845.60	1220.09	1292.60	2310.00	1077.03	998.76	1541.40	5518.10	1868.10	1163.30	1883.50
2015	972.30	802.32	863.90	1508.30	648.89	634.60	1673.60	3940.60	1104.00	670.20	1281.87
2016	1424.40	1022.12	764.20	12.00	878.11	823.33	1962.30	4566.10	1514.50	744.50	1371.16
Avg	**1743**	**1143**	**1204**	**1781**	**926**	**889**	**2276**	**5216**	**1867**	**843**	**1789**

Annexure –IV

The Annual average rainfall data of upper catchment (4D7C9)

Year	Bailahongal	Belawadi	Kadasagatti	Katkol	Murgod	Neginal	Savadatti	Tigadi	Yargatti	Average annual rainfall
	(mm)	(mm)	(mm)	(mm)	(mm)	(mm)	(mm)	(mm)	(mm)	(mm)
1980		566.10	10.00		503.00	1418.90	381.10	766.30		607.6
1981		407.40		481.58	817.60	977.20	670.40	8740.80	507.41	1800.3
1982		402.40		387.37	554.00	901.10	622.00	626.50	401.08	556.4
1983		302.00	411.40	459.02	556.50	720.10	481.70	611.60	483.71	503.3
1984		398.40	1162.00	418.16	574.80	630.50	428.80	678.00	427.95	589.8
1985	475.400	249.80	323.00	381.75	400.60	321.00	307.80	363.40	409.25	359.1
1986	553.900	261.40	293.00	271.81	417.50		351.90		297.09	349.5
1987	519.900	392.50	364.20	453.94	669.10		489.40	317.10	460.64	458.3
1988	623.400	460.50	185.50	504.23	747.90		604.10	643.60	518.84	536.0
1989	521.700	320.80	440.40	449.37	431.90	637.20	440.80	54.60	479.68	419.6
1990	485.000	301.80	568.30	379.87	475.90	557.40	512.80	559.40	386.08	469.6
1991	29.000	469.20	776.80	546.40	855.00	1022.80	737.10	1230.60	585.25	694.7
1992	37.000	477.40	303.80	399.24	693.20	839.60	605.00	557.20	408.21	480.1
1993	649.900	503.50	449.90	515.56	585.60	723.30	698.10	979.80	547.89	628.2
1994	18.000	686.00	591.90	492.12	609.40	620.00	554.90	1193.20	504.87	585.6
1995	452.500	513.20	307.00	414.69	429.20	518.70	538.10	263.50	413.85	427.9
1996	48.000	588.80	323.50	663.18	736.20	694.00	554.90	753.00	656.43	557.6
1997	636.400	455.40	352.80	322.09	559.40	602.50	538.10	991.00	352.24	534.4
1998	726.100	520.20	378.00	590.97	651.80	472.10	0.00	767.00	601.23	523.0
1999	548.800	322.20	408.10	591.55	630.60	671.40	516.40	998.00	630.29	590.8
2000	712.300	475.50	371.40	548.59	560.00	515.60	588.10	802.20	583.38	573.0
2001	421.400	296.80	132.30	506.26	327.10	467.80	464.40	401.00	504.44	391.3
2002	486.500	498.90	301.30	414.16	446.10	467.20	377.20	401.00	432.71	425.0
2003	401.600	258.50	105.50	338.49	423.50	476.50	323.80	718.50	376.47	380.3
2004	683.600	644.00	381.50	451.70	413.00	770.60	487.70	600.40	478.31	545.6
2005	1099.600	1050.00	562.80	739.61	994.80	1013.90	549.10	871.40	752.33	848.2
2006	649.500	779.60	506.00	553.61	406.10	768.80	637.60	757.40	632.21	632.3
2007	1102.400	1042.10	739.40	675.72	666.20	929.40	704.50	954.30	734.24	838.7
2008	737.800	828.30	747.40	441.80	446.90	805.10	687.70	1081.30	447.66	691.6
2009	1102.400	1121.80	889.40	684.33	984.40	1078.20	931.60	1136.60	705.12	959.3
2010	225.200	855.80	902.50	630.69	564.80	970.40	670.80	969.00	688.37	719.7
2011	728.800	531.40	737.00	420.53	449.00	833.20	409.50	1189.80	474.17	641.5
2012	124.600	509.50	293.20	444.54	348.60	515.80	0.00	576.30	444.27	361.9
2013	122.000	493.00	596.90	545.32	397.00	628.00	96.00	941.00	590.42	490.0
2014	122.000	866.30	876.60	512.32	614.50	933.60	697.70	1144.80	559.48	703.0
2015	127.400	605.40	457.10	400.34	448.80	562.90	580.80	779.80	420.24	487.0
2016	473.100	412.80	489.90	449.91	431.40	574.60	544.70	693.00	510.79	508.9
Avg	488.91	536.99	478.28	485.58	562.74	724.69	507.69	975.34	511.29	585.72

Field Photographs during the study Period

1. Measuring Groundwater Head at Khanapur Observation well along with our guide Dr Purandara B.K (Left Most) along with District Groundwater office Senior Geologist D.Arun

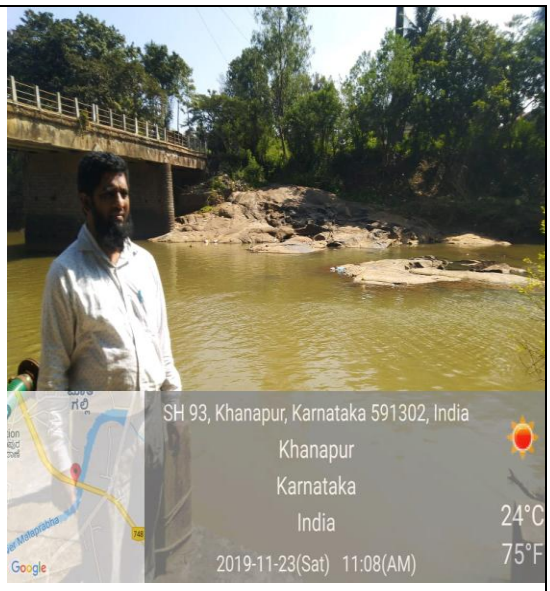

2. Malprabha River at Khanapur guaging station

3.Measuring Groundwater Head at Beedi Observation well along with our guide Dr Purandara B.K (Left Most) along with District Groundwater office Senior Geologist D.Arun

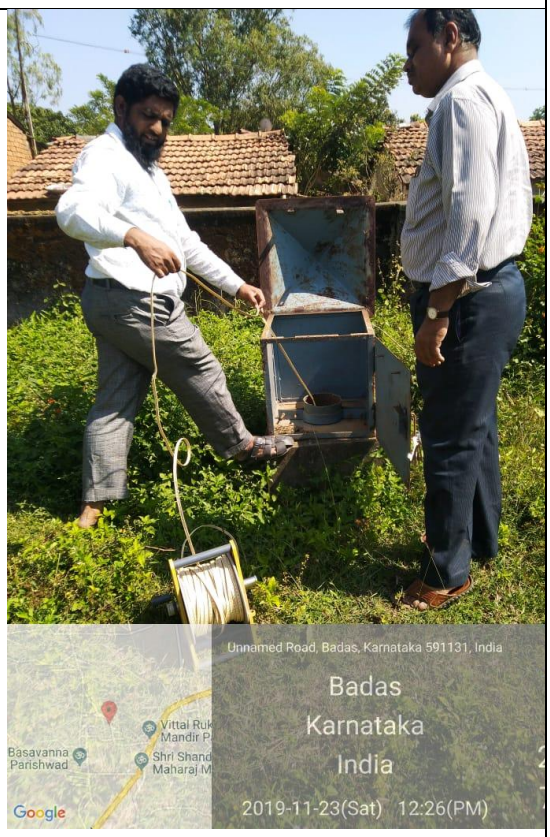

4.Measuring Groundwater Head at Parishwad Observation well along with our guide Dr Purandara B.K and with District Groundwater office Senior Geologist D.Arun

	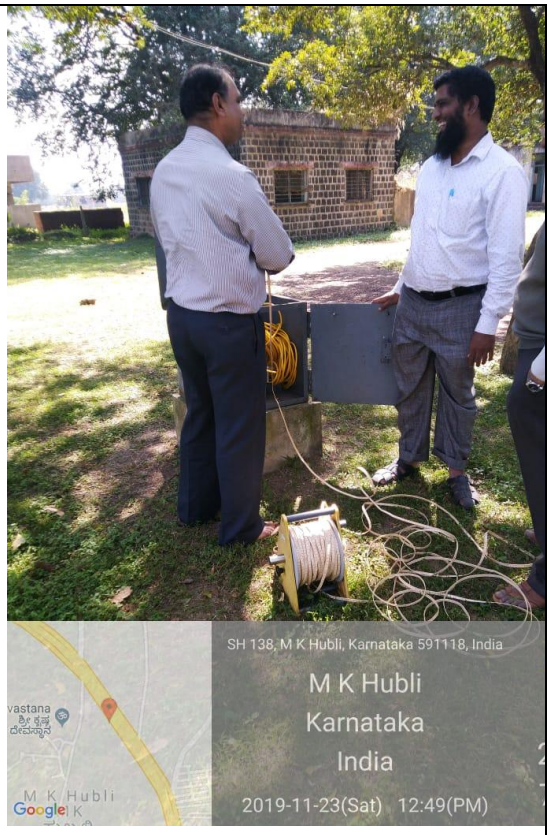
5. Measuring Groundwater Head at Chikkabagewadi Observation well	6. Measuring Groundwater Head at M.K.Hubli Observation well along with our guide Dr Purandara B.K (Left Most) along with District Groundwater office Senior Geologist D.Arun

7. Measuring Groundwater Head at Bailahongal Observation dug well

8. Measuring Groundwater Head at Bailahongal Observation bore well

9. Measuring Groundwater Head at Murkumbi Observation well

10. Measuring Groundwater Head at Munavalli Observation well